A novel effervescent hydrogen-generating tablet – formulation, optimization and in-depth characterization

Dissertation

zur Erlangung des Grades

„Doktor der Naturwissenschaften“

im Promotionsfach Pharmazie

am Fachbereich Chemie, Pharmazie,

Geographie und Geowissenschaften

der Johannes Gutenberg-Universität Mainz

Moritz Rosch

geb. in Wuppertal

Mainz, 2022

1. Berichterstatter:

2. Berichterstatter:

Tag der mündlichen Prüfung:

“May you always remember to enjoy the road, especially when it’s a hard one.”

Kobe Bryant

Für meine Eltern

I hereby declare that I wrote the dissertation submitted without any unauthorized external assistance and used only sources acknowledged in the work. All textual passages which are appropriated verbatim or paraphrased from published and unpublished texts as well as all information obtained from oral sources are duly indicated and listed in accordance with bibliographical rules. In carrying out this research, I complied with the rules of standard scientific practice as formulated in the statutes of Johannes Gutenberg University Mainz to insure standard scientific practice.

Chapters 2, 6, 10 and 13 use text, tables and figures of the following publication:

Rosch M, Lucas K, Al-Gousous J, Pöschl U, Langguth P. Formulation and Characterization of an Effervescent Hydrogen-Generating Tablet. Pharmaceuticals 2021, Vol 14, Page 1327. 2021;14(12):1327-.10.3390/ph14121327

Conflicts of Interest: Kurt Lucas is the inventor, and the Max Planck Society is the assignee of the patent application DE102012217387A1 and related patent family, which served as a starting point for the formulation development.

1. Contents

2. Abstract

Hydrogen, as a medical gas, is a promising emerging treatment for many diseases related to inflammation and oxidative stress. Molecular hydrogen can be generated through hydrogen ion reduction by a metal and an organic acid. Magnesium and citric acid containing effervescent tablets constitute an attractive formulation strategy for oral delivery. In this regard, saccharide-based excipients represent an important class of potential fillers with high water solubility and sweet taste. In this project an effervescent hydrogen-generating tablet was developed optimized with respect to rapid disintegration, sufficient hardness and characterized for all important aspects including content uniformity, disintegration and hardness properties as well as stability. During the development of the hydrogen generating tablet technical problems such as segregation of the excipients during the first attempts of direct compaction, sticking during compaction and slow disintegration were encountered and overcome by fixing the powder's blend status through roller compaction, establishing a milling process to generate small sized adipic acid particles as a water-soluble lubricant and optimization of the formulation's quantitative composition. During the optimization phase the effect of different saccharides on the morphological and mechanical properties and the disintegration of hydrogen-generating effervescent tablets prepared by dry granulation was investigated. Mannitol was found to be superior to other investigated saccharides such as maltose, lactose and glucose and promoted rapid hydrogen generation combined with acceptable mechanical properties. In further product optimization involving investigation of lubricant effects, adipic acid was selected over sodium stearyl fumarate for the optimized tablet, due to regulatory considerations. Moreover, it was soluble in water and didn't form a foam on top of the dispersion. With the aim of eventually gaining market access as a nutritional supplement, the final formulation was further investigated regarding stability and uniformity of dosage units. The technical development and characterization were completed within this thesis.

3. Zusammenfassung

Wasserstoff als medizinisches Gas ist eine vielversprechende neue Behandlung für viele Krankheiten im Zusammenhang mit Entzündungen und oxidativem Stress. Molekularer Wasserstoff kann durch Reduktion von Protonen durch ein Metall und eine organische Säure erzeugt werden. Magnesium und Citronensäure enthaltende Brausetabletten stellen eine attraktive Formulierungsstrategie für die orale Verabreichung dar. In dieser Hinsicht stellen Hilfsstoffe auf Saccharidbasis eine wichtige Klasse potenzieller Füllstoffe mit hoher Wasserlöslichkeit und süßem Geschmack dar. In diesem Projekt wurde eine wasserstofferzeugende Brausetablette entwickelt, die im Hinblick auf schnellen Zerfall, ausreichende Härte optimiert und für alle wichtigen Aspekte wie Gleichförmigkeit des Gehaltes, Zerfalls- und Härteeigenschaften sowie Stabilität charakterisiert wurde. Während der Entwicklung der wasserstofferzeugenden Tablette wurden technische Probleme wie Entmischung der Hilfsstoffe während der ersten Versuche der direkten Kompaktierung, Kleben während der Kompaktierung und langsamer Zerfall festgestellt und überwunden. Der Mischungsstatus des Pulvers wurde durch Walzenkompaktierung fixiert und ein Mahlverfahren zur Erzeugung kleiner Adipinsäure Partikel als wasserlösliches Schmiermittel etabliert. Zudem wurde die quantitative Zusammensetzung der Formulierung optimiert. Während der Optimierungsphase wurde der Einfluss verschiedener Saccharide auf die morphologischen und mechanischen Eigenschaften und den Zerfall von durch Trockengranulation hergestellten wasserstofferzeugenden Brausetabletten untersucht. Es wurde festgestellt, dass Mannitol anderen untersuchten Sacchariden wie Maltose, Lactose und Glucose überlegen war und eine schnelle Wasserstofferzeugung in Kombination mit akzeptablen mechanischen Eigenschaften förderte. In einer weiteren Produktoptimierung, bei der die Schmiermittelwirkung untersucht wurde, wurde aus regulatorischen Gründen für die optimierte Tablette Adipinsäure gegenüber Natriumstearylfumarat ausgewählt. Außerdem ist Adipinsäure wasserlöslich und bildete keinen Schaum auf der Dispersion. Mit dem Ziel, schließlich als Nahrungsergänzungsmittel Marktzugang zu erhalten, wurde die endgültige Formulierung weiter auf Stabilität und Einheitlichkeit der Dosierungseinheiten untersucht. Die technische Entwicklung und Charakterisierung wurden im Rahmen dieser Doktorarbeit abgeschlossen.

4. Introduction

4.1. Hydrogen

Hydrogen is the lightest chemical element of the periodic system. Despite its small size, molecular hydrogen (H_2) offers various applications in many different scientific and economic fields. It has been used for a long time in the chemical industry where it enables key processes like the Haber-Bosch process, which is used for most of the worldwide ammonia production, which in turn is used as fertilizer or as a precursor for various nitrogenous compounds. Many petrochemical processes involve hydrogen as well. For the near future hydrogen is discussed as an energy source for cars and trucks, using fuel cells to provide energy for electric cars without batteries.

This work focused on molecular hydrogen as a medical gas. In recent years a large number of articles focusing on molecular hydrogen as a medical gas have been published, demonstrating positive health effects for various diseases and clinical symptoms [1-4]. In these studies, molecular hydrogen showed antioxidant and anti-inflammatory effects. These effects were initially explained exclusively with radical scavenging effects of reactive oxygen species hydrogen [5]. Given time it was discovered, that the activation of the antioxidant system by molecular hydrogen via the transcription factor Nrf2 plays an important role as well [6-8]. Since many diseases involve inflammatory processes and an increased concentration of reactive oxygen and nitrogen species (ROS/RNS) [9-11], hydrogen was investigated in clinical studies focused on acute cerebral infarction, ischemic stroke, type 2 diabetes, metabolic syndrome and rheumatoid arthritis [12-17]. Moreover, muscular fatigue and performance enhancement were investigated [18-20]. Right now, the use of hydrogen for Covid-19 treatment is investigated in a clinical study (study NCT number: NCT04716985), which makes sense since hydrogen offers treatment potential for in the clinical treatment as investigated in the study as well as for long term effects related to inflammation and oxidative stress.[21, 22]

Application forms of hydrogen include inhalation and injection of hydrogen-enriched saline. While injection of hydrogen-enriched saline allows controlled dosing in animal studies, the most common application form for human use is the application of hydrogen enriched water (HRW) [23]. HRW can be generated by perfusion of water with hydrogen gas, which requires

qualified personnel to be executed safely or by electrolysis, which requires expensive devices. The distribution of professionally prepared HRW would imply difficulties, since it is challenging to store HRW for longer time periods, given that the small gaseous hydrogen molecule will vanish out of the HRW quickly. To prevent that, HRW available on the market is usually distributed in dense, single use aluminum bags that are harmful for the environment and difficult to dispose of. The chemical preparation of HRW constitutes a safer and easier approach for patients and non-qualified persons. Moreover, it makes HRW accessible for people which cannot afford expensive devices to prepare HRW. In this work the formulation development as well as thorough characterization of an effervescent hydrogen-generating tablet is addressed. The tablet contains magnesium powder and organic acids that react in a redox reaction generating hydrogen gas [24]. Effervescent hydrogen-generating tablets are much easier to store, given that proper primary packaging is used and it is sustainable, since it can be transported with much smaller capacities than HRW.

4.2. Effervescent tablets

The European Pharmacopoeia defines effervescent tablets as “uncoated tablets generally containing acid substances and carbonates or hydrogen carbonates which react rapidly in the presence of water to release carbon dioxide. They are intended to be dissolved or dispersed in water before administration“. Effervescent tablets were first monographed in the European Pharmacopeia in 1979, the U.S Pharmacopeia already monographed effervescent tablets in 1965 and the British Pharmacopeia in 1980 [25]. Non pharmaceutical applications include dental compositions containing enzymes, contact lens cleaners, washing powder compositions beverage sweeteners, chewable dentifrices, denture cleansers and surgical instrument sterilizers [26].

The fast disintegration of effervescent tablets allows a rapid release of the active pharmaceutical ingredient [27]. Their application form being a solution or a dispersion promotes a quick uptake and good bioavailability, which is important especially for drug products like analgesics, where an immediate effect is desired [28, 29]. Effervescent tablets are usually larger than non-coated tablets which allows a high amount of the active pharmaceutical ingredient [28]. Patients such as children and elderly people, for which swallowing of a tablet can bear a challenge, can also benefit from the easy administration of the effervescent solutions and dispersions [30]. Moreover, the effervescent solutions and dispersions can replace liquid dosage forms for drugs that are not stable in water for long term storage, because the liquid application form is prepared freshly [31]. The taste of this kind of application is well tolerated by patients, which enhances the patient’s compliance [28, 32]. Due to these advantages, effervescent tablets are used for a variety of different drugs [33, 34].

From a formulator’s point of view effervescent formulations are considered as technically challenging. J.M. Aiache labeled effervescent tablets as a “source of concern” (une source de soucis) [35]. By design, the effervescent agents represent an incompatibility within the tablet. Effervescent agents are usually hygroscopic and the blend is moisture labile. Even small amounts of water can be adsorbed out of the environment and trigger the effervescent reaction of the blend. Consequently, low relative humidity of 20-25% and controlled processing conditions have been recommended for manufacturing of effervescent tablets [31, 36]. High compaction forces have to be used because of the large diameter of these kind of tablets, which also contribute to problems like capping or sticking [37, 38]. Moreover, the increased sodium

intake can result in cardiovascular diseases [39, 40]. This problem however is not present for effervescent hydrogen-generating tablets, as they do not contain sodium.

Generally, an organic acid and a carbonate source are used for the effervescent reaction. For ascorbic acid and sodium bicarbonate the effervescent reaction follows the equation:

$$NaHCO_3 + C_6H_8O_6 \Rightarrow C_6H_7NaO_6 + H_2O + CO_2 \qquad \text{Equation 4.1.}$$

The effervescent reactants can represent up to 75% of the tablets weight.

Common organic acids are citric acid, tartaric acid, malic acid, succinic acid, ascorbic acid, adipic acid and fumaric acid [25, 26, 28, 36]. Salts like sodium dihydrogen phosphate, mono potassium citrate, mono sodium citrate and anhydrides of citric acid and succinic acid are also known as effervescent agents, but are used less frequently.

Citric acid is an organic acid which contains three carboxyl groups with pK_a values of pK_a1 = 3.13 pK_a2= 4.76 and pK_a3 = 6.4. Moreover, it is very soluble in water. Solubility values from 1608 g/kg to 1636 g/kg at 25°C have been reported for the anhydrous form [41-43]. Citric acid is available as monohydrate and anhydrous form. It adds a pleasant taste to an effervescent formulation, which is an important factor for patient compliance. Moreover, it is widely available at reasonable cost. Due to its popularity, there are numerous excipients available on the market, ranging from fine powders to processed compound excipients with coatings for enhanced compactability or moisture resistance. Disadvantages of citric acid are its hygroscopicity and sticking tendency, e.g. to metal surfaces of tablet punch sets or other metal processing parts [44, 45]. Fermentation with *Aspergillus niger* is the most popular industrial processing route to obtain citric acid from raw materials like e.g. molasses and starch based materials [46, 47].

Tartaric acid is a racemic diprotic acid (pK_a1 = 2.98 and pK_a2= 4.34), which is also a very common acid component in effervescent tablets. Similar to citric acid, it is very soluble in water (1396 g/kg to 1436 g/kg at 25°C) [41-43] and has a similar hygroscopicity [44].

Ascorbic acid is a vinylogous monoprotic acid that is freely soluble in water (337g/kg at 25°C [48]). Its acidity is a little weaker than the previous mentioned ones (pK_a = 4.10), however it has other benefits, since it can for example scavenge radicals or act as an antioxidant. Since it

has a very low hygroscopicity it is frequently used in moisture labile effervescent formulations [49]. However it shows sticking and capping tendencies during compaction [50].

Adipic acid has a much lower solubility than the previously mentioned acids (25g/kg at 25°C [42]). However it can be beneficial as a water soluble lubricant, since fatty acid lubricants e.g. magnesium stearate delay the tablet disintegration especially in acidic media and form an unpleasant foam on top of the effervescent solution [51]. The lubricating effect of adipic acid is strongly dependent on the particle size of the substance. In previous works milled qualities showed a much greater effect than coarse qualities. Moreover, adipic acid as a lubricant provides a quick disintegration for effervescent formulations when compared to other lubricants as well as reasonable hardness values of the tablets [52].

As carbonate sources and basic reacting components, sodium bicarbonate and sodium carbonate are the most common carbonate sources for the effervescent reaction. Usually, one of these components or a combination can be used at stoichiometric desired values related to the acid, where a surplus of acid can be beneficial for the taste. Among their disadvantages are the high sodium amount that is consumed by the users as well as the thermal lability and poor compactability [25, 36, 39, 40].

Effervescent diluent binders are usually sugars or sugar derived excipients. They have to be water soluble to yield a clear effervescent solution. Additionally, their taste is usually pleasant, which is also a valuable contributing factor to patient compliance. In this project, sugars like maltose, lactose and dextrates were investigated. Moreover, mannitol was included as a sugar alcohol.

Lubrication of effervescent tablets is more complicated than for usual non-coated tablets, because more hygroscopic excipients with sticking tendencies are used for effervescent formulations and the water insoluble lubricants that are most commonly used for tablets (e.g. magnesium stearate) cannot be used since they form a foam on the dispersion after the tablet disintegrates [53]. For internal lubrication salts of stearic acid and especially magnesium stearate are usually among popular choices for tablets [54]. However, these fatty acids are not water soluble, which results in an unpleasant foam on top of the effervescent solution and extended disintegration time. Water soluble lubricants like adipic acid, fumaric acid, polyethylene glycol 4000-8000 and spray dried l-leucine are known [25]. The problem is

increased by the need of the high compaction forces that are needed for effervescent tablets due to their large diameter compared to regular tablets and the hygroscopicity of citric acid. This results in enhanced sticking of the granules and powders to the punches.

Effervescent tablets are generally manufactured via direct compaction, or previous dry or wet granulation and compaction of the respective granules [25, 55]. Depending on whether the effervescent reactants are processed separately or together during processing steps prior to compaction as blending or granulation, the respective methods are categorized as single-step or multi-step methods [31].

Wet granulation can be performed with various granulation techniques and granulating agents. Fluid bed granulation, spray granulation, high shear granulation and melt granulation techniques have been used for effervescent granulation [25, 26, 28, 31]. Wet granulation processes can include a controlled partial initiation of an effervescent reaction through addition of very small amounts of water. It can be added as steam or via liberation of the crystal water of citric acid with heat and kinetic energy from high speed mixing with a high shear mixer or an external heat source [31, 56, 57]. Moreover, alcoholic organic solvents can contain a very small amount of water, which is barely enough to form a mass of the powder. Alternatively wet granules can be prepared using a binding solution that is sprayed onto or added to the powder. Among popular polymer binders are polyvinylpyrrolidone and polyethylene glycol, which are solved in water, ethanol, isopropyl alcohol and mixtures of them.

Regarding the possible unintended occurrence of the effervescent reaction in the presence of water, it is crucial to control the granulation process carefully. Especially during the single-step method careful monitoring of the amount of added water (usually not more than 1% of the batches weight) as well as a reproducible drying process to achieve a low moisture content (<0.1%) of the granules is crucial [31]. Multi-step methods with separated effervescent reagents minimize this risk. Other processes use heat to melt polyethylene glycol that acts as a binder to receive granules from a fluid bed process [58]. The heat has to be controlled very carefully as well, since sodium bicarbonate already begins to decompose at 50 °C into carbon dioxide, sodium carbonate, and water [59].

As mentioned before, control of the environmental humidity conditions is crucial for manufacturing of effervescent formulations. During compaction a controlled environment with humidity as low as possible is especially important. Ideally, 20% RH at 21°C should not be exceeded [31]. This can be achieved with a small box isolating the compaction zone from the environmental air and flushing the compaction zone with pressurized air as shown by Röscheisen [52]. A considerably larger scaled and more complicated approach is to dehumidify the entire laboratory/manufacturing facility where the tablets are compacted. A cost-effective and feasible approach is to distribute baskets containing calcium chloride in the respective facility. The dehumidifying capacity of this approach is obviously limited, but is a good choice for academic and educational purposes. However, an industrial facility dehumidifier is the more reliable and potent approach to this problem. This applies for storage facilities of excipients and bulk products as well.

In order to remain stable outside of controlled manufacturing and storage environments, effervescent products require humidity resistant packaging. Common packaging concepts for effervescent tablets includes alu blisters and plastic tubes with desiccant caps [26].

An effervescent hydrogen-generating tablet has a modified chemical reaction:

$$\overset{0}{Mg} + 2\ \overset{+I\ \ -I}{HAc} \Rightarrow \overset{+II\ \ -I}{MgAc_2} + \overset{0}{H_2} \qquad \text{Equation 4.2.}$$

Instead of carbon dioxide, the tablet generates hydrogen. Non-noble metals like magnesium reduce protons to hydrogen gas in acidic media. In this case, the organic acids provide the necessary protons. The gaseous solubility is dependent on the partial pressure of the measured gas above the solute and the temperature. Compared to the solubility of carbon dioxide (X_i = 6.15 x 10^{-4}), which is generated by a conventional effervescent tablet, the solubility of hydrogen (X_i = 1.411 x 10^{-5}) in water is much lower. Both values were recorded at atmospheric partial pressure (101.325 kPa) at a temperature of T= 298.15 K [60]. However, in addition to the solved gas there are also dispersed hydrogen bubbles present inside the hydrogen-enriched water. Since the solubility of hydrogen in water is so low, the tablet should provide a sufficient amount of magnesium and acid resulting in an oversaturated solution. Moreover, the hydrogen generation provides rapid disintegration, which is known from regular effervescent tablets and expected by patients that use the tablet. Due to safety considerations, the tablet should have a conventional size for an effervescent tablet, suggesting to the patient, that the tablet is not

intended for immediate swallowing. This has led to the final formulation of a tablet showing a diameter of 18 mm, weighing 1.50 to 1.65 g (depending on the lubricant). This formulation contained 75 mg (3.086 mmol) of magnesium, which required double the molar amount of protons (6.172 mmol) for a quantitative reaction, according to equation 4.2.. One molecule of citric acid (pK_a1 = 3.13, pK_a2 = 4.76 and pK_a3 = 6.4.) can only provide two protons rapidly for the reaction since it requires almost neutral pH value for the third carboxy group to be deprotonated (pK_a3 = 6.4). In order to ensure a quantitative reaction, an excess of protons (~122% of the necessary amount) of 3.753 mmol or 721mg of citric acid was selected. Depending on the formulation, ascorbic acid and adipic acid (18 mg and 150 mg, respectively) were included as well, which provided further protons. Accordingly, one tablet was able to generate 3.086 mmol of hydrogen gas (6.22 mg).

At the beginning of the formulation development, the tablets contained smaller amounts of magnesium (23.34 mg), citric acid (222.42 mg), and tablets of lower weight (425 mg) and diameter (12 mm) were manufactured. First, direct compaction of the excipients without granulation was tested. However, it was immediately visible that grey magnesium particles were accumulating on the top of the visible powder in the hopper. This segregation occurred, because of the movement, the acceleration and the vibration of the feeder shoe, that is always present on an eccentric tablet press during the compaction process [61]. In a powder blend consisting of different excipients, the blend segregates based on the previously mentioned process parameters and the particle characteristics such as density, shape, size and also surface properties [61-63]. During tablet compaction the feeder shoe moves over the die to load it with powder. A previously compacted tablet becomes ejected during this movement as well. Afterwards the feeder shoe is pulled back to ensure a free compaction movement of the punches. During the movement the previously blended powder particles rearrange and segregate. In order to solve this problem a granulation step had to be included. As previously mentioned, there are some restrictions and difficulties for granulation of effervescent powders, since a binder solution that contains water would start the effervescent reaction. For this reason, single-step methods that granulate both effervescent agents in one batch were excluded from the development. The risk to trigger the effervescent reaction was evaluated as too high, since the generated gas amount is much more important for an effervescent hydrogen-generating tablet, than for a conventional effervescent tablet that generates carbon dioxide,

where the gas generation is just a mechanism to ensure a rapid disintegration of the tablet in water. For the effervescent hydrogen-generating tablets, the amount of gas generation is very important, since this is the therapeutic agent. Moreover, residual water in the granulate could contribute to sticking, which is already a well-known problem for effervescent formulations [37, 38]. Consequently, a multi-step method was the next approach of the development. Magnesium and maltose were granulated in a wet granulation process using an oscillating laboratory granulator. Citric acid was granulated separately. For both batches, a binder solution of 5% polyvinylpyrrolidone in isopropyl alcohol was used. While the magnesium-based granules showed good flow properties, the citric acid-based granule showed a very rubbery consistency and heavy sticking, even in the glass beaker where it was stored. Based on the characteristics of the granules, it was decided that the most promising approach for tablet compaction was to blend the magnesium based wet granule with citric acid that was not granulated, which resulted in a first hydrogen-generating prototype of the tablet.

Since the aim was to develop a tablet, that meets the requirements of nutritional supplement regulations of the European Union, the formulation strategy was adjusted in different aspects after consulting an expert for food and supplements.

The magnesium amount was increased to 75 mg, in order to enable the tablet to be marketed with health claims that are associated to magnesium. For this reason, the tablet needs to contain at least 15% of the nutrient reference value (NRV) of 365 mg that was set by the Regulation (EU) No 1169/2011 of the European Parliament and of the Council [64]. This amount also provides for a quick disintegration of the tablets. Ascorbic acid was also included into the formulation, which served several purposes. Since it is a vitamin, 18 mg were included to use its health claims for the tablet. Moreover, it serves as an organic acid which enables the hydrogen-generation and serves as a physiological antioxidant as well as a technical antioxidant for the magnesium in the formulation as well.

Polymers like polyethylene glycol 4000, that was considered as a water-soluble lubricant and polyvinylpyrrolidone, which was used as a binder for wet granulation had to be excluded, since they are only allowed for tablets and capsules by the Regulation (EU) No 1333/2008. Since the tablet has to be disintegrated in water, the form of application is hydrogen enriched

water, which is a liquid. Accordingly, it is at least uncertain, if the polymers were allowed for the formulation and as a consequence they were excluded.

Sodium stearyl fumarate that was used as a lubricant was also excluded, because it is not allowed for nutritional supplements in Europe. Magnesium stearate was considered as an alternative since it is a popular choice as a lubricant [54]. For effervescent tablets it was not suitable, since it delays tablet disintegration in acidic media and forms a foam on top of an effervescent solution [51]. Sodium stearyl fumarate was used for further development but was later replaced by milled adipic acid.

Since granulation was essential to prevent the blend from extensive segregation, the work focused on roller compaction as a binder solution free granulation alternative. Initially, all excipients were granulated in a single process, in the final formulation citric acid was exchanged for Citrocoat® N (citric acid coated with mono sodium citrate) to increase its moisture protection. Citrocoat® N was not included in the roller compacted granule, since the mono sodium citrate coating would have been destroyed during subsequent milling process of the granular ribbons.

In addition to Maltose, which was used as a saccharide-based filler from the beginning of the project, more saccharide-based fillers, specifically mannitol, lactose and dextrates were investigated towards their influence on the formulation, in order to optimize the disintegration time and contribute a sufficient hardness of the tablet for handling and storage.

After the formulation development and the characterization of the formulations, extended investigations directing to a possible market introduction were performed. Different batches of the final formulation were investigated regarding their content uniformity to affirm the reproducibility of the production process.

Moreover, stability analyses were conducted to evaluated the products stability and estimate its shelf life. These studies were performed of unpacked tablets in bulk and of tablets packed in primary packaging tubes. Long term stability storage condition (25°C and 60% RH) and accelerated stability storage condition (40°C and 75% RH) as suggested by the ICH guideline Q1A(R2) “Stability testing of new drug substances and products” were investigated [65].

5. Aims of the thesis

In recent years, hydrogen has emerged as a medical gas for anti-inflammatory and anti-oxidant treatment of various diseases. The aims of this PhD project were to formulate, develop and optimize an effervescent hydrogen-generating tablet that enables patients and other consumers to freshly prepare hydrogen enriched water.

Starting point was a formulation comprising magnesium, citric acid, ascorbic acid and maltose, which was compacted on a manual single punch tablet press. Here a formulation and production process should be developed, which is robust, reliable and can be utilized on automatic eccentric and rotary tablet presses. Furthermore, the tablets should be constituted in accordance with the requirements of nutritional supplement regulations of the European Union.

Compaction of effervescent tablets is challenging [35], since effervescent excipients are hygroscopic as well as moisture-labile during processing and storage. Water uptake of the granules and tablets before and during tableting and storage can result in sticking to the punches of the tableting machine. Further challenges such as segregation of the excipients (components) during the first attempts of direct compaction, sticking during compaction and slow disintegration had to be overcome.

In a future step, it is planned to test this tablet or further modifications of it, for example taste-optimized tablets in a clinical study on patients suffering from chronic fatigue. This frequent syndrome occurs often after infection by COVID-19 and is rarely understood. Some hints make it likely to be a consequence of high oxidative stress [66].

6. Formulation and characterization of an effervescent hydrogen-generating tablet

Note:

The content of this chapter uses text, tables and figures of the following publication:

Rosch M, Lucas K, Al-Gousous J, Pöschl U, Langguth P. Formulation and Characterization of an Effervescent Hydrogen-Generating Tablet. Pharmaceuticals 2021, Vol 14, Page 1327. 2021;14(12):1327-.10.3390/ph14121327

6.1. Introduction

Hydrogen, as a medical gas, is a promising emerging treatment for many diseases related to inflammation and oxidative stress. Molecular hydrogen can be generated through hydrogen ion reduction by a metal, and magnesium-containing effervescent tablets constitute an attractive formulation strategy for oral delivery. In this regard, saccharide-based excipients represent an important class of potential fillers with high water solubility and sweet taste. In this study, we investigated the effect of different saccharides on the morphological and mechanical properties and the disintegration of hydrogen-generating effervescent tablets prepared by dry granulation.

Different formulations using different saccharide binders were prepared and characterized regarding their content uniformity, disintegration, hardness and granular flow properties among others. A formulation based on mannitol as saccharide binder and adipic acid as water soluble lubricant was selected for further characterization regarding stability with dynamic vapor sorption and bulk stability testing in constant climate chambers.

6.2. Materials

Magnesium powder (-325 mesh, 99.8% purity) was purchased from Alfa Aesar (Heysham, England). Citrocoat® N (granule with citric acid core coated with a monosodium citrate shell) was kindly gifted by Jungbunzlauer Suisse AG (Basel, Switzerland). L(+)-ascorbic acid was purchased from Carl Roth GmbH + Co. KG (Karlsruhe, Germany). Samples of Advantose® 100 (maltose) and Kerry Lactose Anhydrous NF DT High Velocity (lactose) were received as a gift from Lehmann &Voss & Co. KG (Hamburg, Germany). Mannogem EZ® (mannitol) was kindly donated by Spi Pharma (Wilmington, NC, USA). Adipic acid Emprove® Essential was generously donated by Merck KGaA (Darmstadt, Germany). Emdex® (dextrates, glucose monohydrate and different polysaccharides derived from starch according to USP 42-NF 37) and Pruv® (sodium stearyl fumarate) were received as a gift from JRS Pharma GmbH + Co. KG (Rosenberg, Germany). Stochiometric quantities of each excipient included in one tablet of the respective batches are listed in Table 6.1.

Table 6.1. Stochiometric quantity of each excipient included in one tablet of the respective batches

Ingredient/tablet (mg)	Maltose	Mannitol	Mannitol/ Adipic Acid	Lactose	Dextrates
Magnesium powder	75	75	75	75	75
Ascorbic acid	18	18	18	18	18
Citrocoat® N	721	721	721	721	721
Maltose	686				
Mannitol		686	686		
Lactose				686	
Dextrates					686
Sodium stearyl fumarate	7.5	7.5		7.5	7.5
Adipic acid			150		

6.3. Methods

6.3.1. Sieving of Powders

The saccharide fillers (maltose, mannitol, lactose, and dextrates) and ascorbic acid were hand-sieved (400 µm or 800 µm sieve mesh size) to disaggregate any agglomerates.

6.3.2. Milling of Adipic Acid

Adipic acid (Emprove® Essential) was milled with a Fritsch Pulverisette Type 00.001 (Fritsch GmbH, Idar-Oberstein, Germany) single ball mill (70 mm agate grinding ball in 95 mm agate grinding bowl; intensity level 10; 3 h). 15 g of adipic acid were milled per cycle and united in a closed vessel afterwards.

6.3.3. Blending of Powders

The powder formulations (50 g of magnesium powder, 12 g of ascorbic acid, and 457.65 g of the respective saccharide fillers (maltose, mannitol, lactose, and dextrates)) were blended with a Turbula® 3D shaker mixer T 2 F (Willy A. Bachofen GmbH, Muttenz, Switzerland), equipped with a 1.6 L mixing basket for 10 min at 49 rpm.

6.3.4. Roller Compaction/Dry Granulation

Dry granulation of the blended powder from Section 6.3.3. was conducted on a roller compactor (TFC-LAB Micro) by Freund-Vector Corp. (Marion, OH, USA), which was equipped with standard compacting rolls "S" (diameter of 50 mm; width 24 mm) by Freund-Vector Corp. (Marion, OH, USA). As input parameters, a compaction force of 4 kN which equals $1.\overline{6}$ kN/cm for the used compacting roll, roll speed of 1 rpm, and a screw speed of 30 rpm, were used to compact the powder to ribbons.

6.3.5 Dry Cone Milling

Milling of the ribbons obtained from 6.3.4. was performed immediately after previous roller compaction step with a U5 Quadro Comil from Quadro Engineering Corp. (Waterloo, ON, Canada) using a 1575 µm rasp mesh screen at 1000 rpm and a round bar impeller (7L160110095).

6.3.6. Blending of Dry Granules with Citrocoat® N

After dry roller compaction and cone milling, 207.86 g of the dry granules and 192.14 g of Citrocoat® N were blended in a Turbula® 3D shaker mixer T 2 F for 10 min.

6.3.7. Addition of Lubricant

2 g of sodium stearyl fumarate (Pruv®) or 40 g adipic acid (Emprove® Essential) were sieved onto 400 g of the blend of dry granules with Citrocoat® N using a 100 µm or 160 µm mesh sieve to disaggregate any agglomerates. Consequently, either 0.5% or 10% of lubricant were added to the granules. Afterwards, the mixture was blended once more with a Turbula® 3D shaker mixer T 2 F for 3 min.

6.3.8. Compaction of Tablets

Tablets were compacted on an instrumented Korsch EK0 eccentric tablet press (Korsch AG, Berlin, Germany) with a Korsch steel punch set (diameter 18 mm). Tablets were compacted at 25 kN (mannitol/adipic acid) or 40 kN (maltose, mannitol, lactose, dextrates). The compaction forces were recorded and processed with a Spider 8 electronic measuring system and Catman 4.5 software (Hottinger Baldwin Messtechnik GmbH, Darmstadt, Germany). 402 g of the granules lubricated with sodium stearyl fumarate (Pruv®) or 440 g of the granules lubricated with adipic acid (Emprove® Essential) were used for the compaction process. Since every tablet should contain 75 mg of magnesium which is included in 1.5g of unlubricated

granules, the theoretical tablet weights were 1.5075 g (granules + 0.5% lubricant) for the granules lubricated with sodium stearyl fumarate (Pruv®) and 1.65 g (granule + 10% lubricant) for the granules lubricated with adipic acid (Emprove® Essential). The measured tablet weights are presented in Table 6.4.. Figure 6.1. shows a flow diagram that summarizes all manufacturing processes.

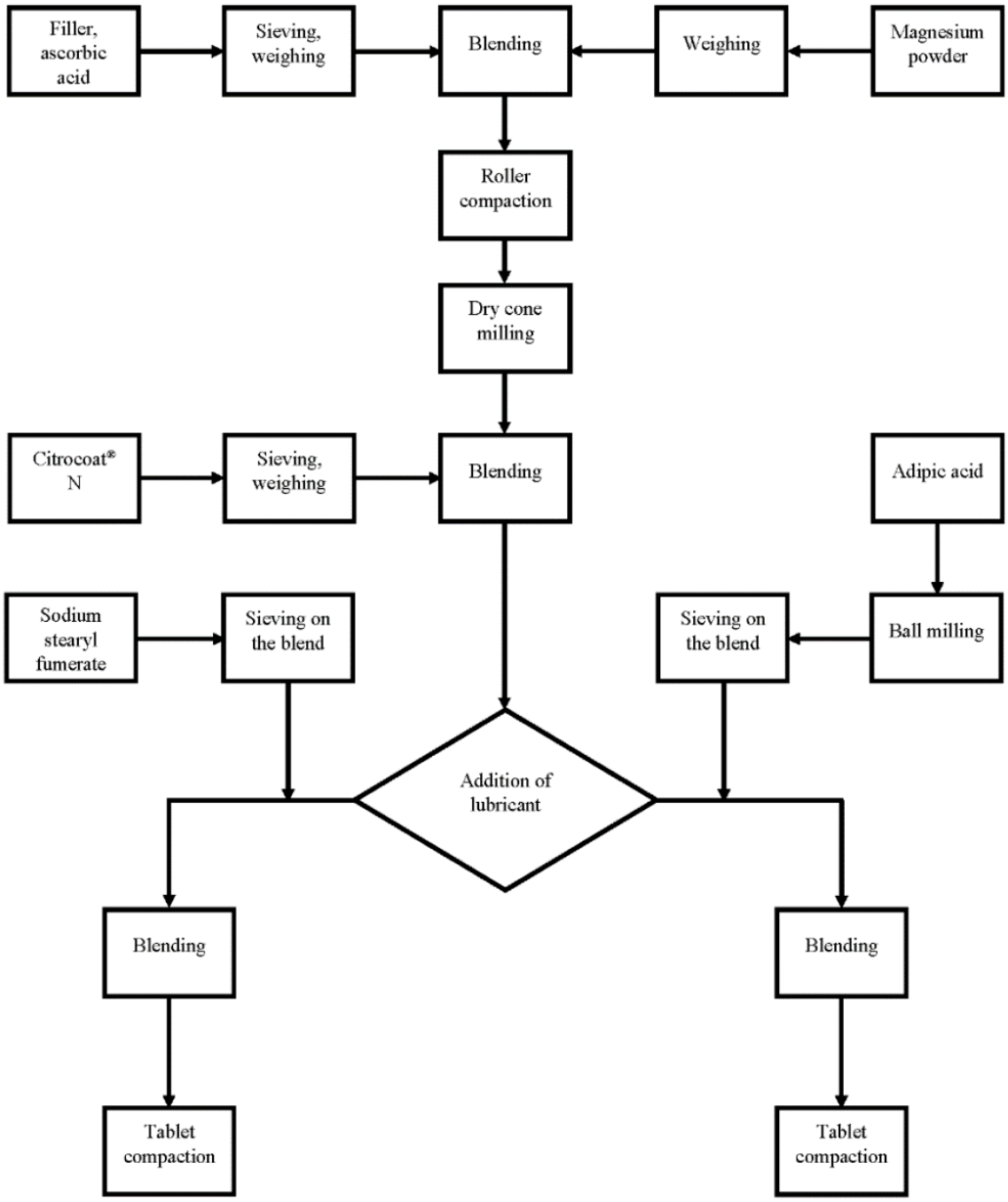

Figure 6.1. Flow diagram of the manufacturing process.

6.3.9. Kinetic Hydrogen Generation Measurement

Kinetic hydrogen generation measurement was conducted with slight modifications to the approach of Brack et al. [67]. Specifically, measurement of hydrogen evolution was similarly performed using a volumetric apparatus and a data logging scale, while the chemical reaction differed to the one in the above-cited article. Brack et al. measured hydrogen that is generated by the reaction of silicon with aqueous sodium hydroxide solutions; whereas, in the present study, hydrogen generated by the reaction of magnesium with the organic acids in the formulations was determined.

A 50 mL Erlenmeyer flask filled with 30 mL of deionized water was used for the chemical reaction. A plastic tube with an inner diameter of 3 mm and a length of 53 cm was used to direct the evolving hydrogen gas to a 250 mL measuring cylinder which was filled with 170 mL of water. The water bath was filled until it flooded slightly. Then, 30 mL of water was added, which was followed by a refractory period of 30 min to make sure that the water bath was completely leveled. Experiments were conducted at room temperature (23 ± 1 °C). The tablets were put into the Erlenmeyer flask, the beaker was closed immediately, and the water displacement was recorded with a data logging Denver S 2002 scale (Denver Instruments, Bohemia, NY, USA) using Sartorius Wedge recording software (Sartorius AG, Goettingen, Germany). When 90% of the expected amount of water was displaced or after 400 s (whichever occurred first), the solution was stirred to recover as much hydrogen as possible.

The volume of displaced water is equivalent to the volume of hydrogen. The amount of hydrogen can then be calculated from its volume employing the equations:

$$p * V = m_{Hydrogen} * R_s * T \qquad \text{Equation 6.1.}$$

p is pressure $[kPa]$; V is volume $[m^3]$; $m_{hydrogen}$ is mass of hydrogen $[kg]$; R_s is specific gas constant of hydrogen $[J/kgK]$; T is temperature $[K]$.

$$V = \frac{m_{water}}{\rho_{water}} \qquad \text{Equation 6.2.}$$

V is volume $[m^3]$; $m_{hydrogen}$ is mass of hydrogen $[kg]$; ρ is density of water (25 °C[997 kg/m^3]).

$$p * \frac{m_{water}}{\rho_{water}} = m_{Hydrogen} * R_s * T \qquad \text{Equation 6.3.}$$

$$m_{Hydrogen} = \frac{p\frac{m_{water}}{\rho_{water}}}{R_S T}$$ Equation 6.4.

f2 values of the hydrogen generation profiles were calculated as suggested by Moore and Flanner [68] in order to evaluate the similarity of the hydrogen generation profiles of the different formulations.

6.3.10. Magnesium Content (Complexometric Titration)

The magnesium content of the tablets was determined according to Ph. Eur. 10.1; 2.5.11. (complexometric titrations/magnesium). A buffered sample was titrated with sodium edetate (0.1 mol/L). Mordant black (Deutsch: Eriochromschwarz) was used as a color indicator. For enhanced visibility, 75 mg mordant black was used. A correction factor of 0.998 was determined (n = 5) by titrating 75 mg of magnesium powder. n = 5 was also used for each batch of tablets.

6.3.11. Disintegration

Disintegration experiments were performed in a beaker with 200 mL of water as described in the monograph of effervescent tablets Ph. Eur. 10.1/0478. According to this monograph, the water has a temperature of 15-25°C and the test is finished, once the evolution of gas around the tablet or the resulting fragments stops. In contrast to the pharmacopeial method, primary and secondary endpoints of disintegration were determined visually. The first measurement was taken when the tablet had disintegrated partially into granular particles. The second measurement was taken as the endpoint, after the tablet and the particles had disintegrated completely. The first measurement was taken additionally, since the Ph. Eur. just determines the complete disintegration. As in the Ph. Eur. Monograph, the measurement was performed for six tablets.

6.3.12. Three-Point Bending Test

The three-point bending test was performed on a Texture Analyzer TA.XTplus equipped with a Three Point Bend Rig ((HDP/3PB) both from Stable Micro Systems Ltd. (Surrey, UK)). Ten measurements of the peak force were performed for each batch. The loading pin was programmed to move 0.05 mm/s starting at a trigger force of 1 N. The gap between the supporting pins was 14 mm.

6.3.13. Friability of Uncoated Tablets

The friability of the dedusted tablets was measured with a TAP friability tester by Erweka (Langen, Germany). One hundred rotations were performed at 21 rpm. Afterwards, the tablets were dedusted again. Tablets were weighed prior to and after the test, and the loss of mass (friability) in % was determined.

6.3.14. Resistance to Crushing

Resistance to crushing was measured as described in Ph. Eur. 10.1/2.9.8 with a PTB-M-manual tablet hardness testing instrument by Pharma Test Apparatebau AG (Hainburg, Germany). Ten measurements were performed on every batch. Prior to this test, every tablet was weighed. Since the tablets are round and symmetrical and have no score line, the orientation of the tablet in the device does not need to receive consideration.

6.3.15. Tensile Strength

Tensile strength (σ) was calculated as suggested by Fell et al. [69] :

$$\sigma = \frac{2P}{\pi DT} \qquad \text{Equation 6.5.}$$

P is crushing strength $[N]$; D is tablet diameter $[mm]$; T is tablet thickness $[mm]$.

Crushing strength was measured with the PTB-M-manual tablet hardness testing instrument from Pharma Test Apparatebau AG (Hainburg, Germany) as mentioned above, and tablet thickness was measured with an ID-C112XBS thickness gage (Mitutoyo Corporation, Kanagawa, Japan).

6.3.16. Porosity and Pore-Size Distribution of Solids by Mercury Porosity

Porosity measurements were performed with Pascal 140 and Pascal 240 porosimeters from Thermo Fisher Scientific (Waltham, MA, USA). The tablets were cut with a band saw in order to fit them into the porosimeter. In the Pascal 140 device, the sample is exposed to mercury at increasing pressures up to 400 kPa. Afterwards, the sample is transferred to the Pascal 240 device and the pressure is increased to 200 MPa.

6.3.17. Helium Pycnometry

True density was measured using a helium pycnometer AccuPyk II 1340 V2.1 (Micrometrics Instrument Corporation; Norcross, GA, USA). Three tablets per batch were analyzed (134.4 kPa helium gas pressure for analysis; 15 purges; equilibration rate: 0.0345 kPa/min)

6.3.18. Particle Size Analysis by Laser Light Diffraction

Particle sizes were measured according to Ph. Eur. 10.1/2.9.31.with a LS 13 320 laser diffraction particle sizing analyzer equipped with a Tornado DPS module (Beckman Coulter, Inc.; Brea, CA, USA). The Fraunhofer method was used to calculate the particle sizes.

6.3.19. Bulk Density and Tapped Density of Powders

Bulk and tapped densities were measured according to Ph. Eur. 10.1/2.9.34; method 1. Therefore, 150 g of sample were used as suggested for samples with high density. Tapped density was measured with an Engelsmann jolting volumeter type EU42E2/114S-WF from J. Engelsmann AG (Ludwigshafen, Germany). The compressibility index and Hausner ratio were calculated as suggested. Each measurement was performed three times.

6.3.20. Angle of Repose

Angle of repose was determined according to Ph. Eur. 10.1/2.9.36 using a funnel and the drained angle of repose method. The measurements were conducted three times with a PTG S3 powder analysis device (Pharma Test Apparatebau AG; Hainburg, Germany).

6.3.21. Flowability

Flowability was determined according to Ph. Eur. 10.1/2.9.16 using nozzle 1. Triplicate measurements were conducted with a PTG S3 powder analysis device (Pharma Test Apparatebau AG; Hainburg, Germany).

6.3.22. Loss on Drying Analysis of the Granules

Loss on drying analysis was conducted with a Precisa moisture analyzer XM60 (Precisa Gravimetrics AG; Dietikon; Switzerland). About 1 g of granule was weighed, then the device was heated to 105 °C. After 2 min, the weight loss (%) was measured. The measurements were performed three times.

6.3.23. Dynamic Vapor Sorption (DVS)

DVS measurements were performed with a DVS Advantage device (Surface Measurement Systems Ltd., London, UK). An effervescent granule formulation containing mannitol was investigated. Two cycles of sorption and desorption were performed, 0%-90%-0% P/P_0 H_20 in 10% increments. Criteria for changing the increment were a mass change smaller than dm/dt = 0.002% min^{-1} [70], stable for 10 min. If the dm/dt criterion was not met, the increment was changed after 600 min.

6.3.24. Bulk Stability Testing

Tablets of the mannitol/adipic acid-based batch were investigated. Tablets were stored in a KBF P 240 constant climate chamber (Binder GmbH, Tuttlingen, Germany) at 25 °C and 60% RH for 0 h, 24 h, 7 days, 14 days, and 8 weeks, respectively. Afterwards, weight gain and kinetic hydrogen generation were measured. The kinetic hydrogen generation measurement was performed as described above. Weight gain was measured on an analytical scale (Sartorius LE225D-0CE; Sartorius AG, Goettingen, Germany). Tablets were also stored in a KBF S 240 constant climate chamber (Binder GmbH, Tuttlingen, Germany) at 40 °C and 75% RH for 24 h. The samples reacted completely and no hydrogen could be generated. A photo of a tablet can be viewed in chapter 13; (Figure 6.8.f)).

6.3.25. Scanning Electron Microscopy

To investigate the tablet surface, the tablets were coated with a gold layer (20 nm thickness) using a sputter coater SCD 050 (Bal-Tec AG; Balzers, Liechtenstein) and stored in an oven for 24 h (70 °C). The samples were investigated with a Leo 1530 scanning electron microscope (Carl Zeiss Microscopy GmbH; Jena, Germany) using an electron high tension of 15 kV for the mannitol/adipic acid-based and 5 kV for all other batches.

6.3.26. Statistical Analysis

IBM SPSS statistics (IBM Corporation; Armonk, NY, USA) was used for statistical calculations of the obtained data. Results were compared with ANOVA. Significance was assumed for p-values < 0.05.

6.4. Results

To develop a hydrogen-generating effervescent tablet based on the chemical redox reaction of an acid and metal, which was the aim of this work, a substance which can reduce the acid's protons by virtue of its lower reduction potential compared to hydrogen is required. Furthermore, both components need to exhibit the exact degree of chemical reactivity which is needed in order to ensure a safe chemical reaction upon contact with water and to ensure sufficiently rapid tablet disintegration within a few minutes. Of course, both components must also be well tolerated physiologically. Suitable candidates include alkali metals such as sodium, alkaline earth metals such as calcium, or even transition metals such as iron. For these reasons a solid acid was chosen as a proton donor, which is commonly found in effervescent tablets [25]. Specifically, elementary magnesium was selected, as it reduces protons to hydrogen gas in an acidic medium. Metals such as sodium were not considered to be safe because of their extremely high chemical reactivity, whereas iron was regarded as chemically too inert. Regarding organic acids, the best results were obtained with ascorbic acid and Citrocoat® N.

6.4.1. Selection of Tableting Excipients

In contrast to a conventional tablet, the formulations described here generate hydrogen instead of carbon dioxide from a chemical redox reaction [24, 71-76] in which elementary magnesium reduces hydrogen in an acidic medium according to the equation

$$\overset{0}{Mg} + 2\ \overset{+I\ -I}{HAc} \Rightarrow \overset{+II\ -I}{MgAc_2} + \overset{0}{H_2} \qquad \text{Equation 6.6.}$$

Magnesium powder of very high purity and small particle size was selected to ensure a quick chemical reaction. With Citrocoat® N (granule with citric acid core coated with a monosodium citrate shell), a functional acid was selected that enables a rapid effervescent reaction that pure citric acid ($pk_a1 = 3.14$, $pk_a2 = 4.77$) would provide and offers a reasonable hygroscopicity by dint of its less hygroscopic monosodium citrate shell. Additionally, effervescent tablets need to disintegrate quickly upon contact with water and since they form oral solutions, taste is an important consideration during product development. Therefore, saccharides and saccharide-derived fillers are often used in such formulations. In addition to their high water solubility and acceptable taste, these excipients tend to exhibit favorable compaction properties. Therefore, one of the main objectives of this study was to evaluate different saccharide fillers

and determine their impact on tablet properties. Highly purified ascorbic acid contributes to the physiological antioxidant effects of the tablet and can also protect the magnesium powder in the formulation from oxidation during processing and storage. The water-soluble lubricants, sodium stearyl fumarate and milled adipic acid (d50 value: < 15 µm), were chosen to avoid delayed disintegration, which would occur especially in acidic media [51], as well as fatty acid layers on top of the effervescent solution created by water-insoluble lubricants like magnesium stearate.

6.4.2. Disintegration, Porosity, Kinetic Hydrogen Generation, and Magnesium Content

The disintegration of the mannitol-based tablets was significantly faster than with other fillers (Figure 6.2., Table 6.2.) with an average disintegration time of 72 ± 3 s (mannitol) and 83 ± 3 s (mannitol/adipic acid), respectively. Interestingly, all fillers bar mannitol took a longer time to disintegrate completely, after partially disintegrating into granular particles. The disintegration into the granular particles took roughly 3 min for maltose, lactose, and dextrates, while the complete disintegration time was 238 ± 25 s for maltose and 257 ± 15 s for dextrates. It took 300 ± 32 s for the lactose-based particles to disintegrate completely, which is significantly longer than for every other formulation. Thus, 116 s was required for the disintegration of the granular lactose particles, while this step was significantly shorter for the maltose-based (46 s) and dextrates-based (66 s) particles and only 15 s or less was required for the complete disintegration of the mannitol-based formulations (7 s for mannitol and 15 s mannitol/adipic acid, respectively).

In conjunction with fast tablet disintegration times, hydrogen generation was also relatively fast for the mannitol-based tablets. They generated more than 80% of the theoretically possible hydrogen content after only 100 s. At this time, the tablets with dextrates as a filler had generated slightly more than 7% of the theoretically possible hydrogen amount.

The amount of generated hydrogen ranged from 91.93 ± 1.59% (lactose) to 105.91 ± 2.08% (mannitol/adipic acid) (Figure 6.2; Table 6.1) of the theoretically possible amount assuming a complete chemical reaction. The mannitol-based formulations generated significantly more hydrogen than the other fillers. No significant differences were observed between mannitol-based tablets. After adjustment for differences in tablet weight, total hydrogen generation averaged 102.8 ± 2.93% (mannitol) and 103.89 ± 1.77% (mannitol/adipic acid), respectively.

Moreover, the magnesium content was determined by complexometric titration of magnesium ions (Table 6.2.). The magnesium content ranged from 100.54 ± 1.70% (lactose) to 106.88 ± 1.95% (dextrates). Only the values of the mannitol-based batches (104.03% and 104.94%) suggest a complete oxidation of the magnesium, leading to hydrogen generation.

The f2 comparison suggests that hydrogen generation curves with a dimensionless value of above 50 can be considered as similar according to SUPAC guidelines (Table 6.3.). The following curves are accordingly considered to be similar: mannitol and mannitol/adipic acid (f2 = 85.95); maltose and lactose (f2 = 64.24); lactose and dextrates (f2 = 54.65).

Figure 6.4. shows that a high porosity is associated with quicker disintegration times. The mannitol-based batches show the highest total porosities (13.13 ± 0.68% and 14.40 ± 0.12%, respectively) and exhibited the lowest median pore size (Table 6.2). The pore sizes were confirmed with scanning electron microscope pictures (Figure 6.5a–e).

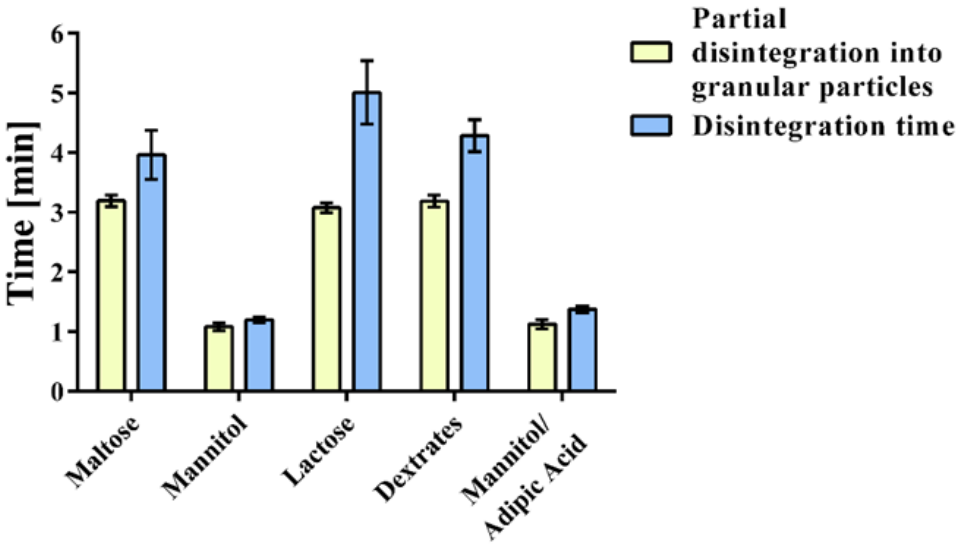

Figure 6.2. Disintegration time of tablets containing different fillers. Experiments were conducted in a beaker with 200 mL of water as described in the monograph of effervescent tablets in the Ph. Eur. 10.1/0478. Primary and secondary endpoints of disintegration were determined visually. The first measurement was taken when the tablet had partially disintegrated into granular particles (DiG = partial disintegration into granular particles). The second measurement was taken as the endpoint, after the tablet and the particles had disintegrated completely (DT = disintegration).

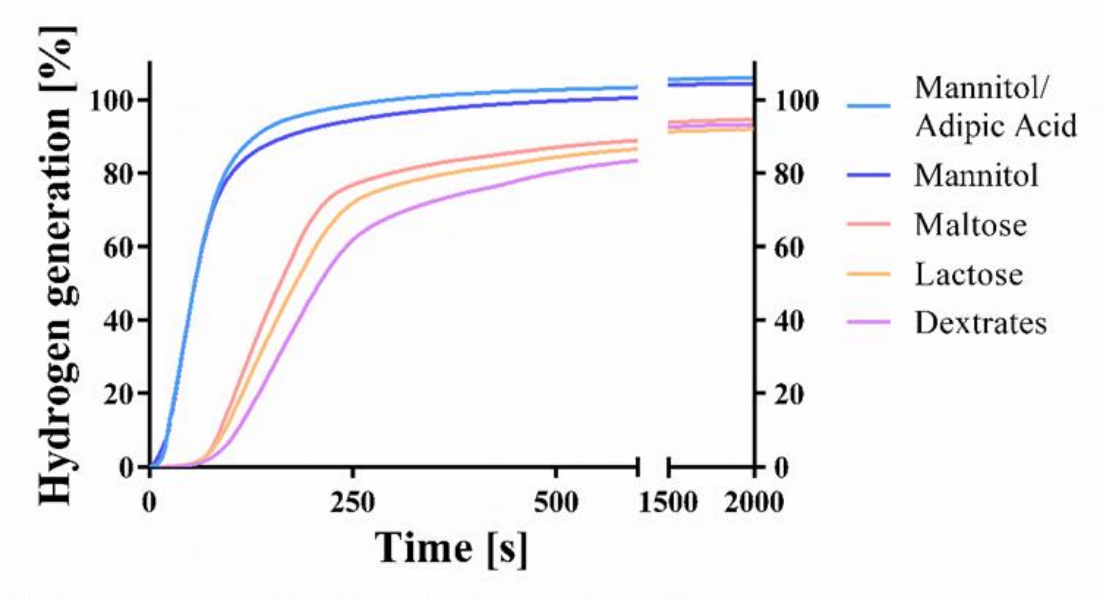

Figure 6.3. Kinetic hydrogen generation measurement (means; n = 3). Kinetics of hydrogen generation were measured using different fillers and lubricants. Means were calculated and plotted against time. SD values can be found in Table 6.2. Graphs of single fillers can be found in chapter 13.

Table 6.2. Content, kinetic hydrogen generation, and disintegration displayed as mean and (SD)

Parameter	Maltose	Mannitol	Mannitol/ Adipic acid	Lactose	Dextrates
H_2 generation (mg)	5.887 (0.027)	6.488 (0.163)	6.589 (0.129)	5.719 (0.099)	5.794 (0.110)
H_2 generation (%)	94.64 (0.43)	104.30 (2.63)	105.91 (2.08)	91.93 (1.59)	93.13 (1.76)
H_2 generation (%) excluding weight incorrectness	92.28 (0.28)	102.80 (2.93)	103.89 (1.77)	92.23 (1.61)	92.61 (1.18)
Mg; complexometric titration (mg)	76.13 (0.36)	78.02 (1.92)	78.70 (1.13)	75.40 (1.28)	80.16 (1.46)

Mg; complexometric titration (%)	101.51 (0.48)	104.03 (2.56)	104.94 (1.51)	100.54 (1.70)	106.88 (1.95)
Partial disintegration into granular particles (mm:ss)	03:11 (00:06)	01:05 (00:04)	01:08 (00:05)	03:04 (00:05)	03:11 (00:06)
Disintegration time (mm:ss)	03:58 (00:25)	01:12 (00:03)	01:23 (00:03)	05:00 (00:32)	04:17 (00:15)
Porosity by Hg intrusion (%)	10.33 (0.29)	13.13 (0.68)	14.40 (0.12)	12.52 (0.23)	11.40 (0.79)
Median pore radius (μm)	0.1912 (0.0124)	0.0502 (0.0073)	0.0745 (0.0294)	0.1330 (0.0143)	0.1545 (0.0151)

Table 6.3. f2 comparison. Kinetic hydrogen generation measurements of tablet batches manufactured with different excipients were compared with the f2 comparison; according to SUPAC guidelines release profiles of tablets with a f2 value between 50 and 100 are considered similar.

Excipient	**Maltose**	**Mannitol**	**Mannitol/ Adipic Acid**	**Lactose**	**Dextrates**
Maltose		16.08	16.18	64.24	44.18
Mannitol	16.08		85.95	15.21	13.60
Mannitol/ Adipic Acid	16.18	85.95		15.62	14.59
Lactose	64.24	15.21	15.62		54.65
Dextrates	44.18	13.60	14.59	54.65	

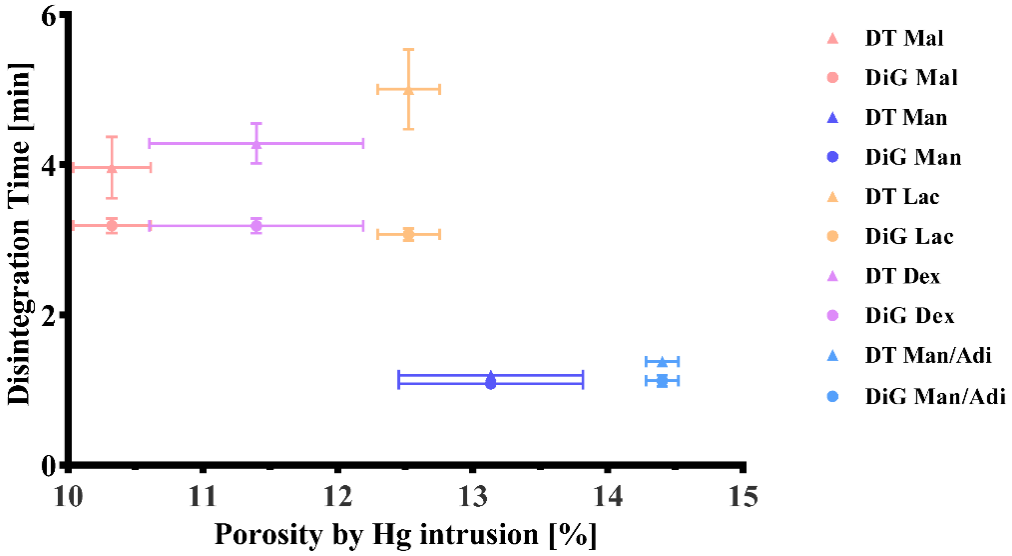

Figure 6.4. Disintegration time vs. porosity. Experiments were conducted in a beaker with 200 mL of water as described in the monograph of effervescent tablets in the Ph. Eur. 10.1/0478. Primary and secondary endpoints of disintegration were determined visually. The first measurement was taken when the tablet had partially disintegrated into granular particles (DiG = partial disintegration into granular particles). The second measurement was taken as the endpoint, after the tablet and the particles had disintegrated completely (DT = disintegration). These values were recorded for different fillers (Mal = maltose; Man = mannitol; Lac = lactose; Dex = dextrates; Man/Adi = mannitol/adipic acid) and were plotted against the porosity of the tablets, which was measured by mercury intrusion.

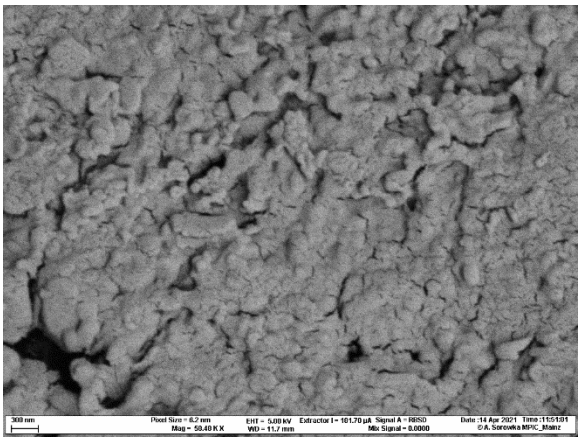

(**a**) maltose-based batch (cf: 40 kN; mag: 58,480×; mpr: 0.1912 ± 0.0124 μm)

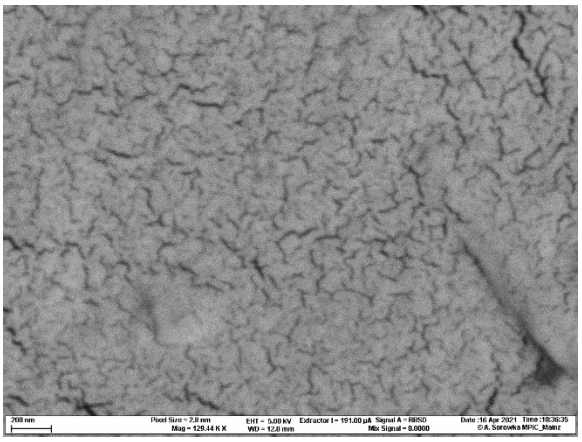

(**b**) mannitol-based batch (cf: 40 kN; mag: 129,440×; mpr: 0.0502 ± 0.0073 μm)

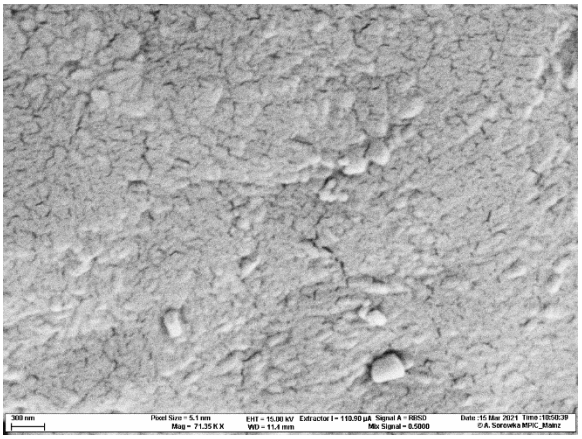

(**c**) the mannitol/adipic acid-based batch (cf 25 kN; mag: 71,350×; mpr: 0.0745 ± 0.0294 μm)

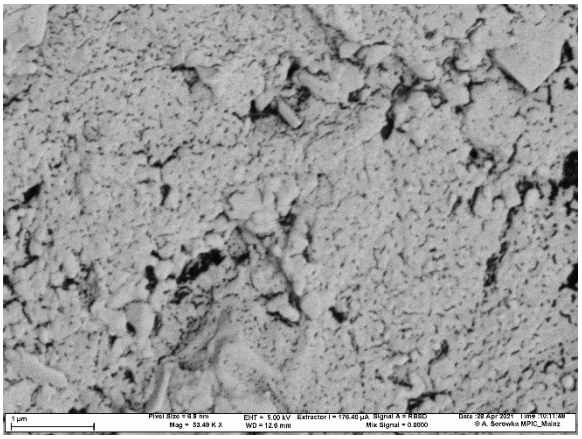

(**d**) he lactose-based batch (cf 40 kN; mag: 53,490× ; mpr: 0.1330 ± 0.0143 μm)

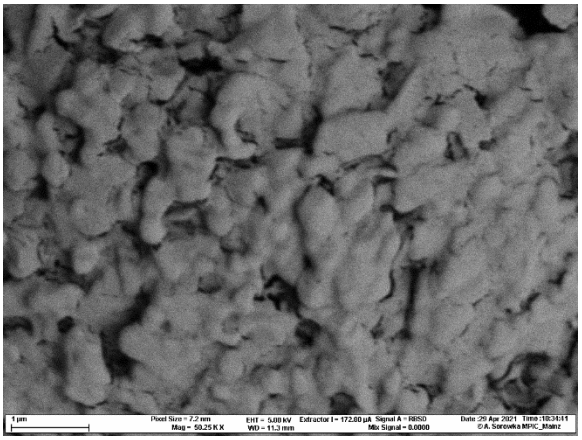

(**e**) the dextrates based-batch (cf: 40 kN; mag: 50,250×; mpr: 0.1545 ± 0.0151 μm)

Figure 6.5. Scanning electron microscope pictures of different saccharide-based tablet surfaces (cf = compaction force; mag = magnification, mpr = median pore radius according to

mercury intrusion (mpr) The analysis confirmed that pores were of the sizes expected based on the mercury porosity measurement(Table 6.2.).

6.4.3. Tablet Hardness

To evaluate the hardness of the tablets, the three-point bending test was performed, and the friability of uncoated tablets and their resistance to crushing were measured (Figure 6.6., Table 6.4.). The mannitol/adipic acid tablets showed the lowest values in all tests (crushing strength = 72.3 ± 4.4 N; tensile strength = 0.513 ± 0.031 N/mm^2; three-point bending test peak force = 28.0 ± 2.1 N), which is not surprising, considering that the compaction force had to be decreased to 25 kN in this batch to avoid capping. All other batches were compacted with a compaction force of 40 kN. The dextrates-based tablets showed significantly higher values than the other batches (crushing strength = 147.4 ± 7.3 N; tensile strength = 1.204 ± 0.063 N/mm^2; three-point bending test peak force = 46.3 ± 4.5 N). Moreover, it was the only batch that passed the test of friability showing 0.72% mass loss. None of the other tablets passed the friability test, which is to be expected for effervescent tablets due to their weights and tensile strengths.

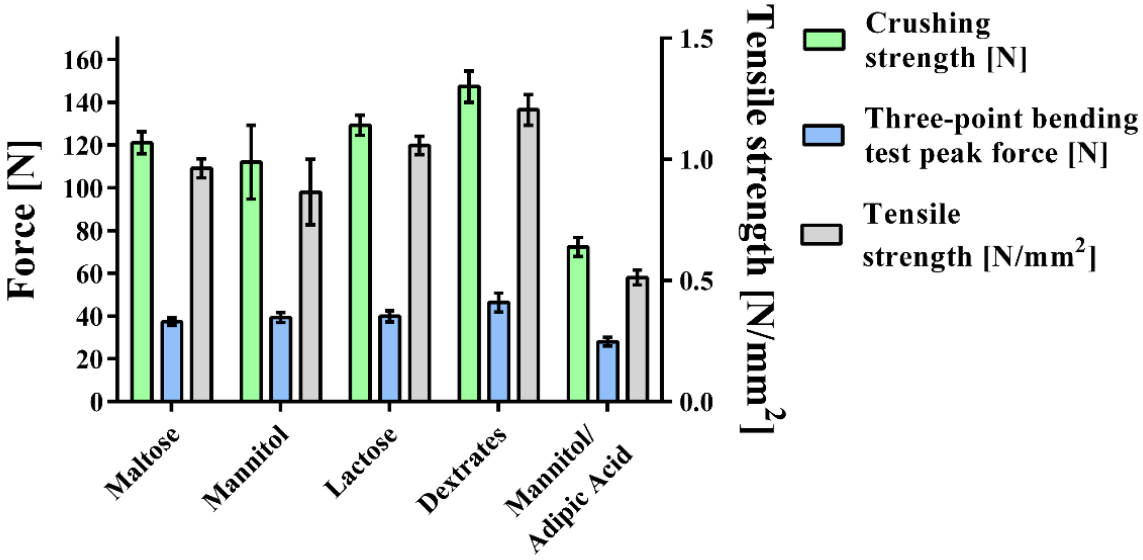

Figure 6.6. Tablet hardness: crushing strength was measured, and the three-point bending test was performed for each formulation (*n* =10). Tensile strength was calculated from the results.

Table 6.4. Tablet hardness characteristics displayed as mean and (SD).

Parameter	Maltose	Mannitol	Mannitol/ Adipic Acid	Lactose	Dextrates
Crushing strength (N)	121.1 (5.1)	112.0 (17.3)	72.3 (4.4)	129.3 (4.7)	147.4 (7.3)
Tensile strength (N/mm^2)	0.963 (0.039)	0.865 (0.135)	0.513 (0.031)	1.057 (0.038)	1.204 (0.063)
Three-point bending test peak force (N)	37.4 (1.7)	39.3 (2.3)	28.0 (2.1)	39.8 (2.6)	46.3 (4.5)
Friability (%)	broken tablets	broken tablets	not tested	broken tablets	0.72
True density (g/mL)	1.624 (0.13)	1.581 (0.007)	1.569 (0.003)	1.603 (0.025)	1.633 (0.006)
Weight (g)	1.545 (0.011)	1.537 (0.019)	1.631 (0.007)	1.495 (0.005)	1.515 (0.011)

6.4.3.1. Three-Point Bending Test

The dextrates-based batches show the highest peak force of 46.3 ± 4.5 N (Figure 6.6., Table 6.4.), which is significantly higher than the peak forces of the three other batches that were compacted with a compaction force of 40 kN. The peak forces for these batches were the following: 39.8 ± 2.6 N (lactose-based), 39.3 ± 2.3 N (mannitol-based), 37.4 ± 1.7 N (maltose-based). Within these batches, there were no significant differences in the measured peak forces. The lowest peak force was measured for the mannitol/adipic acid-based batch that was compacted with a force of 25 kN (28.0 ± 2.1 N).

6.4.3.2. Friability of Uncoated Tablets

The dextrates-based batch showed a friability value of 0.72% (Table 6.4.). For the other three batches, no values could be calculated, since tablets broke during the friability test. During the test of the lactose-based batch one tablet broke, three tablets from the mannitol-based batch broke, and during the test of the maltose-based batch five tablets broke. Since the mannitol/adipic acid tablets showed the lowest values during the other hardness tests, and since broken tablets could therefore be expected for this batch as well, the friability test was omitted for this batch.

6.4.3.3. Resistance to Crushing

As in the other hardness tests, the dextrates-based batch showed the highest values for this test as well, breaking at significantly higher applied force (147.4 ± 7.3 N) than the other batches (Figure 6.6., Table 6.4.). Once more, the lactose-based batch showed the second highest values (129.3 ± 4.7 N). However, this is not significantly higher than the values of the maltose-based batch (121.1 ± 5.1 N). The mannitol-based batch showed the lowest values (112.0 ± 17.3 N) of the batches that were compacted with 40 kN, significantly lower than the value for the lactose-based batches. Comparing the mannitol-based batch to the maltose-based batch, there was no significant difference. For the batch based on mannitol/adipic acid, a significantly lower breaking force was measured (72.3 ± 4.4 N).

6.4.3.4 Tensile Strength

The tensile strength results for the different tablets mirrored those of resistance to crushing (Figure 6.6., Table 6.4.). Dextrates-based tablets showed the highest values for tensile strength (1.204 ± 0.063 N/mm^2), which were significantly higher than the values for lactose-based tablets (1.057 ± 0.038 N/mm^2). There was also a significant difference between lactose- and maltose-based tablets (0.963 ± 0.039 N/mm^2). Mannitol-based batches were characterized by significantly lower tensile strengths than the previously mentioned ones (mannitol (0.865 ± 0.135 N/mm^2) and mannitol/adipic acid (0.513 ± 0.031 N/mm^2)).

6.4.4. Stability

6.4.4.1. Dynamic Vapor Sorption (DVS)

Effervescent formulations are usually very moisture-labile and require careful control of all manufacturing processes and conditions [36]. The formulations' affinity and lability to humidity during processing and storage was evaluated with dynamic vapor sorption measurements. The sample of the mannitol-based effervescent granule mixture was found to have a high affinity for water. The initial mass of the sample (m_0) was 16.0413 mg. The highest value in the first cycle (m_{max1}) was 25.1013 mg, which was a mass increase of 56.5% compared to m_0 (Figures 6.7. and 6.8.). After the first desorption cycle, the lowest value was 17.5162 mg (m_{end1}) which is 109.2% of m_0. In the second cycle, the weight increased to 23.2405 mg (m_{max2}) which was a mass increase of 44.9% over m_0 and an increase of 32.7% relative to the mass after the first cycle m_{end1}. The mass at the end of the second cycle (m_{end2}) was 17.5107 mg, 109.2% of m_0.

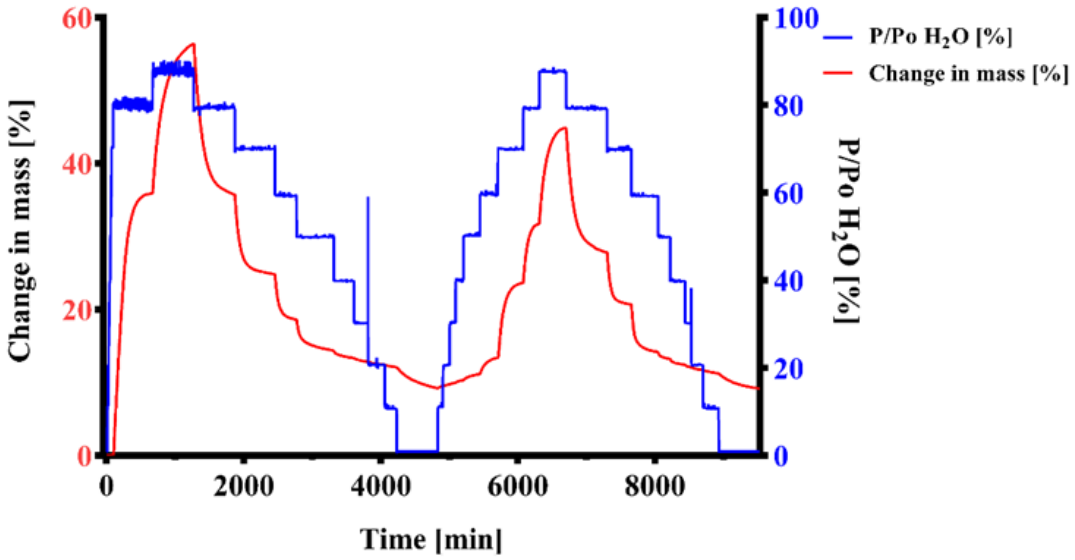

Figure 6.7. Dynamic vapor sorption change in mass analysis. An effervescent granule formulation containing mannitol as filler was investigated. Two cycles of absorption and desorption were performed, 0%-90%-0% P/P_0 in 10% stages. The change in mass was recorded over time. A mass change dm/dt = 0.002% min^{-1} or 600 min (whichever occurred first) were selected as criteria for changing the humidity stage.

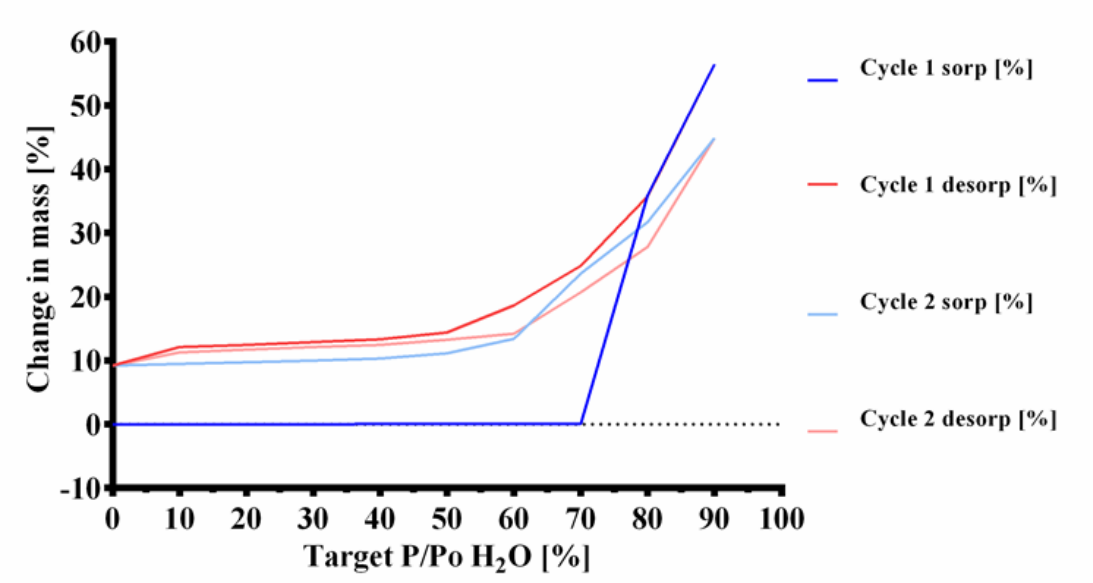

Figure 6.8. Dynamic vapor sorption isotherm analysis. Two sorption and desorption cycles (sorp = sorption; desorp = desorption) of an effervescent granule formulation containing mannitol as a filler from the same DVS measurement as in Figure 6.7. are displayed.

6.4.4.2. Bulk Stability Testing

The total amount of generated hydrogen (Figure 6.8. and Table 6.5.) was not significantly influenced by storage time from starting point t_0 up to 14 days, and the differences were not significant. However, a slightly decreasing trend in hydrogen generation is visible. After 8 weeks, the amount of generated hydrogen decreased significantly. The tablets remained stable under the tested conditions for at least 14 days, but hydrogen generation was slower after longer storage times. f2 comparisons (Table 6.6.) of tablets which were not stored (t_0) or stored for 24 h can be considered similar. With increasing storage time, the hydrogen generation rate decreased, and the samples cannot be considered similar regarding f2 comparison. Tablet weight increased significantly at each sampling time.

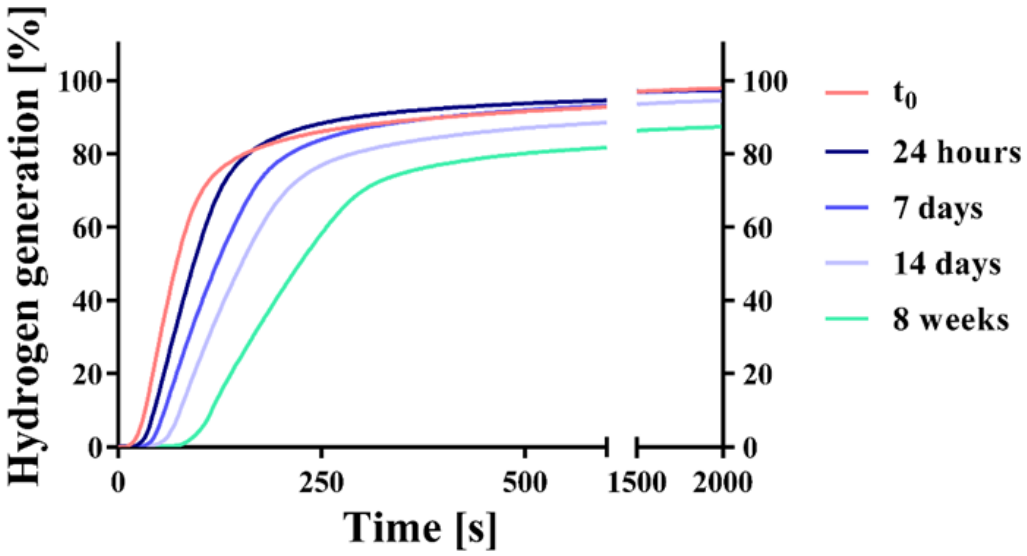

Figure 6.8. Kinetic hydrogen generation measurement (means; *n* = 3). Kinetics of hydrogen generation of unpacked tablets of the mannitol/adipic acid-based batch were measured at the starting point t_0, and after 24 h, 7 days, 14 days, and 8 weeks of storage in a constant climate chamber (25 °C and 60% RH). Single graphs of the storage times can be found in chapter 13.

Table 6.5. Hydrogen generation and weight gain of the bulk stability samples expressed as mean and (SD)

Storage Time	H_2 Generation (%)	Weight Gain (%)
No storage	97.86 (2.98)	-
24 h	97.55 (3.04)	0.504 (0.032)
7 days	97.31 (1.24)	1.029 (0.005)
14 days	94.52 (1.84)	1.289 (0.092)
8 weeks	87.33 (1.47)	2.039 (0.161)

Table 6.6. f2 comparison. Kinetic hydrogen generation measurements of the bulk stability samples were compared with the f2 comparison; according to SUPAC guidelines release profiles of tablets with a f2 value between 50 and 100 are considered similar.

Storage Time	t_0	24 h	7 Days	14 Days	8 Weeks
t_0		51.41	36.07	26.77	17.00
24 h	51.41		45.65	31.54	19.49
7 days	36.07	45.65		48.63	26.76
14 days	26.77	31.54	48.63		38.95
8 weeks	17.00	19.49	26.76	38.95	

6.3.5. Granular Flow Properties

Based on their angle of repose values, the granules showed good (maltose- and dextrates-based granules) to fair flow (lactose- and mannitol-based) [77]. The mannitol/adipic acid-based granule was not measured as it showed insufficient powder flow for the measurement. Flow through orifice values ranging from 7.9 s/100 g (maltose-based granule) to 11.5 s/100 g (lactose-based granules) were recorded. For mannitol-based batches, the powder flow had to be induced. The granules showed good (maltose-, dextrates-, and lactose-based granules) to fair (both mannitol-based granules) Hausner ratios and compressibility indices [77]. The granular characteristics are presented in Table 6.7..

Table 6.7. Granular characteristics displayed as mean and (SD)

Parameter	Maltose	Mannitol	Mannitol/ Adipic Acid	Lactose	Dextrates
Angle of repose (°)	32.47 (0.3)	39.3 (0.8)	-	35.7 (0.6)	33.4 (1.0)
Flow through an orifice (s/100 g)	7.9 (0.1)	-	-	11.5 (0.5)	9.6 (0.0)
Bulk density (g/mL)	0.872 (0.000)	0.795 (0.005)	0.803 (0.005)	0.869 (0.012)	0.855 (0.006)
Tapped density (g/mL)	0.974 (0.000)	0.949 (0.000)	0.991 (0.008)	1.005 (0.008)	0.970 (0.007)
Hausner ratio	1.12 (0.00)	1.19 (0.01)	1.23 (0.01)	1.16 (0.03)	1.13 (0.01)
Compressibility index (%)	10.5 (0.0)	16.3 (0.5)	18.9 (0.5)	13.5 (1.6)	11.8 (0.6)
Particle size d10 (µm)	130.9 (11.9)	28.1 (3.5)	14.0 (2.6)	56.4 (3.0)	90.5 (12.6)
Particle size d50 (µm)	463 (22.6)	461.9 (18.4)	457.28 (15.2)	429.9 (12.3)	458.3 (23.7)
Particle size d90 (µm)	1411.4 (117.4)	1428.6 (40.3)	1430.6 (41.6)	1507.8 (40.0)	1500.2 (116.1)
Loss on drying (%)	1.80 (0.06)	1.03 (0.11)	1.02 (0.18)	1.29 (0.11)	4.32 (0.20)

6.5. Discussion

6.5.1. Content, Kinetic Hydrogen Generation, and Disintegration

Mannitol-based formulations generated the highest amount of hydrogen and showed the quickest disintegration and hydrogen generation (Figures 6.2.-6.4.). Since mannitol is clearly not the most soluble of the investigated binders [59, 78, 79], the major factor responsible for this phenomenon was the porosity of the tablets (Figure 6.2.; Table 6.2.). Mannitol-containing tablets showed the highest porosity of all formulations, although this result can be partly attributed to the lower compaction force that was used for the mannitol/adipic acid-based batch in order to avoid capping. A higher porosity is commonly associated with a quicker disintegration time [80]. The median-sized pores measured by mercury porosimetry were confirmed with scanning electron microscopy (Figure 6.5. a)-e)).

The rapid disintegration of the mannitol-based batches (Figure 6.2.; Table 6.2.) can also be attributed to the low inter- and intragranular binding forces, which are the weakest among all fillers, as indicated by the lower hardness values of the tablets and the significantly higher amounts of fine particles (particle size d10: 14.0 ± 2.6 µm for mannitol/adipic acid-based tablets; 28.1 ± 3.5 µm for the mannitol-based batch, shown in Table 6.2.. It is to be expected that the mannitol-based batches show the highest total porosities, while their median pore radius is significantly lower. It was previously shown that spray-dried mannitol processed by dry granulation yields tablets with favorable disintegration and acceptable hardness values, which is supported by our results [81]. The low SD of the batches' hydrogen generation and magnesium content (Table 6.2.) shows that dry granulation is suitable for avoiding the segregation of excipients during mixing that was observed during previous experiments using direct compaction. Moreover, no recycling and sieving of fines of the granules were performed, because this can have a negative impact on content uniformity [82]. The large differences between partial disintegration into granular particles and the complete disintegration time (Figure 6.1.) suggest that strong deformation and bonding occurred during the dry granulation process of the maltose-, lactose-, and dextrates-based formulations resulting in high intragranular binding forces. The extra granular bonds that were formed during the tableting disintegrated first, most likely on the contact surfaces of the respective granules and Citrocoat® N.

The different values for the hydrogen generation and the magnesium content determined via complexometric titration (Table 6.2.) show that only mannitol-based batches reacted completely. The differences were probably caused by an incomplete reaction of magnesium, which could be related to the following observation: after the disintegration of the tablets manufactured with sodium stearyl fumarate, grey foam forms on top of the water, which resembles the color of the metallic magnesium particles that are most likely covered with sodium stearyl fumarate and are not able to react chemically. As a consequence of the medium's slightly acidic pH-value, the stearyl fumarate anion is at least partly protonated, which decreases the agent's solubility. The mannitol-based batches either do not contain sodium stearyl fumarate (mannitol/adipic acid-based batch) or else the disintegration takes place very quickly (mannitol) and the effect is not manifested. In this case, the time window available for the protonated stearyl fumarate to cover the surface of the magnesium particles and consequently to partly prevent the effervescent reaction before they have dissolved, is smaller.

6.5.2. Tablet Hardness

During formulation development it became clear that manufacturing tablets with good hardness values would be a challenging task (Table 6.4.). Roller compaction causes a reduction in the tabletability of the granules compared to direct compression. However, roller compaction was necessary in order to avoid segregation of the powder particles. The phenomenon of loss of tabletability during roller compaction is known as work hardening and is considered to stem from increased resistance to deformation of a material during multiple compaction cycles [83-86]. Some authors view particle size enlargement and decreased surface area available for bonding during compaction as the main reasons for the loss of tabletability [87] while others [88, 89] suggest that both mechanisms play a role. However, it is crucial to maintain a large enough particle size of the granules in order to avoid segregation after blending with Citrocoat® N, which consists mainly of large particles (d50 = 405.3 µm) of high density. Moreover, a decreased specific surface area of the large particles is beneficial for the lubrication, since it can be expected that the effectiveness of the lubricant depends on the size of the particular surface area that is necessary to be covered [90]. Wet granulation was not considered as a good approach, because a high residual water content in the granules could

exacerbate sticking of the formulation during tableting, as well as trigger the effervescent reaction.

In order to improve the hardness parameters (Figure 6.6.; Table 6.4.), an increased amount of diluent could be beneficial, since these substances show beneficial compactability characteristics. With reference to Heckel's equation [91] to describe compaction mechanisms, the value of yield pressure was introduced [92] and values for yield pressure were characterized. Low values suggest soft and plastically deforming materials, while high values suggest brittle, fragmenting behavior and hard materials [93-95]. The yield pressure values depend on the experimental conditions so the values that are mentioned in different studies serve only as a rough guide [96]. Maltose is known to provide very good flow properties and shows good compactability [97]. Mannitol also shows good compactability [98], is moderately hard as a material, and shows a brittle compaction behavior, which is reflected by yield pressure values ranging from 132–135 MPa [94]. This is also reflected by its relatively lower lubricant sensitivity, which is a typical property of fragmenting materials, since they create new unlubricated bonding sites during fragmentation [99]. Lactose is a moderately hard to hard material according to its yield pressure of 174–233 MPa [100], which is known to consolidate with an initial fragmentation step and deform plastically on newly created bonding sites and within amorphous regions [101, 102]. Dextrates shows a more plastic deformation (yield pressures: 67–166 MPa) as well as some fragmentation during compaction, properties which depend on the formulation before compaction, and the material can be compacted into tablets of high strength [103-106]. According to its yield pressure dextrates can be classified as moderately hard. Hence, it can be concluded that a larger amount of the investigated saccharide fillers would increase the hardness of the formulations although their deformation mechanisms differ slightly. Specifically, the addition of spray-dried maltose to a granular mannitol blend has proven to increase tablet hardness; furthermore, owing to its spherical morphology and good compactability, decreased capping and enhanced flow properties have also been attributed to this filler [97]. However, most studies have investigated directly compactable or wet granulated materials. Based on the particle sizes of the roller-compacted granules, it can be concluded that the mannitol-based batches showed a lower compactability and/or a higher granular fragmentation during the milling process since they exhibited significantly lower d10 particle size values. The lower hardness values and the high number

of fine particles correspond excellently with the fact that mannitol-based batches show the highest total porosity while also showing the lowest average pore size.

To improve tablet hardness, especially of the mannitol/adipic acid-based batch, the citric acid excipient Citrocoat® N (granule with citric acid core coated with a monosodium citrate shell) could be swapped for a compound excipient like citric acid DC, directly compactable citric acid with maltodextrin coating. However, sticking during compaction, which was resolved by the use of Citrocoat® N, would reoccur. Another possibility would be to combine the investigated saccharide fillers in a DOE experiment to find an optimal compromise between improved hardness, good disintegration, and hydrogen generation. The inclusion of an extra granular dry binder might also be useful in this regard. The hardness tests of the different batches showed clearly that the dextrates-based batch was the most favorable filler with respect to hardness parameters.

6.5.3. Dynamic Vapor Sorption (DVS)

In the first stages of humidity (0–70% P/P_0 H_20 at 25 °C) no mass changes greater than the near-equilibrium state criterium ($dm/dt = 0.002\%\ min^{-1}$) were observed (Figures 6.7. and 6.8.). In previous runs, the sorption started already at 70% P/P_0 H_20. In the later stages, starting from 80% P/P_0 H_20 a large increase of mass was observed. Up to 80% P/P_0 H_20 at 25 °C only physisorption occurs, with bulk sorption becoming subsequently dominant [107, 108]. This indicates that the hygroscopic Citrocoat® N had a higher resistance towards humidity than regular anhydrous citric acid, which is known to start sorption of water at 62% P/P_0 H_20 at 25 °C [109]. However, the large maximal mass (m_{max1} = 156.5% of m_0) and the mass at the end of the measurement (m_{end2} = 109.2% of m_0) show that the powder has a high affinity for humidity. The gap between the peak values for m_{max} (m_{max1} = 156.5% and m_{max2} = 144.9%) of the two cycles is too large to be explained by gas generation on account of the low percentage by mass of magnesium in the tablet. The most probable explanation lies in the possible partial dissolution and recrystallization at interparticulate interfaces, which would result in a reduced total surface area available for water sorption. If there was no chemical reaction, two similar sorption and desorption cycles would be expected. No chemical change takes place after cycle 1, since a regular sorption and desorption cycle with $m_{end1} \approx m_{end2}$ can be observed. Comparison of the sorption cycles reveals that, during the second cycle of sorption, the mass of the powder increased at earlier humidity stages (4.17% mass increase at 60% P/P_0 H_20)

than in the first cycle (0.04% mass increase at 60% P/P_0 H_20). This indicates that the protective monosodium citrate coating from Citrocoat® N has been disrupted most probably either through partial dissolution in the adsorbed water film, or through a change in the crystal form, or a combination of both.

6.5.4. Bulk Stability Testing

Data from the dynamic vapor sorption experiments suggested that the investigated mannitol/adipic acid-based formulation was stable up to 25 °C; 60% RH for the selected stability criteria dm/dt = 0.002% min^{-1} (Figures 6.7. and 6.8.). During the bulk stability experiment (Figure 6.9., Table 6.5.) the tablets were exposed to these conditions for up to 8 weeks. During this time, the tablets continuously increased in weight through water sorption. However, the amounts of water taken up were very low and did not cause an extensive reaction in the tablet, at least not in the first 14 days. Upon exposure to humidity, magnesium reacts to form magnesium hydroxide ($Mg(OH)_2$), which passivates its surface [24, 71-76]. $Mg(OH)_2$ is not water-soluble so the surface has to be reactivated. Low pH values as well as organic ligands like citrate or ascorbate are known to enhance the dissolution of $Mg(OH)_2$ and thereby restore the active magnesium surface. Since the amount of generated hydrogen, as well as the rate of generation, decreased during storage time it can be expected that those magnesium surfaces exposed to the gaseous environment (particularly those near the tablet surface) were markedly passivated. This explains the slight reduction in hydrogen generated as well as the decreased hydrogen generation rate, since the passivated surfaces have to be reactivated for the effervescent reaction to start. Furthermore, potential partial solution and recrystallization of Citrocoat® N could lead to a decrease in the specific surface area of the tablet available for effervescent reaction. The significantly lower hydrogen generation after 8 weeks demonstrates that the reaction continues under these conditions (25 °C; 60% RH), although it is very slow. During the whole duration of exposure to these conditions, the tablets continued to gain weight by water vapor sorption, which enabled the continuation of the reaction. In contrast to conventional effervescent tablets, where additional water is a byproduct of their effervescent reaction [26], the effervescent hydrogen-generating tablets do not generate additional water. Without this autocatalytic reaction enhancement, the effervescent hydrogen-generating tablets could be regarded as slightly less moisture-labile than similarly manufactured conventional effervescent tablets. The experiment clearly showed that the tablets need adequate packaging

and controlled environmental conditions for processing and packaging of the tablets and the intermediate products. For primary packaging, we recommend plastic tubes with drying agents in the cap or aluminum/aluminum (alu/alu) blister packs in case that a single unit packaging is preferred. Both options would offer sufficient moisture protection.

6.5.5. Granular Flow Properties

Granule flow was sufficient for subsequent tablet manufacturing (Table 6.7.). The tablets are characterized by low SD in magnesium content and weight deviation (Tables 6.2. and 6.4.). The mannitol-based batches exhibited an inferior powder flow, which is probably related to their high number of fine particles (see d10 particle size values). The batch lubricated with adipic acid (d50 value: < 15 µm) was particularly affected since its level of lubricant is much higher (10% adipic acid addition compared to 0.5% for the other batches). However, the good (maltose-, dextrates-, and lactose-based granules) to fair (both mannitol-based granules) Hausner ratios and compressibility indices as well as the high bulk density ensured a constant filling process of the die of the tablet press.

7. Dynamic vapor sorption investigations of effervescent hydrogen-generating granules

7.1. Introduction

In this chapter, dynamic vapor sorption investigations were performed on three effervescent formulations. Three formulations based on a mannitol/adipic acid-based granule that was prepared as described in chapters 6.3.4 and 6.3.5. were investigated. Three different citric acid excipients were blended with this granule and their impact on stability during dynamic vapor sorption measurements was evaluated. One citric acid powder, a coarser citric acid granule and a coated citric acid granule were evaluated.

7.2. Materials:

Magnesium powder -325 mesh, 99.8% was purchased from Alfa Aesar (Heysham, England). Citrocoat® N (granule with citric acid core coated with a monosodium citrate shell) was kindly gifted by Jungbunzlauer Suisse AG (Basel, Switzerland). L(+)-ascorbic acid was purchased from Carl Roth GmbH + Co. KG (Karlsruhe, Germany). Mannogem EZ® (mannitol) was kindly donated by Spi Pharma (Wilmington, USA). The three following excipients were generously donated by Merck KGaA (Darmstadt, Germany): Adipic acid Emprove® Essential, citric acid anhydrous powder Emprove® Essential and citric acid anhydrous fine granular Emprove® Essential.

7.3. Methods:

A granule (batch MR009-2_6) containing magnesium, mannitol and ascorbic acid was manufactured following the description roller compaction/dry granulation in section 6.3.4. Afterwards the ribbons were milled in a U5 Quadro Comil by Quadro Engineering Corp. (Waterloo, Canada) as previously described in section 6.3.5 (Dry cone milling). After that, either Citrocoat® N, citric acid anhydrous powder, Emprove® Essential or citric acid anhydrous fine granular Emprove® Essential was added using a Turbula® shaker mixer T 2 F (Willy A. Bachofen GmbH, Muttenz, Switzerland), following the description in section 6.3.6 (Blending of dry granules with Citrocoat ® N). To each of the blends adipic acid was added following the description 6.3.7. (Addition of lubricant) using a Turbula® shaker mixer T 2 F (Willy A. Bachofen GmbH, Muttenz, Switzerland). Stochiometric quantities of each excipient included in the respective samples are presented in Table 7.1.

Table7.1. Stochiometric quantity of each excipient included in the measured samples

Sample	MR009-2_6 [g]	Citrocoat® N [g]	Citric acid powder [g]	Citric acid fine granular [g]	Adipic acid[g]
1	51.97	48.15			10.15
2	51.95		48.08		10.07.
3	51.96			48.16	10.13

The dynamic vapor sorption measurements were conducted with a DVS Advantage (Surface Measurement Systems Ltd., London, United Kingdom). Previously solvents were removed from the weighing pans using a 200°C/30 min preheat program. The sample was weighed inside the DVS device and the samples were exposed to 25°C and 0% P/P_0 H_2O for 4h to remove adsorbed water from the sample. Afterwards the sample was exposed to a cycle 0%-90% P/P_0 H_2O (5% intervals) and back to 0% P/P_0 H_2O (3 steps 90% 50% and 0%). Each step was performed until an equilibrium was reached (%dm/dt= 0.002% min^{-1} or 600 min).

7.4. Results:

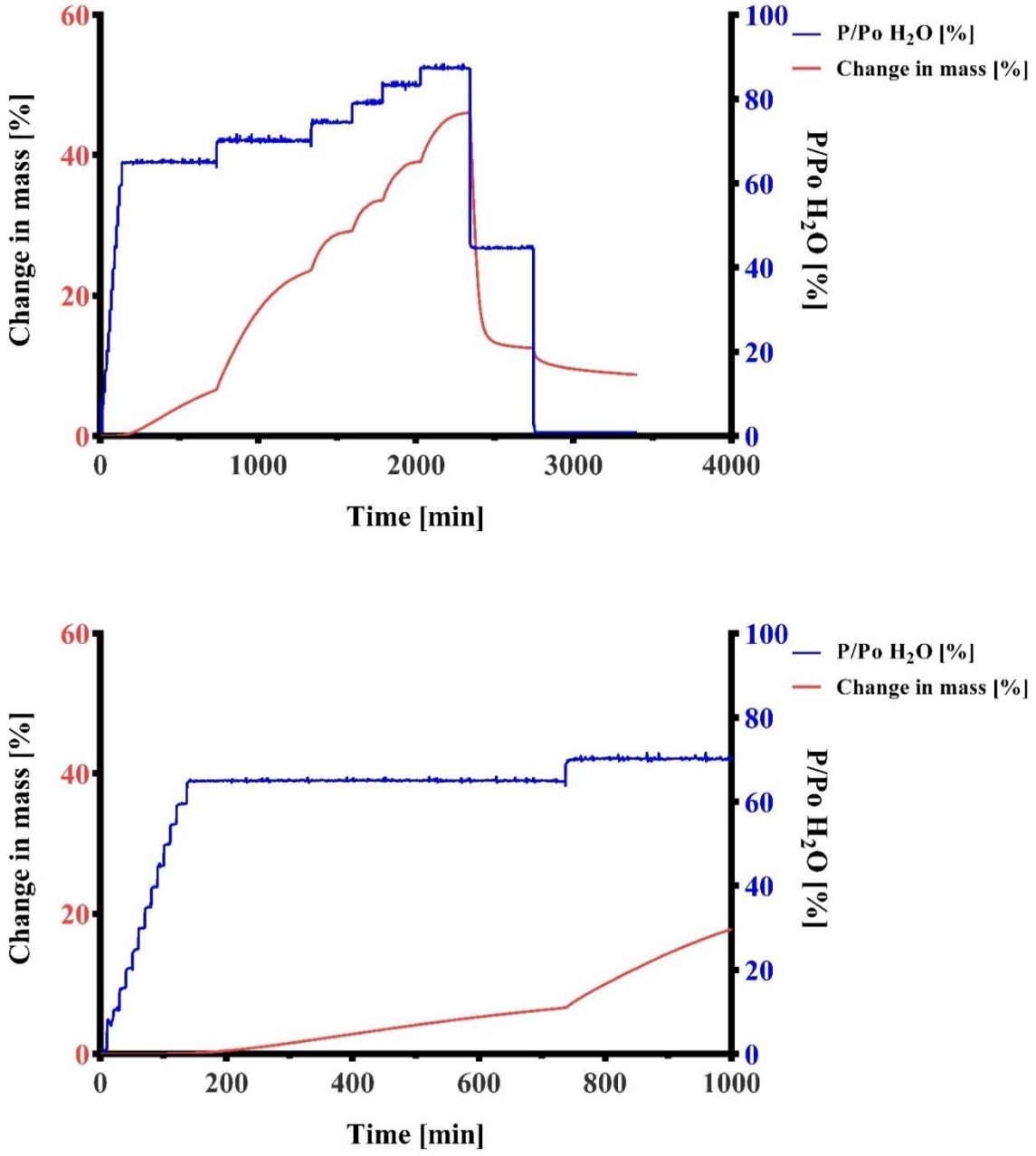

Figure 7.1. Dynamic vapor sorption change in mass analysis. An effervescent granule formulation containing Citrocoat ® N (sample 1) was investigated. A cycle of absorption and desorption was performed, 0%-90% P/P_0 H_2O in 5% stages. 90%-0% P/P_0 H_2O was performed in 3 steps (90%, 50% and 0%). The change in mass was recorded over time. The first graph shows an overview of the whole measurement, while the second graph shows a smaller time frame that focusses on the onset of the moisture uptake of the sample.

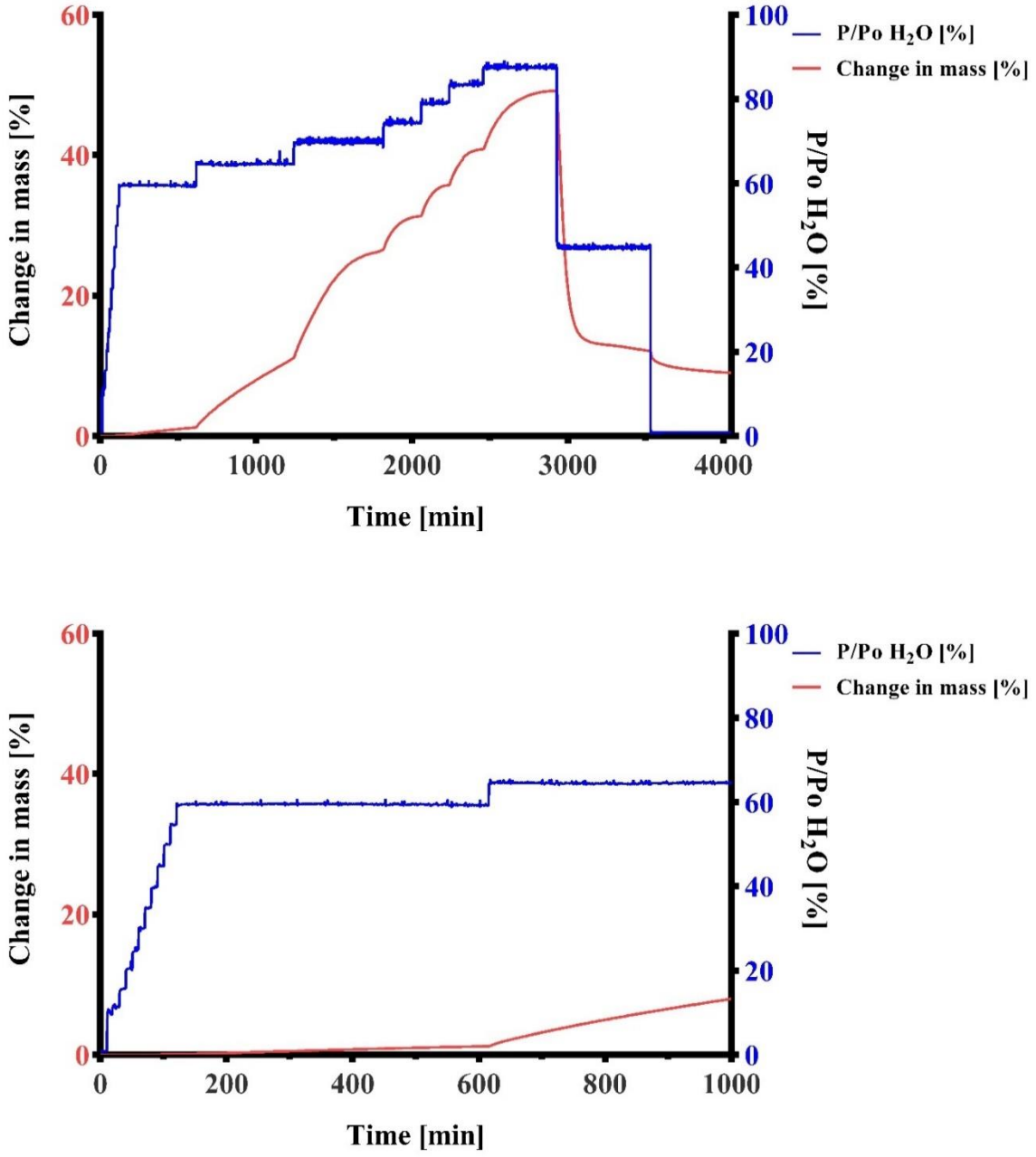

Figure 7.2. Dynamic vapor sorption change in mass analysis. An effervescent granule formulation containing citric acid anhydrous powder (sample 2) was investigated. A cycle of absorption and desorption was performed, 0%-90% P/P_0 H_2O in 5% stages. 90%-0% P/P_0 H_2O was performed in 3 steps (90%, 50% and 0%). The change in mass was recorded over time. The first graph shows an overview of the whole measurement, while the second graph shows a smaller time frame that focusses on the onset of the moisture uptake of the sample.

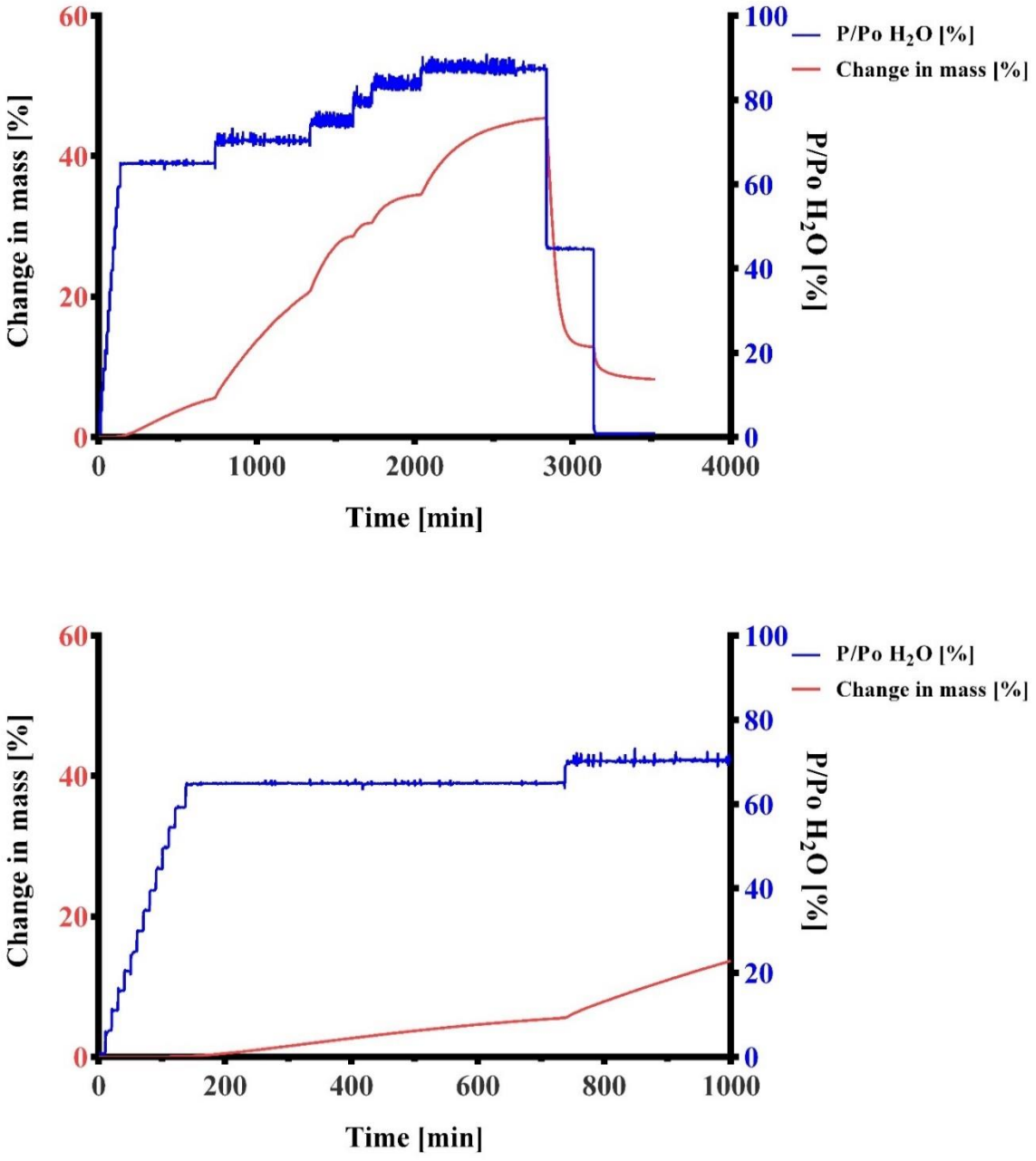

Figure 7.3. Dynamic vapor sorption change in mass analysis. An effervescent granule formulation containing citric acid anhydrous fine granular (sample 3) was investigated. A cycle of absorption and desorption was performed, 0%-90% P/P_0 H_2O in 5% stages. 90%-0% P/P_0 H_2O was performed in 3 steps (90%, 50% and 0%). The change in mass was recorded over time. The first graph shows an overview of the whole measurement, while the second

graph shows a smaller time frame that focusses on the onset of the moisture uptake of the sample.

No blend increased its weight by more than 0.05% during the stages of 0-55% P/P_0 H_2O. The citric acid powder-based sample 2 (Figure 7.2.) shows the earliest water sorption of all three blends. It already increased its weight by 1.21% at 60% P/P_0 H_2O and took longer to reach equilibrium state (criterion: %dm/dt< 0.002% min^{-1} for 10 minutes). The citric granule-based samples 1 (Figure 7.1.) and 3 (Figure 7.3.) showed no relevant mass increase during the 60% P/P_0 H_2O stage. Sample 3 increased its mass by 0.06% while it was 0.07% for sample 1. During the 65% humidity stage all batches showed a meaningful amount of water adsorption. Sample 2 increased its total weight by 10.77%, while the citric granule-based samples 3 and 1 showed much smaller amounts of adsorption (5.60% and 6.62%). None of the batches reached the equilibrium state at this stage. Instead of allowing equilibrium to be reached, the stage was terminated by the time limit of 600 min for all batches. During the 65% P/P_0 H_2O stage the granular samples 3 and 1 showed a slower adsorption of water compared to the powder-based sample 2. Their average mass change per minute was lower. Sample 3 showed the slowest mass increase by an average %dm/dt= 0.00951 % min^{-1} followed by sample 1 (average %dm/dt= 0.01126 % min^{-1}). The citric acid powder-based sample 2 showed the quickest mass increase during this stage (average %dm/dt= 0.01640 % min^{-1}). The total amounts of water adsorption were 49.19% for sample 2, 45.43% for sample 3 and 46.02% for sample 1. Most of the mass was desorbed during the desorption phase, indicating physisorption. At P/P_0 H_2O =0%, sorption masses of 8.21% (sample 3), 8.73% (sample 1) and 8.99% (sample 2) remained in the samples as bulk sorption or chemisorption.

7.5. Discussion:

The samples are very moisture labile, which was expected for effervescent granules. After an initial resistance at lower humidities, the samples adsorbed large amounts of water. Since the mass amount of citric acid is equal in all formulations it makes sense that the total mass increase during the experiment is relatively similar, while there are differences in the starting point of the sorption process and the sorption rate. This can be explained with the higher specific surface area of the smaller powder particles (sample 2 containing citric acid anhydrous powder) compared to the granular citric acid-based samples 1 and 3. Comparing the granular citric acid-based samples there are no noticeable differences. This could be attributed to the high amount of fine, milled adipic acid particles (wt%: 9.1), which were present in both blends and represented a large part of the particular accessible surface area. Adipic acid is much less hygroscopic than citric acid, which is the most hygroscopic excipient in the blend [45]. It could be possible that the influence of Citrocoat® N's protective mono sodium citrate coating is negated by the adipic acid which provides a hydrophobic accessible surface for both granules.

It can be concluded, that granular citric acid excipients show a slower rate of water adsorption, which begins in higher P/P_0 H_2O environments compared to the powder containing sample. Thus, they are less susceptible to humidity during short time intervals occurring at manufacturing and processing. However, a benefit in long term stability would need to be proven. For tablets, which have a smaller specific surface compared to powders and granules, and should therefore be more resistant towards humidity. The condition of 25°C and 60% P/P_0 H_2O, which did not lead to mass increase during the dynamic vapor sorption experiments, was identified as a condition for the investigation of the bulk stability of the tablets for longer storage intervals in a constant climate chamber.

8. Stability analysis of effervescent hydrogen-generating tablets

8.1. Introduction

Stability analysis of tablets was conducted with three identically manufactured batches. The batches were stored for up to 6 months in two constant climate chambers with long term- and accelerated stability storage conditions as suggested by the ICH.

One batch (MR010-2_7) was used for bulk stability studies. The results are described in sections 6.3.24; 6.4.4. and 6.5.4.

The two other investigated batches were packed in tubes and stored for up to six months. Hydrogen generation was frequently determined as described in section 6.3.9. (Kinetic Hydrogen Generation Measurement) and compared using f2 comparison.

8.2. Materials:

Effervescent hydrogen releasing tablets of the batches MR010-2_7, MR010-2_11 and MR010_12 were used for the stability study. All batches were manufactured identically and contained mannitol as filler and adipic acid as lubricant. A detailed list of the respective excipients can be found in table 6.1. The tablets were either packed in tubes closed with caps (tube: R344AWG cap: V344-01 / TR20,1 SPOG; Jaco - Dr. Jaeniche GmbH & Co. KG; Kehl, Germany) or as loose unpacked bulk material and stored in constant climate chambers (KBF P 240 and KBF S 240; Binder GmbH; Tuttlingen, Germany) For bulk stability studies tablets were weighed on an analytical scale (Sartorius LE225D-0CE; Sartorius AG, Goettingen, Germany).

8.3. Methods:

Methods, results and discussion of the bulk stability investigations can be found in sections 6.3.24; 6.4.4.; and 6.5.4..

Stability studies of packed tablets were performed with the batches MR010-2_11 and MR010_12 at 25°C and 60% RH (long term stability storage condition). and at 40°C and 75% RH (accelerated stability storage condition). The respective batches were compacted as described in section 6.3.8. with 25 kN compaction force. The samples of the long-term stability storage condition were stored for 4 weeks, 3 months and 6 months. The samples of the accelerated stability storage condition were stored for 3 months and 6 months. After taking

them out of the constant climate chamber at the respective sampling point and prior to storage, the samples were analyzed with the method “Kinetic hydrogen generation measurement” as described in section 6.3.9.. Measurements of the starting values (t_0) of batches MR010-2_11 and MR010_12 were performed once and were accounted as starting values for both conditions. Measurements of the starting values (t_0) of MR010-2_7 were performed as described in section 6.3.24 and used for comparison to the other batches.

IBM SPSS statistics (IBM Corporation; Armonk, NY, USA) was used for statistical calculations. The values were compared with ANOVA. Significance was assumed for p-values < 0.05.

8.4. Results

The compaction process proved to be reproducible, compaction forces were recorded and are shown in the following Figure 8.1 a)-c).:

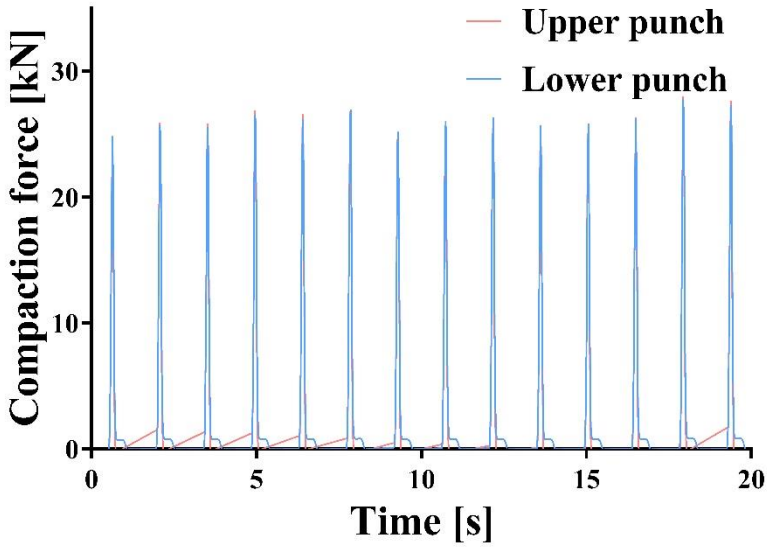

Figure 8.1.a) Tablet compaction data of batch MR010-2_7 on an instrumented Korsch EK0 eccentric tablet press. Upper and lower punch forces were recorded and plotted against time.

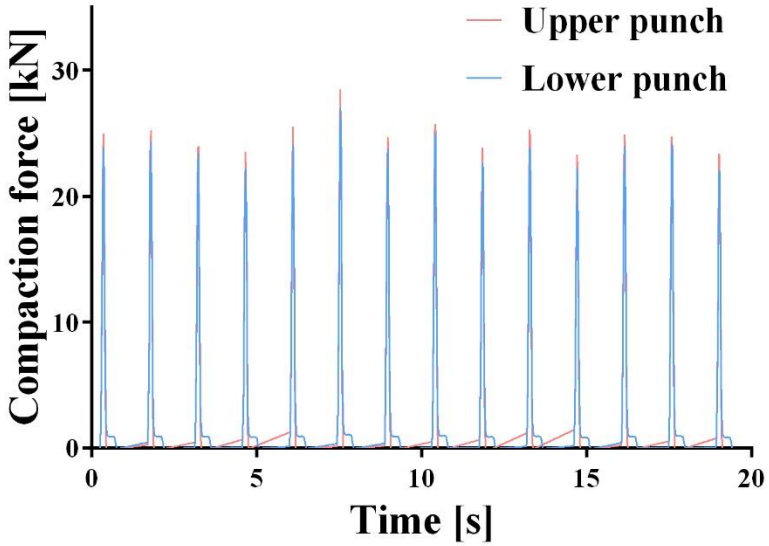

Figure 8.1.b) Tablet compaction data of batch MR010-2_11 on an instrumented Korsch EK0 eccentric tablet press. Upper and lower punch forces were recorded and plotted against time.

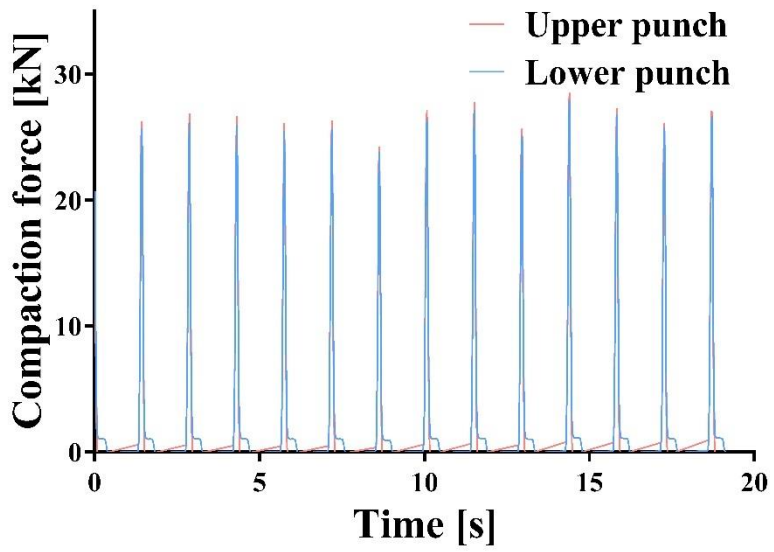

Figure 8.1.c) Tablet compaction data of batch MR010-2_12 on an instrumented Korsch EK0 eccentric tablet press. Upper and lower punch forces were recorded and plotted against time.

The mean hydrogen generation of the batches MR010-2_11 and MR010-2_12 ranged from 97.58 ± 3.00% to 103.98 ± 5.44% during the long-term stability storage condition of 25°C and 60% RH. In accelerated stability storage conditions of 40°C and 75% RH the contents ranged from 96.98 ± 1.76% to 102.22 ± 1.90%. The measured hydrogen generations can be found in Table 8.1.a)-d). The hydrogen generation kinetics of the batches MR010-2_11 and MR010-2_12 in the respective storage conditions are presented in Figure 8.2.a)-d). The measurements of similar storage time and storage conditions were compared using f2 tests. Moreover, the starting points (t_0) of the two batches were compared to the starting point (t_0) of batch MR010-2_7, which was used in the bulk stability study. Further f2 tests were calculated comparing different storage times of a single batch. The values of all compared sampling points of all batches were always over 50 and could thus all be considered similar.

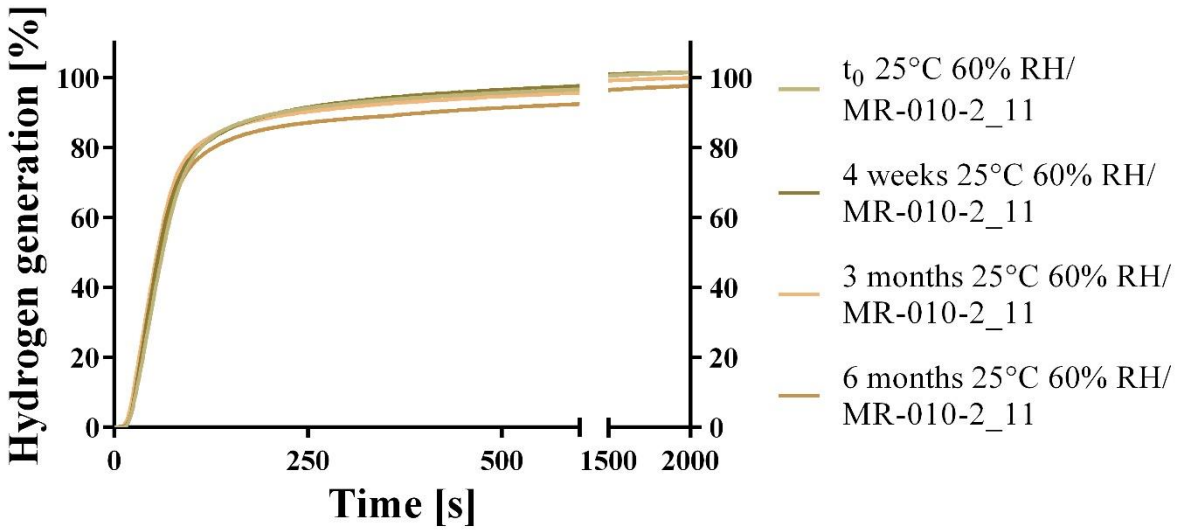

Figure 8.2.a) Kinetic hydrogen generation measurement (means; n = 3). Kinetics of hydrogen generation of packed tablets of batch MR010-2_11 were measured at the starting point t0, after 4 weeks, 3 months and 6 months of storage in a constant climate chamber (25°C and 60% RH). Single graphs of the storage times can be found in chapter 13.

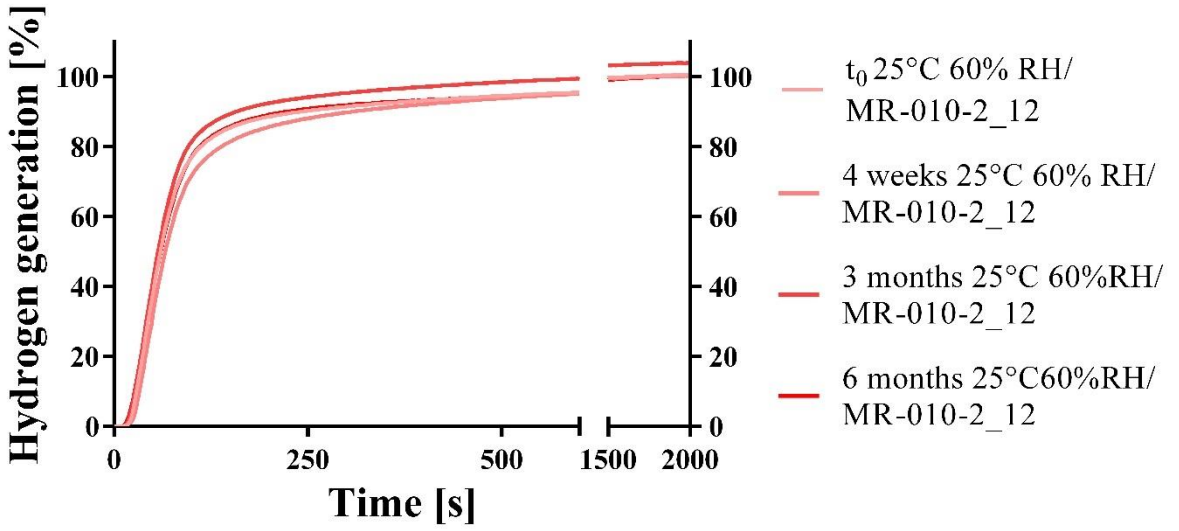

Figure 8.2.b) Kinetic hydrogen generation measurement (means; n = 3). Kinetics of hydrogen generation of packed tablets of batch MR010-2_12 were measured at the starting point t0, after 4 weeks, 3 months and 6 months of storage in a constant climate chamber (25°C and 60% RH). Single graphs of the storage times can be found in chapter 13.

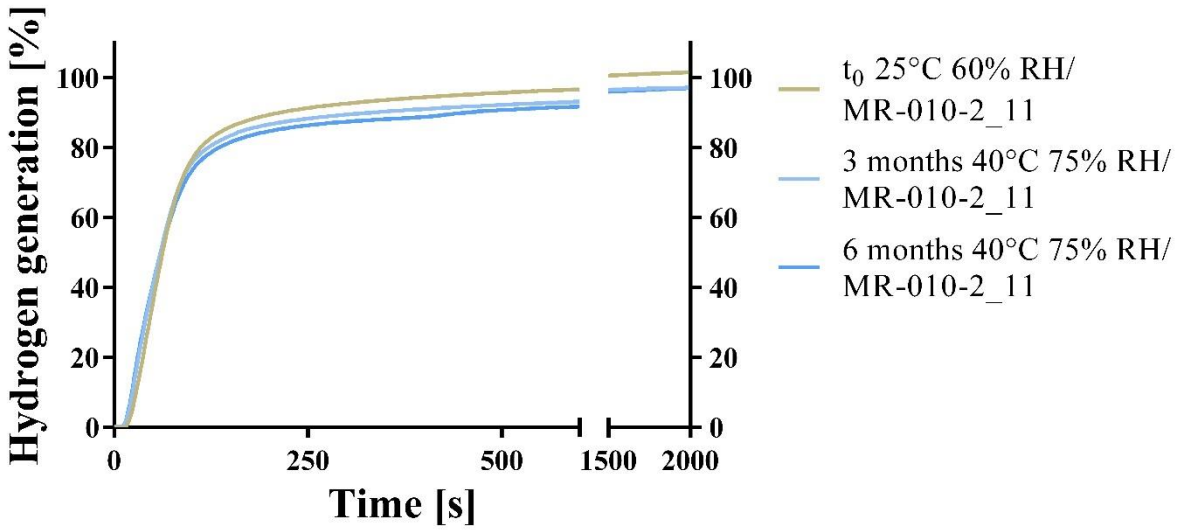

Figure 8.2.c) Kinetic hydrogen generation measurement (means; n = 3). Kinetics of hydrogen generation of packed tablets of batch MR010-2_11 were measured at the starting point t0, after 3 months and 6 months of storage in a constant climate chamber (40°C and 75% RH). Single graphs of the storage times can be found in chapter 13.

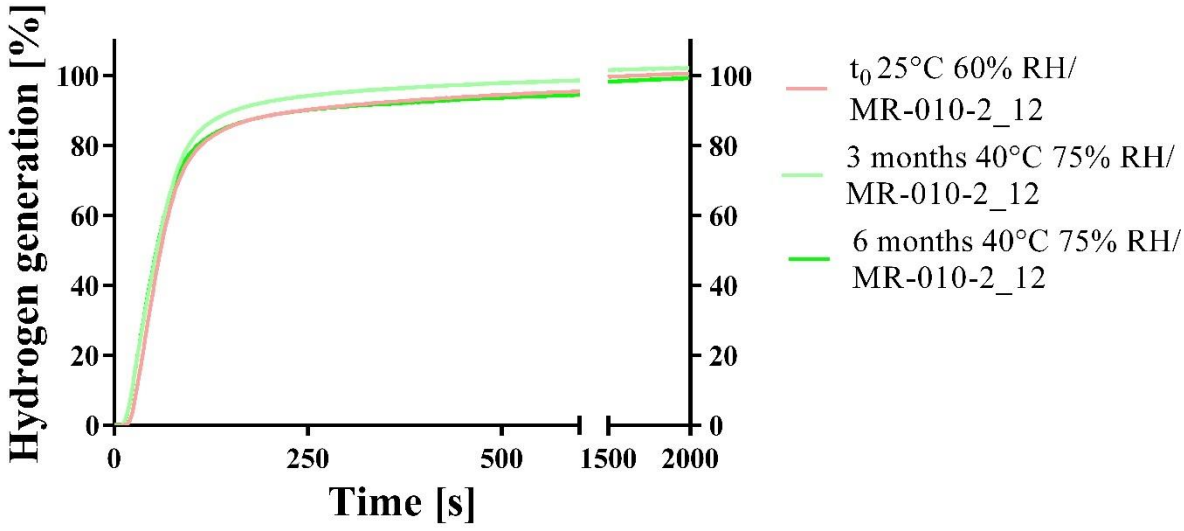

Figure 8.2.d) Kinetic hydrogen generation measurement (means; n = 3). Kinetics of hydrogen generation of packed tablets of batch MR010-2_12 were measured at the starting point t0, after 3 months and 6 months of storage in a constant climate chamber (40°C and 75% RH). Single graphs of the storage times can be found in chapter 13.

Tables 8.1.a)-d) Kinetic hydrogen measurements of batches MR-010-2_11 and MR010-2_12 stored at 25°C 60% RH or 40°C 75%RH in constant climate chambers for 4 weeks up to 6 months or without storage (t_0).

a) 25°C 60%RH; batch MR-010-2_11

Storage time	Hydrogen 1 (%)	Hydrogen 2 (%)	Hydrogen 3 (%)	Mean (%)	SD (%)
t_0	102.58	99.84	102.05	101.49	1.45
4 weeks	100.01	102.23	102.25	101.50	1.29
3 months	98.18	100.10	101.42	99.90	1.63
6 months	99.74	98.85	94.15	97.58	3.00

b) 25°C 60%RH; batch MR-010-2_12

Storage time	Hydrogen 1 (%)	Hydrogen 2 (%)	Hydrogen 3 (%)	Mean (%)	SD (%)
t_0	98.79	99.66	103.19	100.55	2.33
4 weeks	99.75	98.01	102.95	100.24	2.51
3 months	97.81	106.03	108.10	103.98	5.44
6 months	99.21	102.54	99.21	100.32	1.92

c) 40°C 75%RH/ batch MR-010-2_11

40°C 75%RH/ MR-010-2_11	Hydrogen 1 (%)	Hydrogen 2 (%)	Hydrogen 3 (%)	Mean (%)	SD (%)
t_0	102.58	99.84	102.05	101.49	1.45
3 months	98.71	99.06	93.74	97.17	2.97
6 months	96.70	95.38	98.86	96.98	1.76

d) 40°C 75%RH/ batch MR-010-2_11

40°C 75%RH/ MR-010-2_12	Hydrogen 1 (%)	Hydrogen 2 (%)	Hydrogen 3 (%)	Mean (%)	SD (%)
t_0	98.79	99.66	103.19	100.55	2.33
3 months	103.04	100.05	103.56	102.22	1.90
6 months	97.72	99.78	100.34	99.28	1.38

Tables 8.2. a)-g) f2 comparisons. Kinetic hydrogen generation measurements of the stability samples were compared with the f2 comparison; according to SUPAC guidelines release profiles of tablets with a f2 value between 50 and 100 are considered similar.

Table 8.2. a) f2 comparisons of batches MR010-2_7, MR010-2_11 and MR010-2_12 at the starting point (t_0).

t_0	**MR010-2_7**	**MR-010-2_11**	**MR010-12**
MR010-2_7		58.07	55.38
MR-010-2_11	58.07		88.42
MR010-12	55.38	88.42	

Table 8.2. b) f2 comparisons of batches MR010-2_11 and MR010-2_12 of similar storage times and similar storage condition of 25°C 60%RH

MR-010-2_11 vs MR010-12	**t_0**	**4weeks**	**3 months**	**6 months**
t_0	88.42			
4 weeks		59.79		
3 months			81.82	
6 months				84.09

Table 8.2. c) f2 comparisons of different storage times of batch MR010-2_11 with similar storage condition of 25°C 60%RH

MR-010-2_11	**t_0**	**4weeks**	**3 months**	**6 months**
t_0		76.55	65.95	77.77
4 weeks	76.55		81.65	80.76
3 months	65.95	81.65		71.10
6 months	77.77	80.76	71.10	

Table 8.2. d) f2 comparisons of different storage times of batch MR010-2_12 with similar storage condition of 25°C 60%RH

MR-010-2_12	t_0	4weeks	3 months	6 months
t_0		64.92	72.09	90.24
4 weeks	64.92		53.36	62.91
3 months	72.09	53.36		72.75
6 months	90.24	62.91	72.75	

Table 8.2. e) f2 comparisons of batches MR010-2_11 and MR010-2_12 of similar storage times and similar storage condition of 40°C 75%RH

MR-010-2_11 vs MR010-12	t_0	3 months	6 months
t_0	88.42		
3 months		67.74	
6 months			68.17

Table 8.2. f) f2 comparisons of different storage times of batch MR010-2_11 with similar storage condition of 40°C 75%RH

MR-010-2_11	t_0	3 months	6 months
t_0		73.87	68.38
3 months	73.87		85.78
6 months	68.38	85.78	

Table 8.2. g) f2 comparisons of different storage times of batch MR010-2_12 with similar storage condition of 40°C 75%RH

MR-010-2_12	t_0	3 months	6 months
t_0		63.88	68.03
3 months	63.88		84.98
6 months	68.03	84.98	

8.5. Discussion:

The contents of the batches MR010-2_7 at (the starting point t_0), MR010-2_11 and MR010-2_12 showed no significant differences throughout the entire stability studies. During the long-term stability storage condition (25°C and 60% RH) and at the accelerated stability storage condition (40°C and 75% RH) no significant decreases of hydrogen generation were observed. In contrast to the bulk stability studies, no significant decrease of hydrogen content as well as no decrease in hydrogen generation speed was observed throughout the study. The values of sample MR010-2_11 show a trend of decreasing content in the stability storage condition. However, the decrease is not yet significant after storage for 6 months. This shows, that the primary packaging of plastic tubes with sealed desiccant containing cap was very important for the formulation's stability. Although the formulation proved some resistance towards the long-term stability storage conditions in bulk as shown in chapters 6.3.24; 6.4.4.; and 6..4., the effervescent reaction took place extensively in the accelerated stability storage condition. In this condition the bulk tablets changed their appearance drastically (see Figure 6.8.f) and showed no more hydrogen generation upon contact with water after only 24h of storage. The packed tablets showed no decreased hydrogen generation amount even after 6 months of storage. Alu alu blisters could serve as an option, if single dose packaging was desired. The investigated batches can be considered similar regarding f2 values as well, which proves the robustness of packed tablets in the packaging as well as a robust production process.

9. Uniformity of dosage units investigation of effervescent hydrogen-generating tablets

9.1. Introduction

Uniformity of dosage investigations according to Ph. Eur. 2.9.40 were performed on three identically manufactured batches. The same three batches, whose hydrogen generation was determined in section 8 were once more evaluated in this section. For this investigation the pharmacopeial quantification method complexometric titration according to Ph. Eur. 10.1; 2.5.11. was chosen to determine the magnesium content of the samples. This study was conducted to prove reproducible and exact dosing with the developed manufacturing process as well as low batch to batch variability.

9.2. Materials

Effervescent hydrogen releasing tablets of the batches MR010-2_7, MR010-2_11 and MR010_12 were used. All batches were manufactured identically contained mannitol as filler and adipic acid as lubricant.

9.3. Methods

9.3.1. Uniformity of dosage test

Uniformity of dosage units according to the European Pharmacopeia (Ph. Eur. 9.2.40.) was determined for three batches. Since the theoretical Magnesium content of the formulation is only 4.55 % referring to the tablets total mass, content uniformity was determined instead of mass variation. Only if the dose of the active substance would have been under 25 mg or 25 % the test for mass variation would also have been possible. For each batch 10 samples were analyzed and the acceptance value (AV) was calculated. For mean values $(\bar{X})$ over 101.5 % the equation

$$AV = |\bar{X} - M| + ks \qquad \text{Equation 9.1.}$$

was used, where M is the reference value (M =101.5 % if $\bar{X}$ is over 101.5%), k is the acceptability constant (k = 2.4 for n=10) and s is the sample standard deviation.

9.3.2. Complexometric titration

For each batch 10 samples were analyzed using complexometric titration of magnesium ions according to Ph. Eur. 10.1; 2.5.11. The samples were prepared as described for the monograph of magnesium citrate. Therefore, the samples were introduced into a 500 mL conical flask. 50 mL of deionized water were added so that the effervescent reaction could take place. Afterwards the complexometric titration was conducted. First, the samples were diluted with deionized water to 300 mL. Afterwards, 10 mL of ammonium chloride buffer solution pH 10.0 R were added. Then 75 mg of mordant black 11 triturate R were added and the solution was heated to 40 °C. The titration was performed with 0.1 M sodium edetate (EDTA) until the color of the solution changed from violet to full blue. A correction factor (f) was established using about 75mg of magnesium powder as a reference, since the color change of the titration was determined visually. 1000 mg of Citrocoat® N was added to enable the effervescent reaction. The following equation was used:

$$f = \frac{m_{weighed}(Magnesium\ powder)}{m_{measured}(Mg^{2+})} \qquad \text{Equation 9.2.}$$

$where\ m_{weighed}(Magnesium\ powder)\ is\ the\ mass\ of\ weighed\ magnesium\ powder\ [mg]$

$$f = \frac{m_{weighed}(Magnesium\ powder)}{V(EDTA)*C(EDTA)*M(Mg^{2+})} \qquad \text{Equation 9.3.}$$

$V(EDTA)\ is\ the\ volume\ of\ 0.1M\ sodiumedetate\ [ml],$

$C(EDTA) is\ the\ concentration\ of\ 0.1\ M\ sodiumedetate [mol/l],$

$M(Mg^{2+})\ is\ the\ molar\ mass\ of\ magnesium\ [g/mol]$

$$= \frac{m_{weighed}(Magnesium\ powder)}{V(EDTA)*2.431\ mg/ml} \qquad \text{Equation 9.4.}$$

The correction factor was used to calculate the content of the samples:

$$m(Mg) = V(EDTA) * 2{,}431\ mg/ml * f \qquad \text{Equation 9.5.}$$

9.4. Results

The determination of the correction factor worked very well, a mean magnesium content of 100.21% of the previously weighed amount and a SD of 0.12% were determined resulting in a correction factor (f) of 0.998. Results are shown in table 9.1..

Table 9.1. Correction factor (f)

Sample	Mg powder[mg]	V(EDTA) [mL]	m(Mg) [mg]	*f*
1	75.5	31.1	75.60	0.999
2	76.9	31.7	77.06	0.998
3	75.2	31.0	75.36	0.998
4	74.3	30.7	74.63	0.996
5	78.7	32.4	78.76	0.999
6	75.1	31.0	75.24	0.997
7	75.2	31.0	75.36	0.998
Mean	75.84	31.3	76.00	0.998
SD	1.48	0.6	1.43	0.001

The three batches showed mean weights ranging from 1622.90 mg to 1671.68 mg, and mean magnesium contents of 102.45 ± 2.10% to 104.52 ± 0.72%.

The batch MR010-2_7 showed 104.36 ± 1.36% mean content, with single contents ranging from 102.22% to 106.43%. The results are shown in table 9.2.. A mean content of 102.45 ± 2.10% was measured for batch MR010-2_11, where values from 99.96% to 105,46% were measured. Table 9.3. shows the results of this batch. The highest mean content as well as the lowest SD (104.52 ± 0.72%) were recorded for batch MR010-2_12. Values ranged from 103.19% to 105.46%.

Table 9.2. Uniformity of content determination batch MR010-2_7

Sample	Tablet weight [mg]	V(EDTA)[mL]	m(Mg)[mg]	Content[%]
1	1633.85	31.7	76.91	102.54
2	1612.74	32.3	78.36	104.49
3	1631.89	32.9	79.82	106.43
4	1634.82	32.7	79.33	105.78
5	1623.56	32.6	79.09	105.46
6	1631.99	32.4	78.61	104.81
7	1630.09	32.3	78.36	104.49
8	1606.2	32.0	77.64	103.52
9	1628.78	31.6	76.67	102.22
10	1637.54	32.1	77.88	103.84
Mean	1627.15	32.3	78.27	104.36
SD	10.16	0.4	1.02	1.36
AV	6.11			

Table 9.3. Uniformity of content determination batch MR010-2_11

Sample	Tablet weight [mg]	V(EDTA)[mL]	m(Mg)[mg]	Content[%]
1	1603.29	31.1	75.45	100.60
2	1607.38	31.4	76.18	101.57
3	1614.29	31.9	77.39	103.19
4	1610.8	32.0	77.64	103.52
5	1640.78	32.5	78.85	105.13
6	1659.23	32.6	79.09	105.46
7	1610.06	30.9	74.97	99.96
8	1612.65	30.9	74.97	99.96
9	1632.83	32.2	78.12	104.16
10	1637.66	31.2	75.70	100.93
Mean	1622.90	31.7	76.84	102.45
SD	18.47	0.6	1.58	2.10
AV	5.99			

Table 9.4. Uniformity of content determination batch MR010-2_12

Sample	Tablet weight [mg]	V(EDTA)[mL]	m(Mg)[mg]	Content[%]
1	1672.32	32.4	78.61	104.81
2	1657.05	32.1	77.88	103.84
3	1664.97	32.3	78.36	104.49
4	1704.8	32.6	79.09	105.46
5	1668.67	32.3	78.36	104.49
6	1689.66	31.9	77.39	103.19
7	1641.41	32.4	78.61	104.81
8	1698.67	32.1	77.88	103.84
9	1662.49	32.4	78.61	104.81
10	1656.78	32.6	79.09	105.46
Mean	1671.68	32.3	78.39	104.52
SD	20.11	0.2	0.54	0.72
AV	4.75			

9.5. Discussion

Although the test is not required for vitamin and trace-element preparations by the Ph.Eur., it is able to provide relevant insights into batch-to-batch variation of the tablets. Each batch fulfills the Ph.Eur. criteria of a maximum allowed acceptance value of less than 15.0 while no single unit showed a higher deviation than allowed as well. It is known, that roller compaction is a suitable method to reduce segregation during tableting. The differences between the particle sizes of the excipients are large, ranging from d50 values of <13.7 µm for adipic acid and 35.1 µm for magnesium to 384 µm for Citrocoat® N which is why a dry granulation step had to be included in order for the excipients not to segregate during the automatic compaction process in an eccentric tablet press. The small magnesium particles are necessary to ensure an equal statistical distribution in the powder mixture, which leads to an appreciable content uniformity of the respective tablets, provided that the powder does not segregate and the variation of the tablet weight is low [110]. The powder excipients were blended in a Turbula mixer for 10 min prior to granulation. This was important to achieve a good distribution of the excipients. The consequent dry granulation step fixed the current state of distribution of the powders and ensured a much lower susceptibility for segregation, allowing two subsequent blending steps with Citrocoat® N and milled adipic acid for 10 min and 3 min respectively. The very small adipic acid particles stabilize the blend as well. They decrease the flow properties due to their cohesive character as a very fine powder. Cohesive materials tend to form more stable blends, once they are transferred into a well-blended status. Especially when exposed to vibration as in tableting of an eccentric press, coarser particles tend to segregate faster [111]. In chapter 6.4. the decreased flow properties of the mannitol/adipic acid-based batch was shown very clearly. Compared to the other batches that were tested it was not able to flow through an orifice equipped with nozzle 1 (10 mm diameter) and form a cone for the angle of repose measurement. Resulting from its high density, the blend shows a fair Hausner ratio and compressibility index. It could be assumed that the parameters characterizing flow are not sufficient to ensure a constant filling process of the die during compaction. However, the large diameter of the die (18 mm) offers some advantages compared to smaller die sizes, since its diameter is 12.6 times the size of the largest granular particles (d90 1430.6 µm ± 41.6 µm). It is recommended that the biggest particles do not exceed 1/3 of the die diameter, which is clearly not the case here, since a particle size that exceeds 1/3 of the die diameter can be

problematic for constant die filling [112]. Moreover, the stirring blade of the feed shoe provides for a constant die filing process.

Complexometric titration proved to be a suited analytical method for the determination of the magnesium content. Although its endpoint is determined visually, a low standard deviation (1.48 during correction factor determination) and a correction factor of 0.998 suggest that this method is well suited for quality control purposes of magnesium content determination. Magnesium ions and sodium edetate form a relatively weak complex ($pK_{MgY}^{2\ominus}$ = 8.7)[113]. In order to determine the content as accurately as possible, the temperature was constantly monitored during the titration, since it is crucial for the complex formation [113]. The magnesium content of batch MR010-2_7 (104.36 ± 1.36 %) corresponds very well with the kinetic hydrogen measurement for this sample where 105.91 ± 2.08 % were determined. Contrary to the kinetic hydrogen generation measurement, the method is not able to account for the tablet's release kinetics. However, a titration is much easier to conduct than a kinetic hydrogen measurement where one measurement takes roughly two hours. Together with the disintegration test for effervescent tablets Ph. Eur. 10.1/0478 it can represent a good alternative to the kinetic hydrogen generation measurement in situations where a stability-indicating method is not necessary.

10. Conclusion and Outlook

The aim of the project was to formulate an effervescent hydrogen-generating tablet, establish a robust production process and characterize each technological and scientific aspect of the tablet as carefully as possible. This was achieved through careful selection and optimization of the excipients and the manufacturing processes and process parameters. Several challenges were encountered during the manufacturing process, such as segregation, sticking of the formulation to punch surfaces and other processing equipment, slow disintegration of the tablets and low hardness of the tablets. All problems were solved in one final formulation containing mannitol as a filler and adipic acid as lubricant.

Mannitol-based formulations showed by far the quickest disintegration although it is the least soluble filler investigated in this study. Its formulations showed the highest total porosity, which indicates that the latter is the chief factor governing the disintegration rate of the compact. Therefore, they were selected for further development and stability testing. Additionally, mannitol-based tablets showed satisfactory hardness values. Dextrates-based formulations performed best regarding hardness. Moreover, they facilitated a precise and rapid generation of hydrogen.

The volumetric, kinetic hydrogen generation measurement proved to be a useful method for quantitative and kinetic measurements of hydrogen gas generation. Since it is volumetric it could easily be transferred to formulation development and quality control of conventional effervescent tablets and provide a more detailed insight into the disintegration kinetics than the pharmacopeial disintegration test.

As expected, this formulation proved to be moisture-labile. The mannitol-based formulation and its intermediate products such as the granules were investigated very carefully using Dynamic Vapor Sorption analysis and through stability studies that were performed with packed and unpacked tablets. It can be concluded that the unpacked tablets are stable at moderate conditions and time frames for a short time, while the primary packaging was able to protect the tablets very well for months.

Through the uniformity of dosage testing and the stability test of the mannitol-based formulation it was confirmed, that the batch-to-batch variability of the magnesium content,

the hydrogen generation amount and time is low. That accounts for a reproducible and robust production process.

Regulatory considerations concerning a possible market release of the tablet were made in a very early stage of the development. It is planned to register the tablet as a nutritional supplement and release it on the German and European market. Clinical studies and animal research revealed large benefits for several diseases. Thus, it is planned to test this tablet in a clinical study as well.

11. References

1. LeBaron TW, Kura B, Kalocayova B, Tribulova N, Slezak J. A New Approach for the Prevention and Treatment of Cardiovascular Disorders. Molecular Hydrogen Significantly Reduces the Effects of Oxidative Stress. Molecules. 2019;24(11):2076-.10.3390/molecules24112076

2. Ge L, Yang M, Yang NN, Yin XX, Song WG. Molecular hydrogen: A preventive and therapeutic medical gas for various diseases. Oncotarget. 2017;8(60):102653-73.10.18632/oncotarget.21130

3. Ichihara M, Sobue S, Ito M, Ito M, Hirayama M, Ohno K. Beneficial biological effects and the underlying mechanisms of molecular hydrogen - Comprehensive review of 321 original articles. Medical Gas Research. 2015;5(1):1-21.10.1186/s13618-015-0035-1

4. Ohno K, Ito M, Ichihara M, Ito M. Molecular hydrogen as an emerging therapeutic medical gas for neurodegenerative and other diseases. Oxidative Medicine and Cellular Longevity. 2012;2012.10.1155/2012/353152

5. Ohsawa I, Ishikawa M, Takahashi K, Watanabe M, Nishimaki K, Yamagata K, et al. Hydrogen acts as a therapeutic antioxidant by selectively reducing cytotoxic oxygen radicals. Nature Medicine. 2007;13(6):688-94.10.1038/nm1577

6. Chen W, Zhang HT, Qin SC. Neuroprotective Effects of Molecular Hydrogen: A Critical Review. Neuroscience Bulletin. 2020:1-16.10.1007/s12264-020-00597-1

7. Murakami Y, Ito M, Ohsawa I. Molecular hydrogen protects against oxidative stress-induced SH-SY5Y neuroblastoma cell death through the process of mitohormesis. PLoS ONE. 2017;12(5):1-14.10.1371/journal.pone.0176992

8. Yuan J, Wang D, Liu Y, Chen X, Zhang H, Shen F, et al. Hydrogen-rich water attenuates oxidative stress in rats with traumatic brain injury via Nrf2 pathway. Journal of Surgical Research. 2018;228:238-46.10.1016/j.jss.2018.03.024

9. Chen L, Deng H, Cui H, Fang J, Zuo Z, Deng J, et al. Inflammatory responses and inflammation-associated diseases in organs. Impact Journals LLC; 2018. p. 7204-18.

10. Uttara B, Singh AV, Zamboni P, Mahajan RT. Oxidative Stress and Neurodegenerative Diseases: A Review of Upstream and Downstream Antioxidant Therapeutic Options. Current neuropharmacology. 2009;7(1):65-74.

11. Lucas K, Maes M. Role of the toll like receptor (TLR) radical cycle in chronic inflammation: Possible treatments targeting the TLR4 pathway. Humana Press Inc.; 2013. p. 190-204.

12. Nagatani K, Nawashiro H, Takeuchi S, Tomura S, Otani N, Osada H, et al. Safety of intravenous administration of hydrogen-enriched fluid in patients with acute cerebral ischemia: initial clinical studies. Medical Gas Research. 2013;3(1):13-.10.1186/2045-9912-3-13

13. Li H, Luo Y, Yang P, Liu J. Hydrogen as a complementary therapy against ischemic stroke: A review of the evidence. Elsevier B.V.; 2019. p. 240-6.

14. Nakayama M, Nakano H, Hamada H, Itami N, Nakazawa R, Ito S. A novel bioactive haemodialysis system using dissolved dihydrogen (H2) produced by water electrolysis: A clinical trial. Nephrology Dialysis Transplantation. 2010;25(9):3026-33.10.1093/ndt/gfq196

15. Kajiyama S, Hasegawa G, Asano M, Hosoda H, Fukui M, Nakamura N, et al. Supplementation of hydrogen-rich water improves lipid and glucose metabolism in patients with type 2 diabetes or impaired glucose tolerance. Nutrition Research. 2008;28(3):137-43.10.1016/j.nutres.2008.01.008

16. Nakao A, Toyoda Y, Sharma P, Evans M, Guthrie N. Effectiveness of hydrogen rich water on antioxidant status of subjects with potential metabolic syndrome - An open label pilot study. Journal of Clinical Biochemistry and Nutrition. 2010;46(2):140-9.10.3164/jcbn.09-100

17. Ishibashi T. Molecular Hydrogen: New Antioxidant and Anti-inflammatory Therapy for Rheumatoid Arthritis and Related Diseases. Current Pharmaceutical Design. 2013;19(35):6375-81.10.2174/13816128113199990507

18. LeBaron TW, Laher I, Kura B, Slezak J. Hydrogen gas: from clinical medicine to an emerging ergogenic molecule for sports athletes. Canadian Journal of Physiology and Pharmacology. 2019;97(9):797-807.10.1139/cjpp-2019-0067

19. Mikami T, Tano K, Lee H, Lee H, Park J, Ohta F, et al. Drinking hydrogen water enhances endurance and relieves psychometric fatigue: a randomized, double-blind, placebo-controlled study. Canadian Journal of Physiology and Pharmacology. 2019;97(9):857-62.10.1139/cjpp-2019-0059

20. Aoki K, Nakao A, Adachi T, Matsui Y, Miyakawa S. Pilot study: Effects of drinking hydrogen-rich water on muscle fatigue caused by acute exercise in elite athletes. Medical Gas Research. 2012;2(1):12-.10.1186/2045-9912-2-12

21. Alwazeer D, Liu FFC, Wu XY, Lebaron TW. Combating Oxidative Stress and Inflammation in COVID-19 by Molecular Hydrogen Therapy: Mechanisms and Perspectives. Oxidative Medicine and Cellular Longevity. 2021;2021.10.1155/2021/5513868

22. Mazza MG, Palladini M, De Lorenzo R, Magnaghi C, Poletti S, Furlan R, et al. Persistent psychopathology and neurocognitive impairment in COVID-19 survivors: Effect of inflammatory biomarkers at three-month follow-up. Brain, Behavior, and Immunity. 2021;94:138-.10.1016/j.bbi.2021.02.021

23. Ohta S. Recent Progress Toward Hydrogen Medicine: Potential of Molecular Hydrogen for Preventive and Therapeutic Applications. Current Pharmaceutical Design. 2011;17(22):2241-52.10.2174/138161211797052664

24. Taub IA, Roberts W, … SLTJoP, undefined. Mechanism of Dihydrogen Formation in the Magnesium− Water Reaction. ACS Publications. 2002;106(35):8070-8.10.1021/jp0143847

25. Schmidt PC, Christin I. Effervescent tablets--a nearly forgotten drug form. Die Pharmazie. 1990;45(2):89-101.

26. Mohrle R, Lieberman L, Lachmnann L, Schwartz JB. Pharmaceutical dosage forms: Tablets; Volume 1; Second Edition. New York NY, USA: Marcdel Dekker Inc.; 1989. 285-92 p.

27. Patel SG, Siddaiah M. Formulation and evaluation of effervescent tablets: a review. Journal of Drug Delivery and Therapeutics. 2018;8(6):296-303.10.22270/jddt.v8i6.2021

28. Bauer-Brandl A, Ritschel WA. Die Tablette: Handbuch der Entwicklung, Herstellung und Qualitätssicherung. 3.Auflage ed: ECV Editio Cantor; 2012. 51-5 p.

29. Møller PL, Nørholt SE, Ganry HE, Insuasty JH, Vincent FG, Skoglund LA, et al. Time to onset of analgesia and analgesic efficacy of effervescent acetaminophen 1000 mg compared to tablet acetaminophen 1000 mg in postoperative dental pain: A single-dose, double-blind, randomized, placebo-controlled study. Journal of Clinical Pharmacology. 2000;40(4):370-8.10.1177/00912700022009071

30. Aslani A, Jahangiri H. Formulation, characterization and physicochemical evaluation of ranitidine effervescent tablets. Advanced Pharmaceutical Bulletin. 2013;3(2):315-22.10.5681/apb.2013.051

31. Parikh DM, (ed.), Bertuzzi G. Handbook of Pharmaceutical Granulation Technology. 4th ed: CRC Press; 2021. 469-84 p.

32. Yanze MF, Duru C, Jacob M, Bastide JM, Lankeuh M. Rapid therapeutic response onset of a new pharmaceutical form of chloroquine phosphate 300 mg: Effervescent tablets. Tropical Medicine and International Health. 2001;6(3):196-201.10.1046/j.1365-3156.2001.00681.x

33. Aslani A, Sharifian T. Formulation, characterization and physicochemical evaluation of amoxicillin effervescent tablets. 2014.10.4103/2277-9175.143252

34. Aslani A, Fattahi F. Formulation, characterization and physicochemical evaluation of potassium citrate effervescent tablets. Advanced Pharmaceutical Bulletin. 2013;3(1):217-25.10.5681/apb.2013.036

35. Aiache JM. Les Comprimes Effervescents. Pharmaceutica Acta Helvetiae. 1974;491(5-6):169-78.

36. Sendall FEJ, Staniforth JN, Rees JE, Leatham MJ. Effervescent tablets. Pharm J. 1983;230:289-94.

37. Sendall FEJ, Staniforth JN. A study of powder adhesion to metal surfaces during compression of effervescent pharmaceutical tablets. Journal of Pharmacy and Pharmacology. 1986;38(7):489-93.10.1111/j.2042-7158.1986.tb04620.x

38. Zheng X, Wu F, Hong Y, Shen L, Lin X, Feng Y. Improvements in sticking, hygroscopicity, and compactibility of effervescent systems by fluid-bed coating. RSC Advances. 2019;9(54):31594-608.10.1039/c9ra05884b

39. George J, Majeed W, Mackenzie IS, MacDonald TM, Wei L. Association between cardiovascular events and sodium-containing effervescent, dispersible, and soluble drugs: Nested case-control study. BMJ (Online). 2013;347.10.1136/bmj.f6954

40. Mozaffarian D, Fahimi S, Singh GM, Micha R, Khatibzadeh S, Engell RE, et al. Global sodium consumption and death from cardiovascular causes. N Engl J Med. 2014;371(7):624-34.10.1056/NEJMoa1304127

41. Dalman LH. The Solubility of Citric and Tartaric Acids in Water. Journal of the American Chemical Society. 1937;59(12):2547-9.10.1021/ja01291a018

42. Apelblat A, Manzurola E. Solubility of oxalic, malonic, succinic, adipic, maleic, malic, citric, and tartaric acids in water from 278.15 to 338.15 K. The Journal of Chemical Thermodynamics. 1987;19(3):317-20.10.1016/0021-9614(87)90139-x

43. Apelblat A, Dov M, Wisniak J, Zabicky J. The vapour pressure of water over saturated aqueous solutions of malic, tartaric, and citric acids, at temperatures from 288 K to 323 K. The Journal of Chemical Thermodynamics. 1995;27(1):35-41.10.1006/jcht.1995.0004

44. Peng C, Chan MN, Chan CK. The hygroscopic properties of dicarboxylic and multifunctional acids: Measurements and UNIFAC predictions. Environmental Science and Technology. 2001;35(22):4495-501.10.1021/es0107531

45. Joutsensaari J, Vaattovaara P, Vesterinen M, Hämeri K, Laaksonen A. A novel tandem differential mobility analyzer with organic vapor treatment of aerosol particles. Atmospheric Chemistry and Physics. 2001;1(1):51-60.10.5194/acp-1-51-2001

46. Show PL, Oladele KO, Siew QY, Aziz Zakry FA, Lan JCW, Ling TC. Overview of citric acid production from Aspergillus niger. Frontiers in Life Science. 2015;8(3):271-83.10.1080/21553769.2015.1033653

47. Kubicek CP, Röhr M, Rehm HJ. Citric acid fermentation. Critical Reviews in Biotechnology. 1985;3(4):331-73.10.3109/07388558509150788

48. Apelblat A, Manzurola E. Solubility of ascorbic, 2-furancarboxylic, glutaric, pimelic, salicylic, and o-phthalic acids in water from 279.15 to 342.15 K, and apparent molar volumes of ascorbic, glutaric, and pimelic acids in water at 298.15 K. The Journal of Chemical Thermodynamics. 1989;21(9):1005-8.10.1016/0021-9614(89)90161-4

49. Amela J, Salazar R, Cemeli J. Effervescent tablets of ascorbic acid. I. Physical study of the possible components to be used. Drug Development and Industrial Pharmacy. 1996;22(5):407-16.10.3109/03639049609069349

50. Kawaguchi T, Sunada H, Yonezawa Y, Danjo K, Hasegawa M, Makino T, et al. Granulation of Acetaminophen by a Rotating Fluidized-Bed Granulator. Pharmaceutical development and technology. 2000;5(2):141-51.10.1081/pdt-100100529

51. Ariyasu A, Hattori Y, Otsuka M. Delay effect of magnesium stearate on tablet dissolution in acidic medium. International Journal of Pharmaceutics. 2016;511(2):757-64.10.1016/j.ijpharm.2016.07.034

52. Röscheisen G. Optimierung von Schmiermitteln für Brausetabletten: Eberhard Karls Universität Tübingen; 1994.

53. Li J, Wu Y. Lubricants in pharmaceutical solid dosage forms. Lubricants. 2014;2(1):21-43.10.3390/lubricants2010021

54. Li J, Wu Y. Lubricants in pharmaceutical solid dosage forms. MDPI AG; 2014. p. 21-43.

55. Jivraj M, Martini LG, Thomson CM. An overview of the different excipients useful for the direct compression of tablets. 2000. p. 58-63.

56. Murray RB. New approach to the fusion method for preparing granular effervescent products. Journal of Pharmaceutical Sciences. 1968;57(10):1776-9.10.1002/jps.2600571032

57. Jassim ZE, Rajab NA, Mohammed NH. Study the effect of wet granulation and fusion methods on preparation, characterization, and release of lornoxicam sachet effervescent granules. Drug Invention Today. 2018;10(9):1612-6.

58. Yanze FM, Duru C, Jacob M. A process to produce effervescent tablets: Fluidized bed dryer melt granulation. Drug Development and Industrial Pharmacy. 2000;26(11):1167-76.10.1081/ddc-100100988

59. Rowe RC, Sheskey PJ, Quinn ME. Handbook of Pharmaceutical Excipients. 6th ed. London (UK) and Washington DC (USA): Pharmaceutical Press and American Pharmacists Association; 2009.

60. Lide D, Gevantman L. CRC Handbook of Chemistry and Physics. Boca Raton, Florida: CRC Press; 2004. pp. 8-87 p.

61. Shah KR, Badawy SIF, Szemraj MM, Gray DB, Hussain MA. Assessment of segregation potential of powder blends. Pharmaceutical development and technology. 2007;12(5):457-62.10.1080/10837450701556834

62. He X, Han X, Ladyzhynsky N, Deanne R. Assessing powder segregation potential by near infrared (NIR) spectroscopy and correlating segregation tendency to tabletting performance. Powder Technology. 2013;236:85-99.10.1016/j.powtec.2012.05.021

63. Mateo-Ortiz D, Muzzio FJ, Méndez R. Particle size segregation promoted by powder flow in confined space: The die filling process case. Powder Technology. 2014;262:215-22.10.1016/j.powtec.2014.04.023

64. Official Journal of the European Union REGULATION (EU) No 1169/2011 OF THE EUROPEAN PARLIAMENT AND OF THE COUNCIL. [18.01.22];

]. Available from: https://eur-lex.europa.eu/legal-content/EN/TXT/HTML/?uri=CELEX:32011R1169&from=DE.

65. ICH Harmonised Tripartite Guideline Q1A(R2) “Stability testing of new drug substances and products. [19.01.2022]; Available from: https://database.ich.org/sites/default/files/Q1A%28R2%29%20Guideline.pdf.

66. Lucas K, Rosch M, Langguth P. Molecular hydrogen (H2) as a potential treatment for acute and chronic fatigue. Archiv der Pharmazie. 2021;354(4):2000378-.10.1002/ardp.202000378

67. Brack P, Dann S, Upul Wijayantha KG, Adcock P, Foster S. A simple, low-cost, and robust system to measure the volume of hydrogen evolved by chemical reactions with aqueous solutions. Journal of Visualized Experiments. 2016;2016(114):1-7.10.3791/54383

68. Moore JW, Flanner HH. Mathematical comparison of dissolution profiles. Pharmaceutical technology. 1996;20(6):64-74.

69. Fell JT, Newton JM. The tensile strength of lactose tablets. Journal of Pharmacy and Pharmacology. 1968;20(8):657-9.10.1111/j.2042-7158.1968.tb09832.x

70. Price R, Young PM. Visualization of the Crystallization of Lactose from the Amorphous State. Journal of Pharmaceutical Sciences. 2004;93(1):155-64.10.1002/jps.10513

71. Yu SH, Uan JY, Hsu TL. Effects of concentrations of NaCl and organic acid on generation of hydrogen from magnesium metal scrap. International Journal of Hydrogen Energy. 2012;37(4):3033-40.10.1016/j.ijhydene.2011.11.040

72. Uan JY, Yu SH, Lin MC, Chen LF, Lin HI. Evolution of hydrogen from magnesium alloy scraps in citric acid-added seawater without catalyst. International Journal of Hydrogen Energy. 2009;34(15):6137-42.10.1016/j.ijhydene.2009.05.133

73. Pokrovsky OS, Schott J. Experimental study of brucite dissolution and precipitation in aqueous solutions: surface speciation and chemical affinity control. Geochimica et Cosmochimica Acta. 2004;68(1):31-45.10.1016/s0016-7037(03)00238-2

74. Pokrovsky OS, Schott J, Castillo A. Kinetics of brucite dissolution at 25°C in the presence of organic and inorganic ligands and divalent metals. Geochimica et Cosmochimica Acta. 2005;69(4):905-18.10.1016/j.gca.2004.08.011

75. Wan W-L, Lin Y-J, Shih P-C, Bow Y-R, Cui Q, Chang Y, et al. An In Situ Depot for Continuous Evolution of Gaseous H 2 Mediated by a Magnesium Passivation/Activation Cycle for Treating Osteoarthritis. Angewandte Chemie. 2018;130(31):10023-7.10.1002/ange.201806159

76. Mou F, Chen C, Ma H, Yin Y, Wu Q, Guan J. Self-Propelled Micromotors Driven by the Magnesium–Water Reaction and Their Hemolytic Properties. Angewandte Chemie International Edition. 2013;52(28):7208-12.10.1002/anie.201300913

77. Carr RL. Classifying flow properties of solids. Chemical Engineering. 1965;72(3):69-72.

78. Park JS, Shim JY, Park JS, Choi YW, Jeong SH. A novel three-layered tablet for extended release with various layer formulations and in vitro release profiles. Drug Development and Industrial Pharmacy. 2011;37(6):664-72.10.3109/03639045.2010.535211

79. Bouchard A, Hofland GW, Witkamp G-J. Properties of Sugar, Polyol, and Polysaccharide Water-Ethanol Solutions. Journal of Chemical & Engineering Data. 2007;52(5):1838-42.10.1021/je700190m

80. Sunada H, Bi Y. Preparation, evaluation and optimization of rapidly disintegrating tablets. Powder Technology. 2002;122(2-3):188-98.10.1016/s0032-5910(01)00415-6

81. Wagner CM, Pein M, Breitkreutz J. Roll compaction of mannitol: Compactability study of crystalline and spray-dried grades. International Journal of Pharmaceutics. 2013;453(2):416-22.10.1016/j.ijpharm.2013.05.024

82. Sheskey PJ, Cabelka TD. Use of roller compaction in the preparation of hydrophilic sustained-release matrix tablets. Pharmaceutical technology. 1994;18(9):132-50.

83. Malkowska S, Khan KA. Effect of re-conpression on the properties of tablets prepared by dry granulation. Drug Development and Industrial Pharmacy. 1983;9(3):331-47.10.3109/03639048309044678

84. Sheskey PJ, Hendren J. The effects of roll compaction equipment variables, granulation technique, and HPMC polymer level on a controlled-release matrix model drug formulation. Pharmaceutical technology. 1999;23(3):90-106.

85. Sheskey PJ, Cabelka TD. Reworkability of Sustained-Release Tablet Formulations Containing HPMC Polymers. Pharmaceutical technology. 1992;16(6):60-74.

86. Bultmann JM. Multiple compaction of microcrystalline cellulose in a roller compactor. European Journal of Pharmaceutics and Biopharmaceutics. 2002;54(1):59-64.10.1016/s0939-6411(02)00047-4

87. Sun C, Himmelspach MW. Reduced tabletability of roller compacted granules as a result of granule size enlargement. Journal of Pharmaceutical Sciences. 2006;95(1):200-6.10.1002/jps.20531

88. Herting MG, Kleinebudde P. Studies on the reduction of tensile strength of tablets after roll compaction/dry granulation. European Journal of Pharmaceutics and Biopharmaceutics. 2008;70(1):372-9.10.1016/j.ejpb.2008.04.003

89. Patel S, Dahiya S, Calvin Sun C, Bansal AK. Understanding size enlargement and hardening of granules on tabletability of unlubricated granules prepared by dry granulation. Journal of Pharmaceutical Sciences. 2011;100(2):758-66.10.1002/jps.22315

90. Mosig J, Kleinebudde P. Evaluation of lubrication methods: How to generate a comparable lubrication for dry granules and powder material for tableting processes. Powder Technology. 2014;266:156-66.10.1016/j.powtec.2014.06.022

91. Heckel RW. Density-Pressure Relationships in Powder Compaction. Transactions of the Metallurgical Society of AIME. 1961;221:671-5.

92. Hersey JA, Rees JE. Deformation of Particles during Briquetting. Nature Physical Science. 1971;230(12):96-.10.1038/physci230096a0

93. York P. Crystal engineering and particle design for the powder compaction process. Drug Development and Industrial Pharmacy. 1992;18(6-7):677-721.10.3109/03639049209058558

94. Nordström J, Klevan I, Alderborn G. A protocol for the classification of powder compression characteristics. European Journal of Pharmaceutics and Biopharmaceutics. 2012;80(1):209-16.10.1016/j.ejpb.2011.09.006

95. Humbert Droz P, Gurny R, Mordier D, Doelker E. Densification behaviour of drugs presenting availability problems. International Journal of Pharmaceutical Technology and Product Manufacture. 1983;4(2):29-35.

96. Humbert-Droz P, Mordier D, Doelker E. Méthode rapide de détermination du comportement à la compression pour des études de préformulation. Pharm Acta Helv. 1982;57:136-43.

97. Bowe KE. Recent advances in sugar-based excipients. Pharmaceutical Science and Technology Today. 1998;1(4):166-73.10.1016/s1461-5347(98)00043-1

98. Ohrem HL, Schornick E, Kalivoda A, Ognibene R. Why is mannitol becoming more and more popular as a pharmaceutical excipient in solid dosage forms? Pharmaceutical development and technology. 2014;19(3):257-62.10.3109/10837450.2013.775154

99. Tarlier N, Soulairol I, Bataille B, Baylac G, Ravel P, Nofrerias I, et al. Compaction behavior and deformation mechanism of directly compressible textured mannitol in a rotary tablet press simulator. International Journal of Pharmaceutics. 2015;495(1):410-9.10.1016/j.ijpharm.2015.09.007

100. Shukla AJ, Price JC. Effect of moisture content on compression properties of directly compressible high beta-content anhydrous lactose. Drug Development and Industrial Pharmacy. 1991;17(15):2067-81.10.3109/03639049109048533

101. Vromans H, De Boer AH, Bolhuis GK, Lerk CF, Kussendrager KD, Bosch H. Studies on tableting properties of lactose - Part 2. Consolidation and compaction of different types of crystalline lactose. Pharmaceutisch Weekblad Scientific Edition. 1985;7(5):186-93.10.1007/bf02307575

102. Lerk CF. Consolidation and compaction of lactose. Drug Development and Industrial Pharmacy. 1993;19(17-18):2359-98.10.3109/03639049309047195

103. Olmo IG, Ghaly ES. Compressional characterization of two dextrose-based directly compressible excipients using an instrumented tablet press. Pharmaceutical development and technology. 1999;4(2):221-31.10.1081/pdt-100101356

104. Olmo IG, Ghaly ES. Evaluation of two dextrose-based directly compressible excipients. Drug Development and Industrial Pharmacy. 1998;24(8):771-8.10.3109/03639049809082725

105. Malamataris S, Goidas P, Dimitriou A. Moisture sorption and tensile strength of some tableted direct compression excipients. International Journal of Pharmaceutics. 1991;68(1-3):51-60.10.1016/0378-5173(91)90126-9

106. Shukla AJ, Price JC. Effect of Moisture Content on Compression Properties of Two Dextrose-Based Directly Compressible Diluents. Pharmaceutical Research: An Official Journal of the American Association of Pharmaceutical Scientists. 1991;8(3):336-40.10.1023/a:1015889414533

107. Lennard-Jones JE. Processes of adsorption and diffusion on solid surfaces. Transactions of the Faraday Society. 1932;28(0):333-59.10.1039/tf9322800333

108. Huber F, Berwanger J, Polesya S, Mankovsky S, Ebert H, Giessibl FJ. Chemical bond formation showing a transition from physisorption to chemisorption. Science. 2019;366(6462):235-8.10.1126/science.aay3444

109. Fischer M, Schepky G. The effect of hygroscopic formulation ingredients on the sorption characteristics of tablets. Drug Development and Industrial Pharmacy. 1995;21(3):279-300.10.3109/03639049509048111

110. Zhang Y, Johnson KC. Effect of drug particle size on content uniformity of low-dose solid dosage forms. International Journal of Pharmaceutics. 1997;154(2):179-83.10.1016/s0378-5173(97)00134-8

111. Ahmad K, Smalley IJ. Observation of particle segregation in vibrated granular systems. Powder Technology. 1973;8(1-2):69-75.10.1016/0032-5910(73)80064-6

112. Zhao J, Yin D, Rowe J, Badawy S, Nikfar F, Pandey P. Understanding the Factors That Control the Quality of Mini-Tablet Compression: Flow, Particle Size, and Tooling Dimension. Journal of Pharmaceutical Sciences. 2018;107(4):1204-8.10.1016/j.xphs.2017.12.002

113. Bracher F, Heisig P, Langguth P, Mutschler E, Schirmeister T, Scriba GKE, et al. Arzneibuch-Kommentar, Wissenschaftliche Erläuterungen zum Arzneibuch: Wissenschaftliche Verlagsgesellschaft Stuttgart; 2021. Kommentar zu Ph.Eur. 2.5.11 p.

12. Publications

Peer reviewed articles:

- Rosch M, Lucas K, Al-Gousous J, Pöschl U, Langguth P. Formulation and Characterization of an Effervescent Hydrogen-Generating Tablet. Pharmaceuticals 2021, Vol 14, Page 1327. 2021;14(12):1327-.10.3390/ph14121327

- Lucas K, Rosch M, Langguth P. Molecular hydrogen (H2) as a potential treatment for acute and chronic fatigue. Archiv der Pharmazie. 2021;354(4):2000378-.10.1002/ardp.202000378

Oral presentations:

- "Formulation and testing of an effervescent hydrogen releasing tablet"; Working group presentation of Working Group Langguth, Department of Biopharmaceutics and Pharmaceutical Technology, Mainz, Germany, 24.01.2020

- "DVS analysis of different citric acid excipients for pharmaceutical formulation of effervescent tablets"; Online Workshop: Sorption Analysis in Pharmaceuticals Formulation; Surface Measurement Systems Ltd., London, United Kingdom, 16.11.2021

Poster presentations:

- “Formulation and evaluation of effervescent hydrogen generating granulates using wet (oscillating granulation) and dry (roller compacting) granulation”; Max Planck Institute for Chemistry poster day, Mainz, Germany, 26.06.19

- “Formulation and evaluation of effervescent hydrogen generating granulates using wet and dry granulation “; DPhG Annual meeting; Heidelberg, Germany, 01.-04.09.2019

- “Formulation and evaluation of an effervescent hydrogen generating tablet”; Max Planck Institute for Chemistry, Multiphase Chemistry Department retreat, Stromberg, Germany, 11-13.11.2019

- “Dynamic vapor sorption investigations of hydrogen generating granules”; Max Planck Institute for Chemistry poster day, Mainz, Germany, 17.06.21

- “Dynamic vapor sorption investigations of hydrogen generating granules” Max Planck Institute for Chemistry, Max Planck Institute for Chemistry, Multiphase Chemistry Department retreat, Mainz, Germany, 27.-29.11.2021

13. Supplementary materials

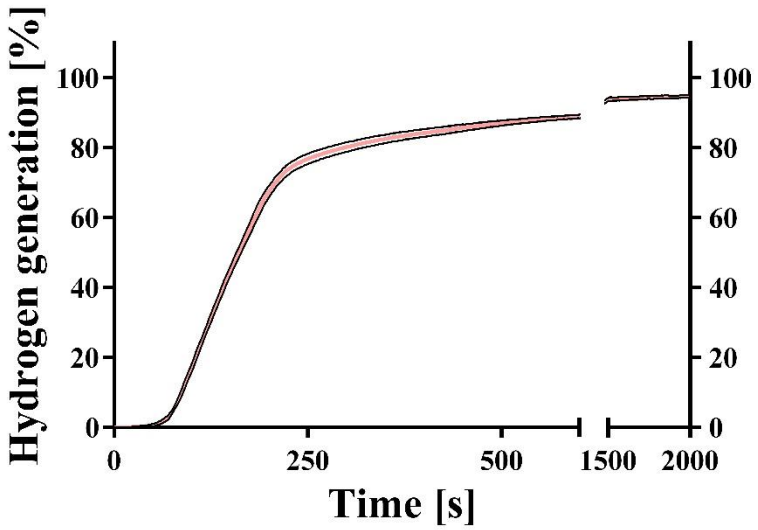

Figure 6.3.a) Kinetic hydrogen generation measurement (mean; n = 3). Kinetics of hydrogen generation were measured using a maltose-based batch. Means were calculated and plotted against time. SD values are shown as black lines.

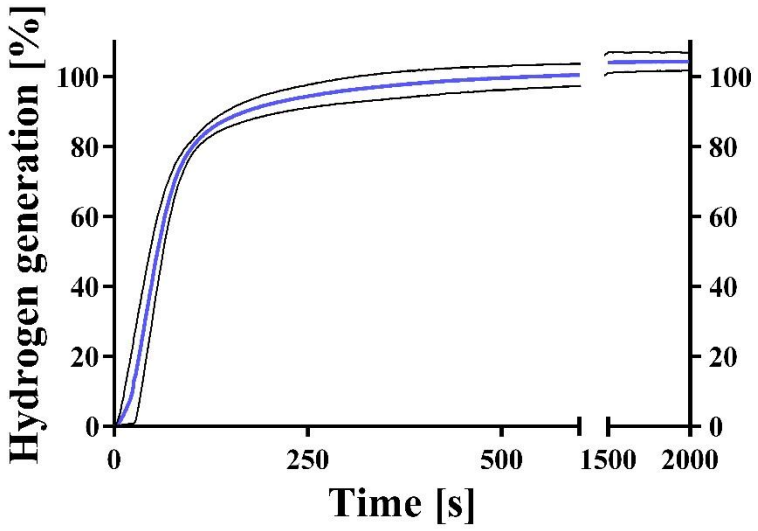

Figure 6.3.b) Kinetic hydrogen generation measurement (mean; n = 3). Kinetics of hydrogen generation were measured using a mannitol-based batch. Means were calculated and plotted against time. SD values are shown as black lines.

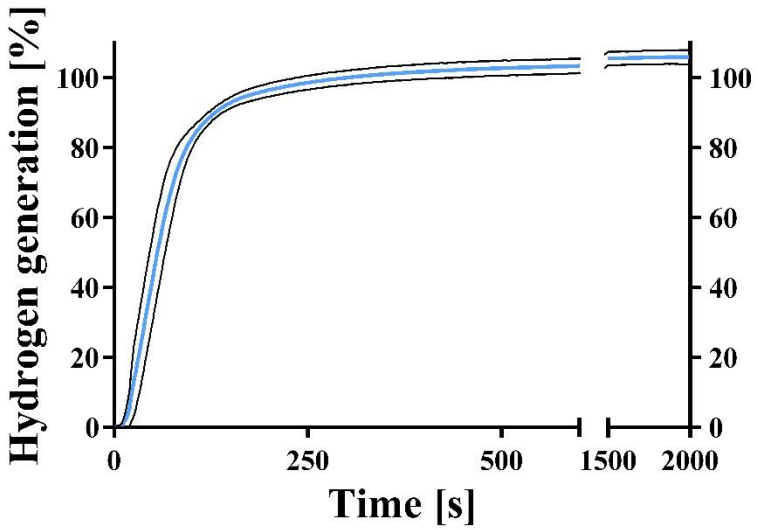

Figure 6.3.c) Kinetic hydrogen generation measurement (mean; n = 3). Kinetics of hydrogen generation were measured using a mannitol/adipic acid-based batch. Means were calculated and plotted against time. SD values are shown as black lines.

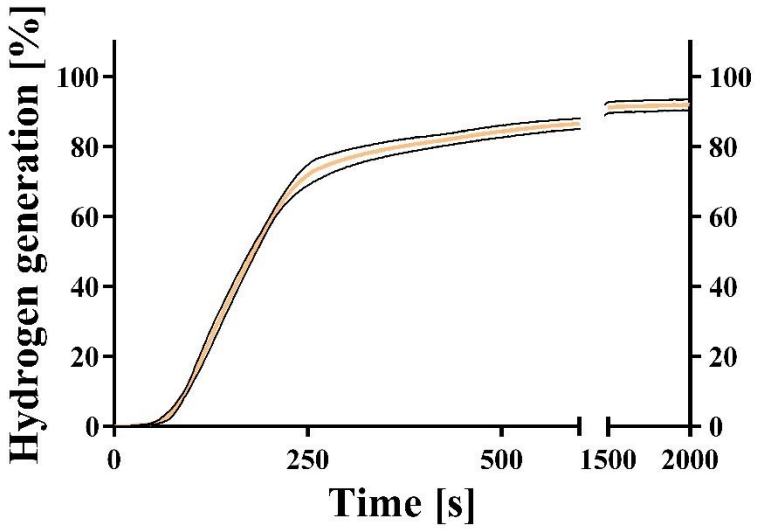

Figure 6.3.d) Kinetic hydrogen generation measurement (mean; n = 3). Kinetics of hydrogen generation were measured using a lactose-based batch. Means were calculated and plotted against time. SD values are shown as black lines.

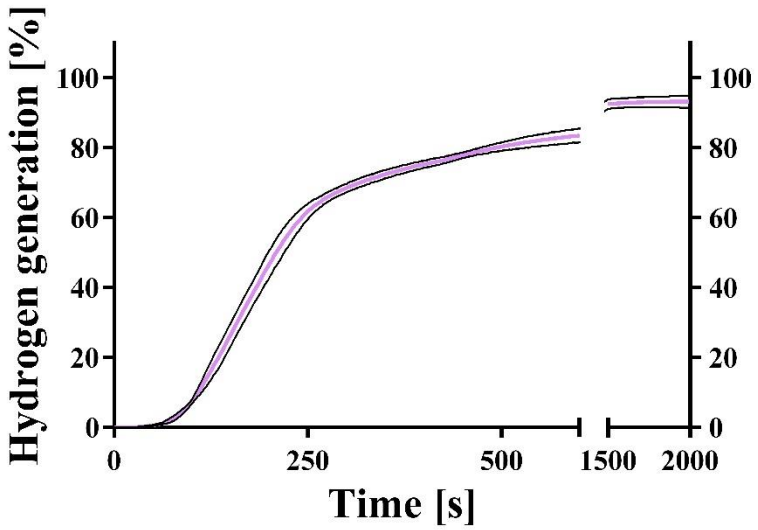

Figure 6.3.e) Kinetic hydrogen generation measurement (mean; n = 3). Kinetics of hydrogen generation were measured using a dextrates-based batch. Means were calculated and plotted against time. SD values are shown as black lines.

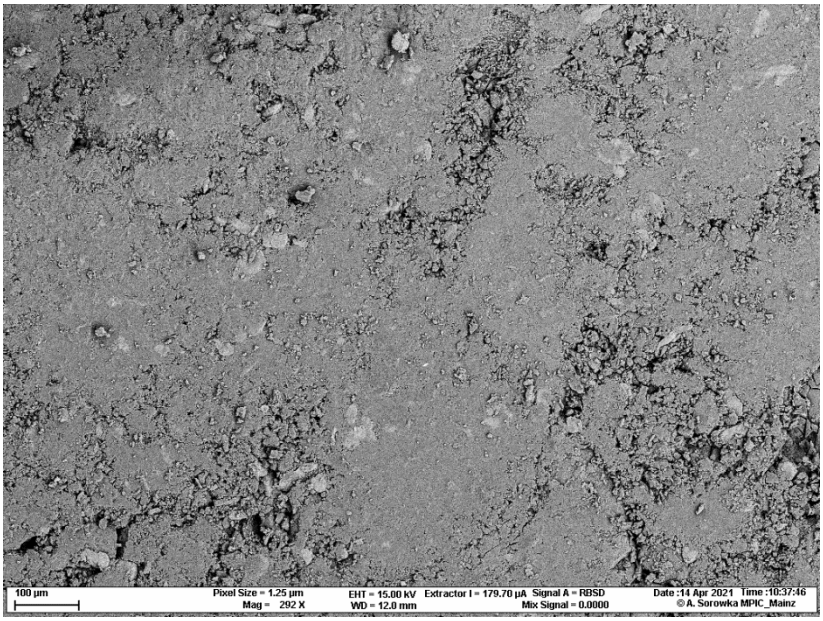

Figure 6.5.f) Scanning electron microscope pictures of a maltose-based batch (compaction force 40 kN; magnification: 292×)

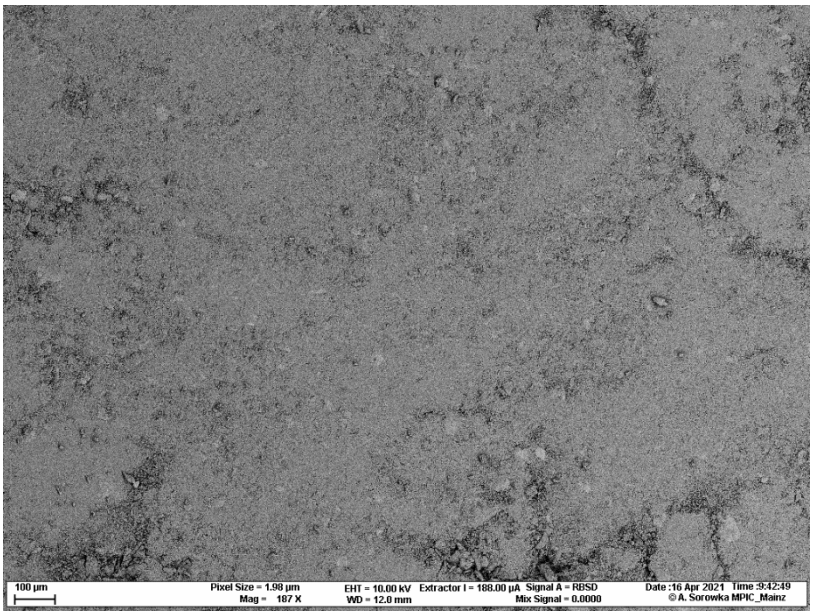

Figure 6.5.g) Scanning electron microscope pictures of a mannitol-based batch (compaction force 40 kN; magnification: 187×)

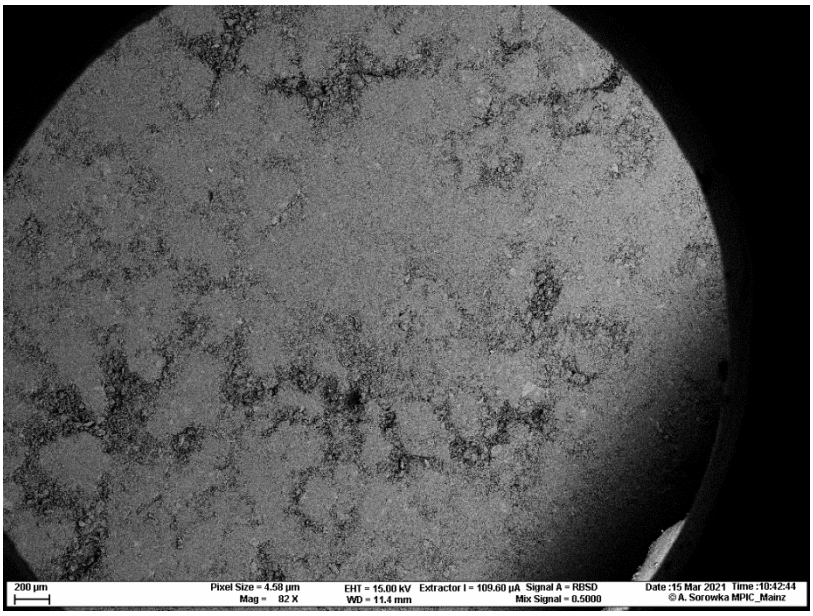

Figure 6.5. h) Scanning electron microscope pictures of a mannitol/adipic acid-based batch (compaction force 25 kN; magnification: 82×)

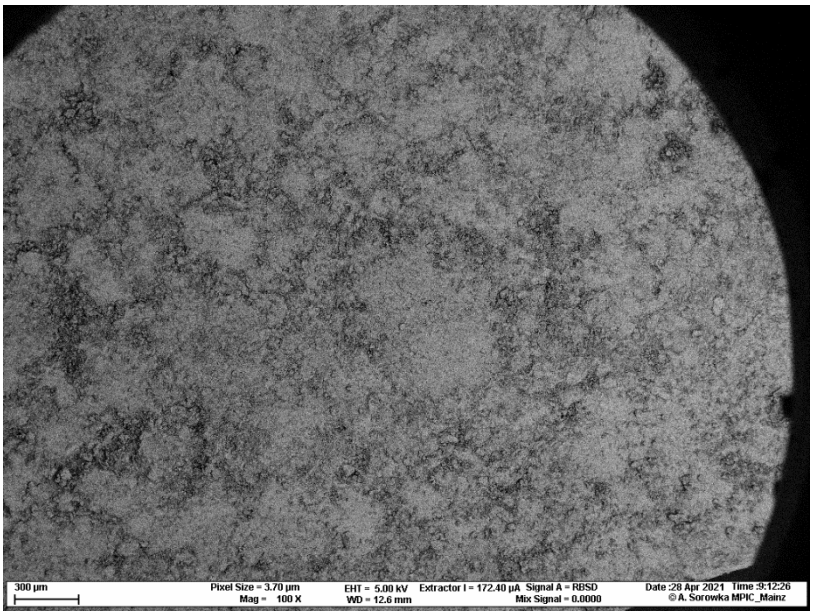

Figure 6.5.i) Scanning electron microscope pictures of a lactose-based batch (compaction force 40 kN; magnification: 100×)

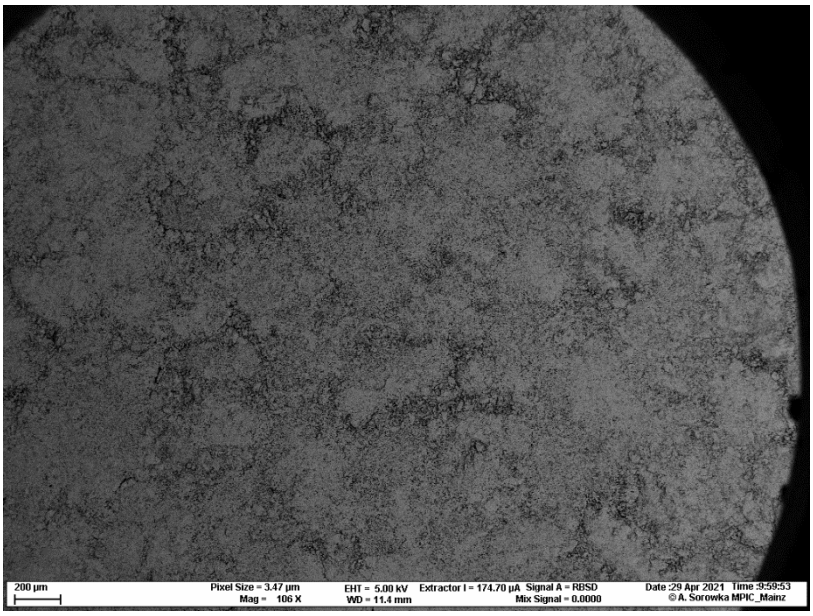

Figure 6.5.j) Scanning electron microscope pictures of a dextrates-based batch (compaction force 40 kN; magnification: 106×)

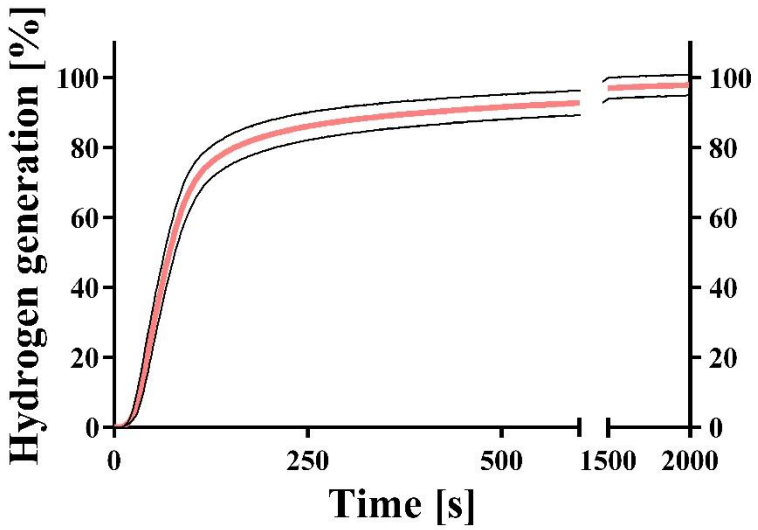

Figure 6.8.a) Kinetic hydrogen generation measurement (mean; *n* = 3). Kinetics of hydrogen generation of unpacked tablets of the mannitol/adipic acid-based batch MR010-2_7 was measured at the starting point t_0 without storage in a constant climate chamber (25 °C and 60% RH). SD values are shown as black lines.

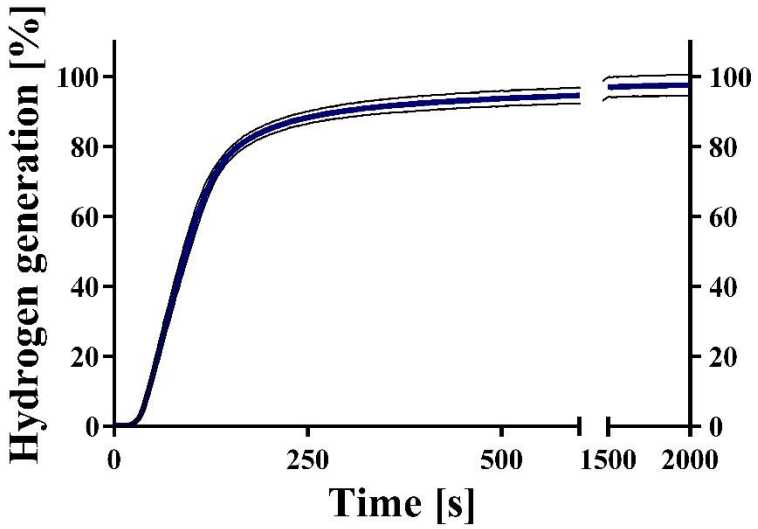

Figure 6.8.b) Kinetic hydrogen generation measurement (mean; *n* = 3). Kinetics of hydrogen generation of unpacked tablets of the mannitol/adipic acid-based batch MR010-2_7 was measured after 24h of storage in a constant climate chamber (25 °C and 60% RH). SD values are shown as black lines.

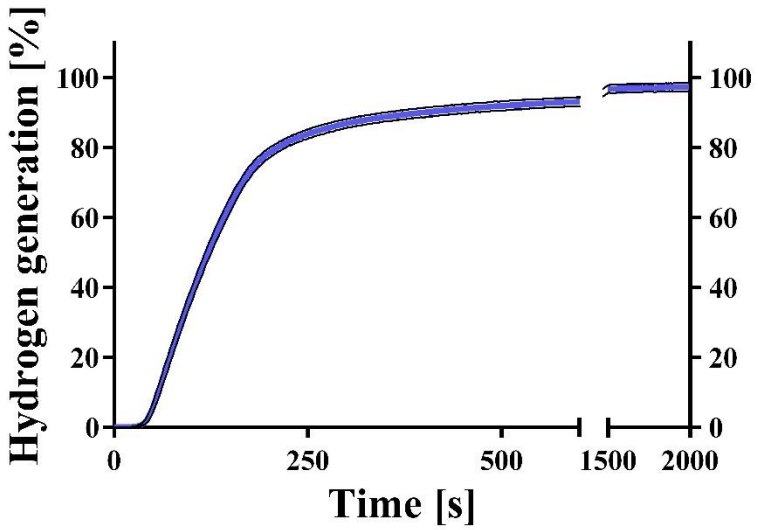

Figure 6.8.c) Kinetic hydrogen generation measurement (mean; *n* = 3). Kinetics of hydrogen generation of unpacked tablets of the mannitol/adipic acid-based batch MR010-2_7 was measured after 7 days of storage in a constant climate chamber (25 °C and 60% RH). SD values are shown as black lines.

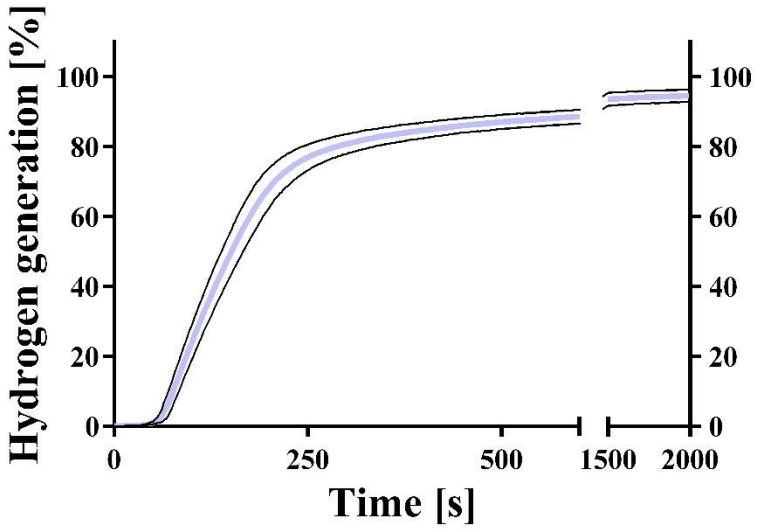

Figure 6.8.d) Kinetic hydrogen generation measurement (mean; *n* = 3). Kinetics of hydrogen generation of unpacked tablets of the mannitol/adipic acid-based batch MR010-2_7 was measured after 14 days of storage in a constant climate chamber (25 °C and 60% RH). SD values are shown as black lines.

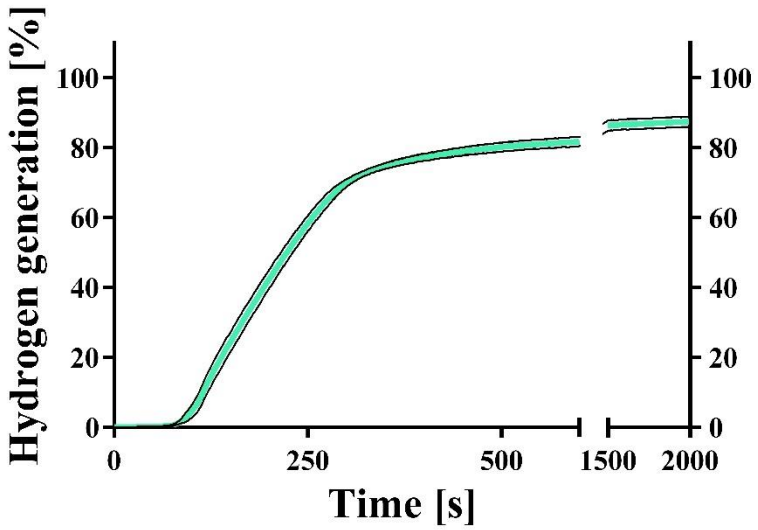

Figure 6.8.e) Kinetic hydrogen generation measurement (mean; *n* = 3). Kinetics of hydrogen generation of unpacked tablets of the mannitol/adipic acid-based batch MR010-2_7 was measured after 8 weeks of storage in a constant climate chamber (25 °C and 60% RH). SD values are shown as black lines.

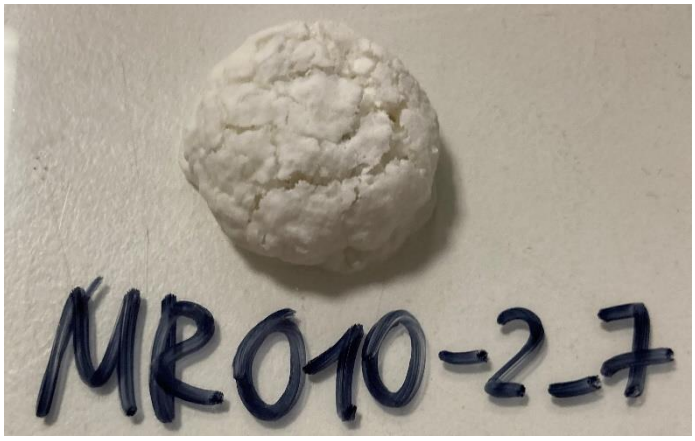

Figure 6.8.f) Photo of an unpacked tablet of the mannitol/adipic acid-based batch MR010-2_7 after storage in a constant climate chamber (40 °C and 75% RH) for 24h.

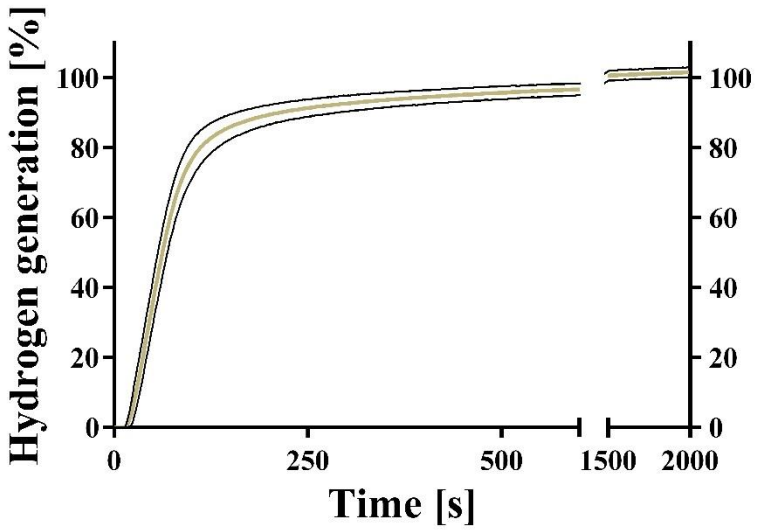

Figure 8.2.e) Kinetic hydrogen generation measurement (mean; n = 3). Kinetics of hydrogen generation of packed tablets of the mannitol/adipic acid-based batch MR010-2_11 was measured at the starting point t_0 without constant climate chamber storage. SD values are shown as black lines.

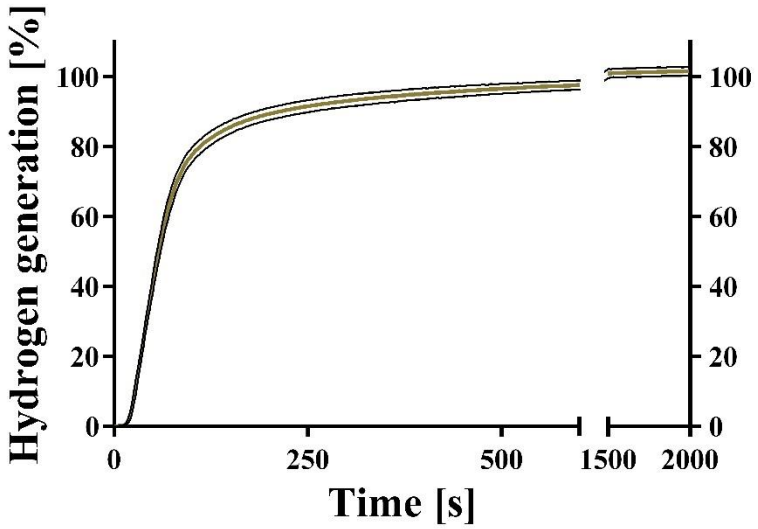

Figure 8.2.f) Kinetic hydrogen generation measurement (mean; n = 3). Kinetics of hydrogen generation of packed tablets of the mannitol/adipic acid-based batch MR010-2_11 was measured after 4 weeks of storage in a constant climate chamber (25 °C and 60% RH). SD values are shown as black lines.

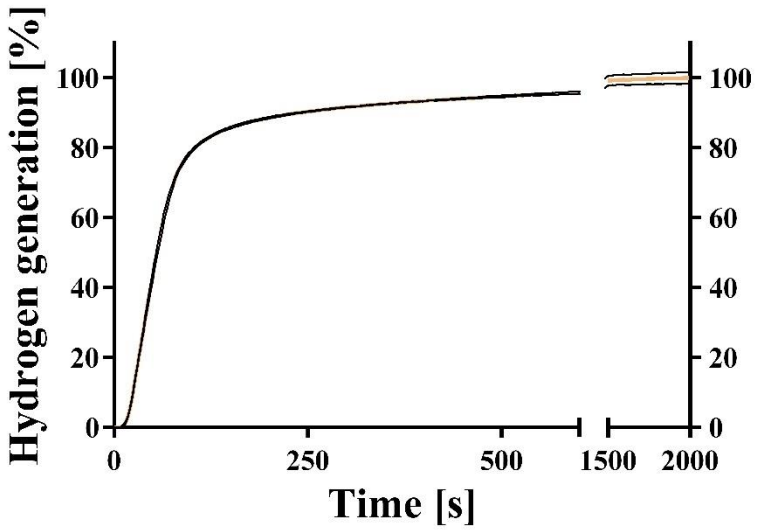

Figure 8.2.g) Kinetic hydrogen generation measurement (mean; n = 3). Kinetics of hydrogen generation of packed tablets of the mannitol/adipic acid-based batch MR010-2_11 was measured after 3 months of storage in a constant climate chamber (25 °C and 60% RH). SD values are shown as black lines.

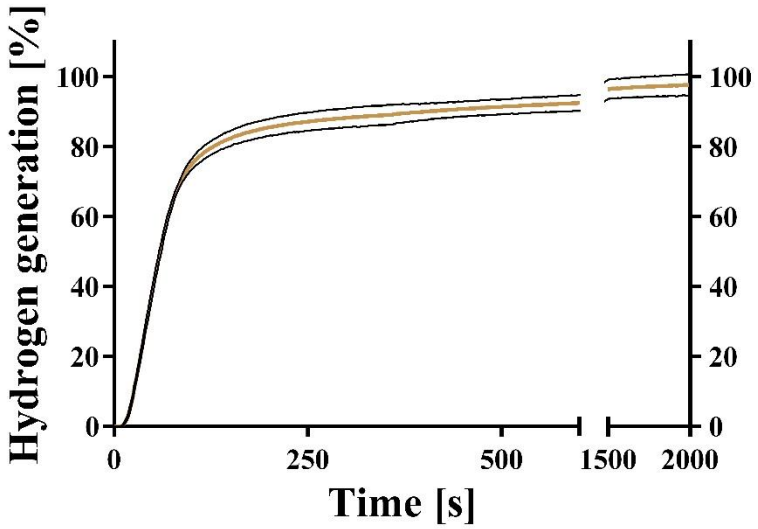

Figure 8.2.h) Kinetic hydrogen generation measurement (mean; n = 3). Kinetics of hydrogen generation of packed tablets of the mannitol/adipic acid-based batch MR010-2_11 was measured after 6 months of storage in a constant climate chamber (25 °C and 60% RH). SD values are shown as black lines.

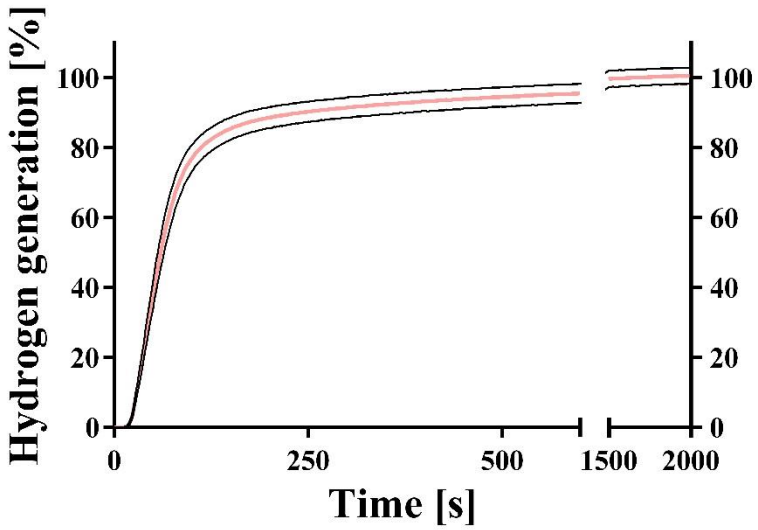

Figure 8.2.i) Kinetic hydrogen generation measurement (mean; n = 3). Kinetics of hydrogen generation of packed tablets of the mannitol/adipic acid-based batch MR010-2_12 was measured at the starting point t0 without constant climate chamber storage. SD values are shown as black lines.

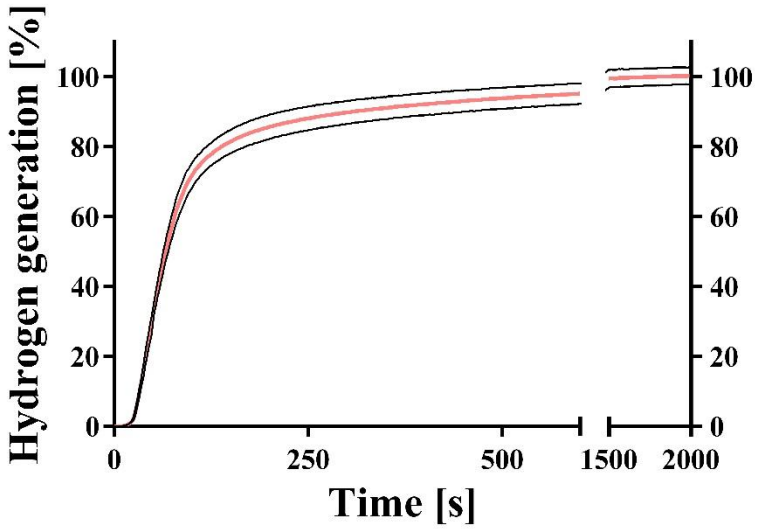

Figure 8.2.j) Kinetic hydrogen generation measurement (mean; n = 3). Kinetics of hydrogen generation of packed tablets of the mannitol/adipic acid-based batch MR010-2_12 was measured after 4 weeks of storage in a constant climate chamber (25 °C and 60% RH). SD values are shown as black lines.

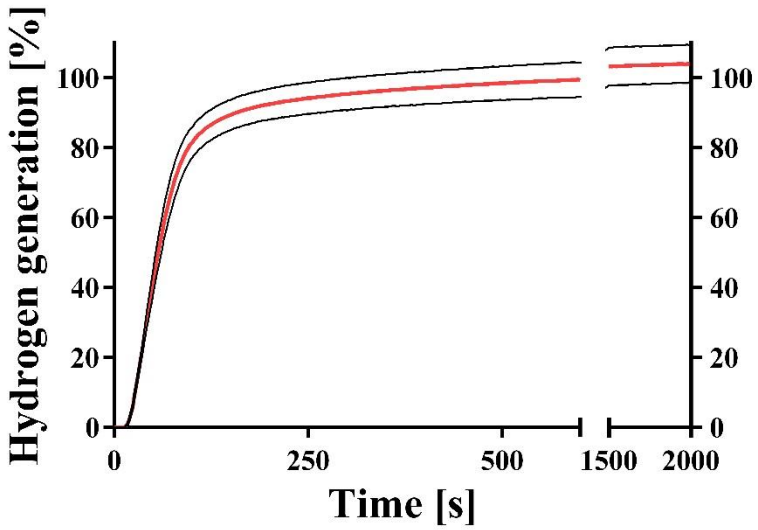

Figure 8.2.k) Kinetic hydrogen generation measurement (mean; n = 3). Kinetics of hydrogen generation of packed tablets of the mannitol/adipic acid-based batch MR010-2_12 was measured after 3 months of storage in a constant climate chamber (25 °C and 60% RH). SD values are shown as black lines.

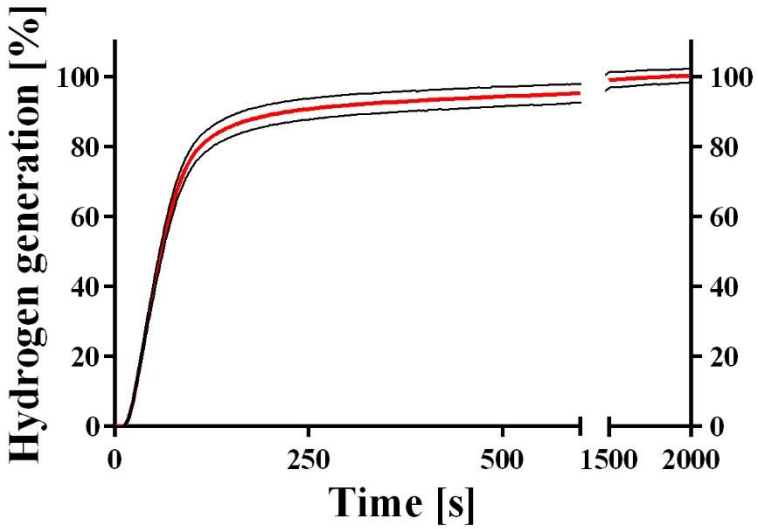

Figure 8.2.l) Kinetic hydrogen generation measurement (mean; n = 3). Kinetics of hydrogen generation of packed tablets of the mannitol/adipic acid-based batch MR010-2_12 was measured after 3 months of storage in a constant climate chamber (25 °C and 60% RH). SD values are shown as black lines.

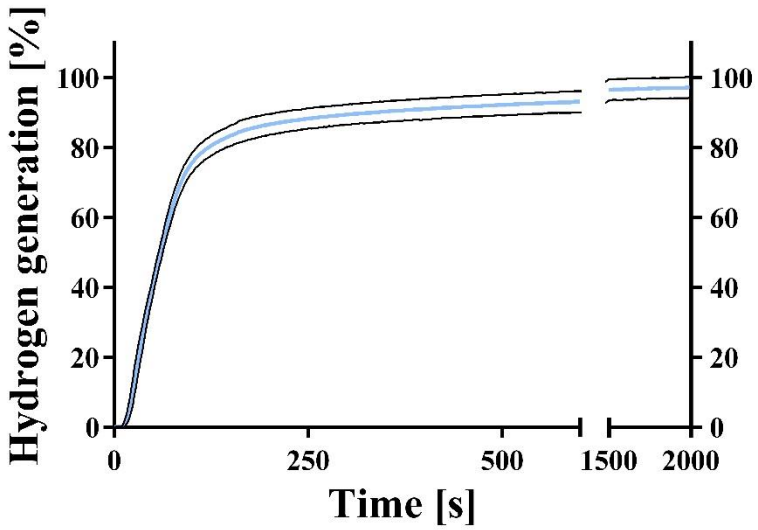

Figure 8.2.m) Kinetic hydrogen generation measurement (mean; n = 3). Kinetics of hydrogen generation of packed tablets of the mannitol/adipic acid-based batch MR010-2_11 was measured after 3 months of storage in a constant climate chamber (40°C and 75% RH). SD values are shown as black lines.

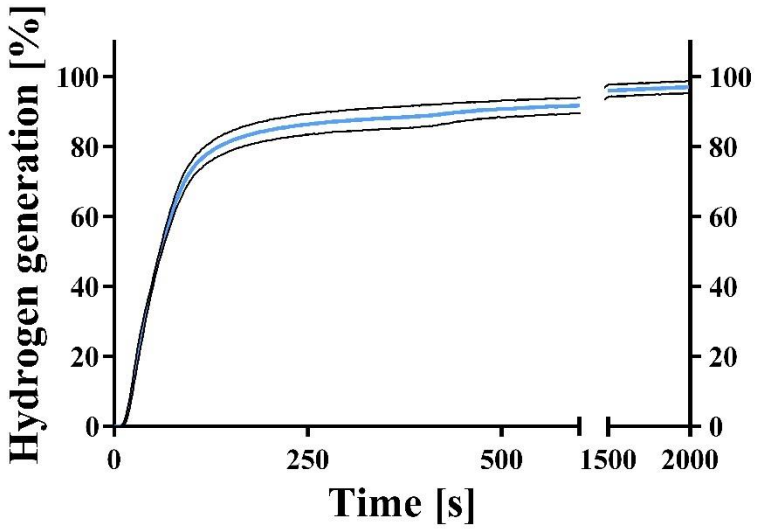

Figure 8.2.n) Kinetic hydrogen generation measurement (mean; n = 3). Kinetics of hydrogen generation of packed tablets of the mannitol/adipic acid-based batch MR010-2_11 was measured after 6 months of storage in a constant climate chamber (40°C and 75% RH). SD values are shown as black lines.

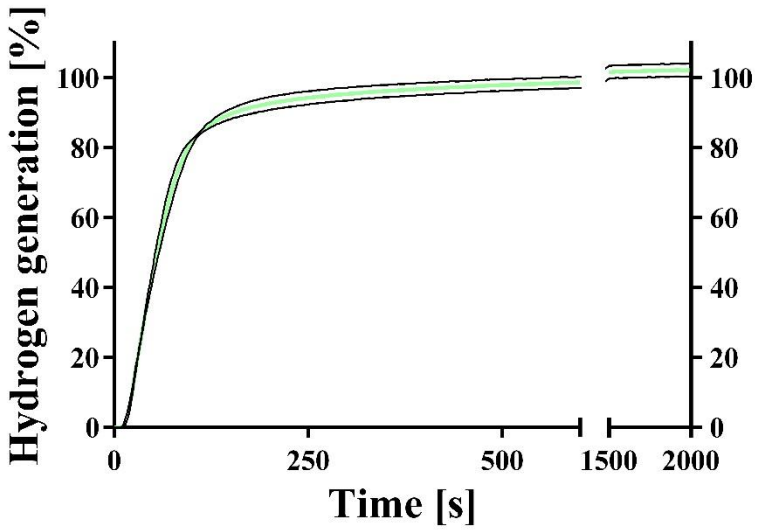

Figure 8.2.o) Kinetic hydrogen generation measurement (mean; n = 3). Kinetics of hydrogen generation of packed tablets of the mannitol/adipic acid-based batch MR010-2_12 was measured after 3 months of storage in a constant climate chamber (40°C and 75% RH). SD values are shown as black lines.

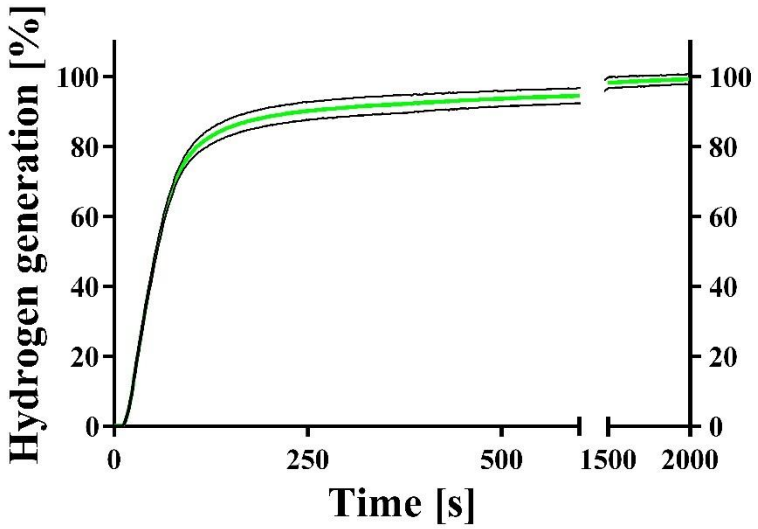

Figure 8.2.p) Kinetic hydrogen generation measurement (mean; n = 3). Kinetics of hydrogen generation of packed tablets of the mannitol/adipic acid-based batch MR010-2_12 was measured after 6 months of storage in a constant climate chamber (40°C and 75% RH). SD values are shown as black lines.

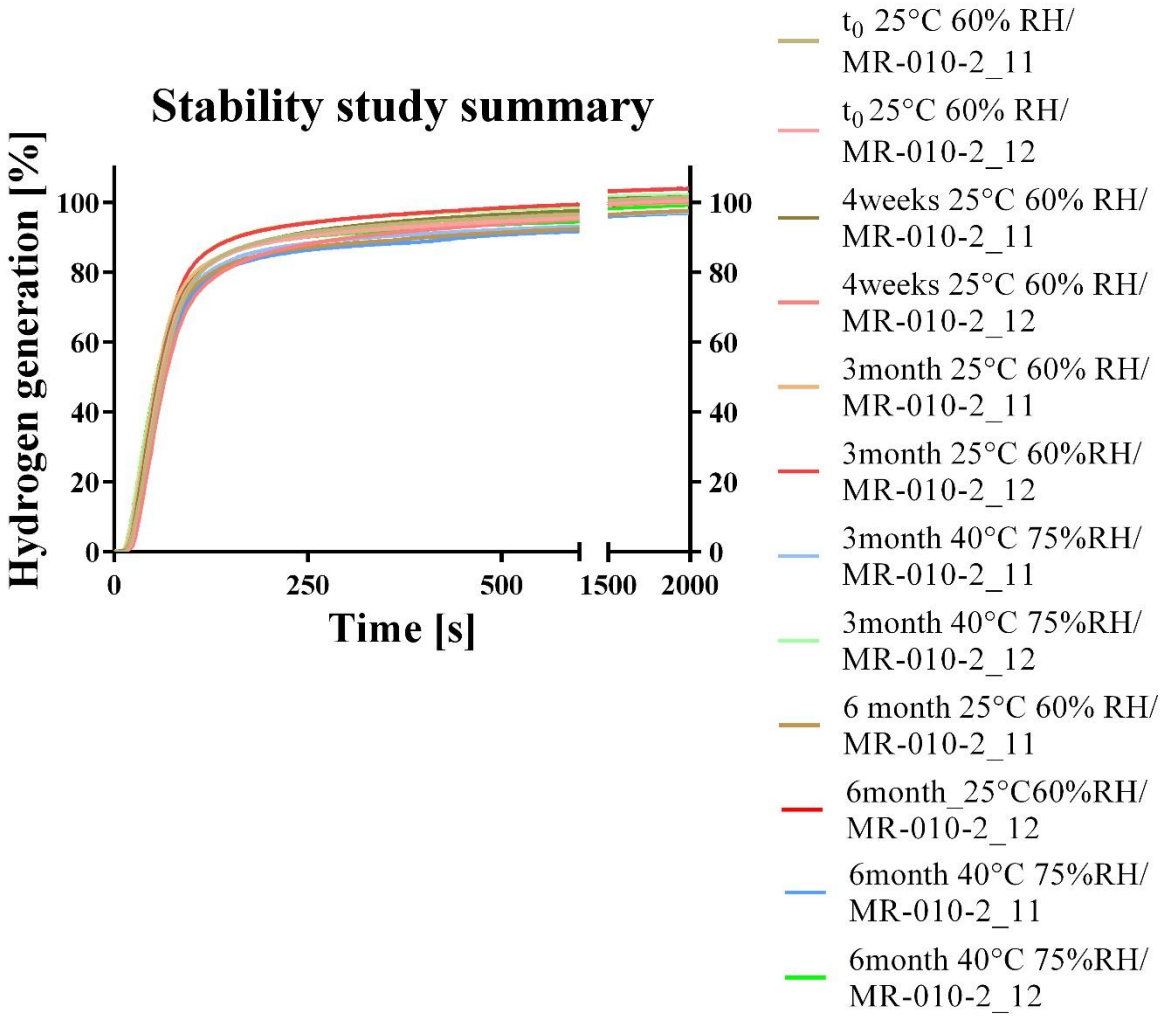

Figure 8.2.q) Kinetic hydrogen generation measurement (mean; n = 3). Kinetics of hydrogen generation of packed tablets of the mannitol/adipic acid-based batch MR010-2_11 and MR010-2_12. All means and of each sampling point of both conditions was measured.

14. Acknowledgements

The Acknowledgement section is only available in the printed version of the thesis.